GREENHOUSE GAS LIFE-CYCLE ASSESSMENT OF ADVANCED LIQUID BIOFUELS SUPPLY CHAINS

A consistent assessment of different European and global supply chains for the production of advanced liquid biofuels for road and aviation markets

MSc. Thesis – MSc. Energy Science
8-11-2019

Author
Guus de Jong
Utrecht University
g.a.dejong@students.uu.nl

First Supervisor
Dr. Ric Hoefnagels
Copernicus Institute of Sustainable Development
Utrecht University
r.hoefnagels@uu.nl

Second Supervisor
Prof. Dr. Martin Junginger
Copernicus Institute of Sustainable Development
Utrecht University
H.M.Junginger@uu.nl

Universiteit Utrecht

ADVANCEFUEL

Abstract

Advanced biofuels create an opportunity to reduce the lifecycle Greenhouse-Gas (GHG) emissions in transport, however a consistent comparison between the different production systems, end uses and corresponding lifecycle GHG emissions is missing. The conducted research therefore focussed on creating a dynamic model for calculating lifecycle GHG emissions of multiple advanced biofuels for road and aviation markets, made from lignocellulosic biomass, based on the calculation rules of the Revised Renewable Energy Directive (RED-II). The selected conversion processes have a Technological Readiness Level of four or higher as covered in the H2020 project ADVANCEFUEL. The results provide insight in possible ranges in GHG emission performance of possible feedstock-conversion combinations and assess whether they reach the GHG emission saving threshold set by the RED-II.

The results show that there are large ranges for each type of fuel produced (see figure 1). The large ranges are the effect of four important variables within each supply chain including feedstock type, transportation distance, pelletisation and energy source of Hydrogen (H_2) production. Additionally to these possible ranges, location specific case studies were assessed next to the impact of different methods of dealing with multifunctionality.

Biofuels produced from residues have lower GHG emissions compared to dedicated energy crops. The transportation mode and distance also demonstrate a significant impact, where a supply chain of 17500km compared 500km can double the GHG emissions. Pre-treatment (pelletising) reduces transportation emissions, however these are generally offset by the increased emissions from the pelletising process unless transported over distances of 175000km. For production systems that rely on hydrotreatment like pyrolysis, hydrothermal liquefaction and ethanol upgrading, the H_2 production energy source also demonstrates a significant impact. Electrolysers with fossil based electricity create higher GHG emissions compared to steam methane reformers (SMR) or biomass gasification. Using renewable H_2 can reduce the GHG emissions to a quarter compared to SMR. The method of dealing with multifunctionality causes differences where mass allocation often increases the GHG emissions and economic allocation as well as the displacement method decreases the GHG emissions compared to energy allocation used throughout this research.

The results of this study confirm that, although advanced biofuels reduce GHG emissions compared to fossil based fuels, many important variables can affect the GHG performance resulting in large possible ranges. Some conversion processes have better performance than others, however the total GHG performance of the production systems also heavily depends on the supply chain design (feedstock & transportation) as well as the design of the system itself (H_2 source and pre-treatment technology). Additionally it is strongly dependent on the method of dealing with co-products.

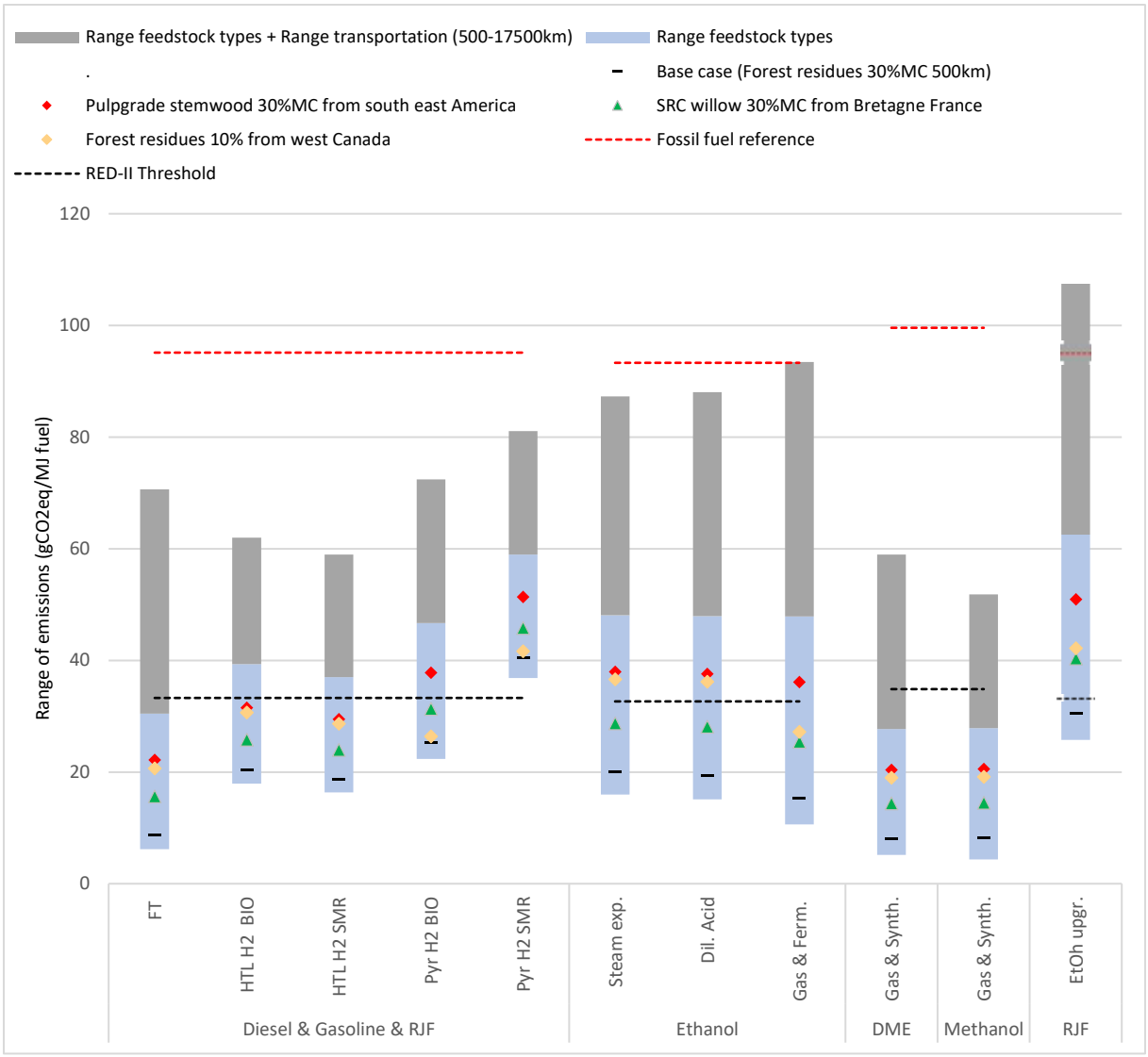

Figure 1- Total GHG emissions of advanced biofuel supply chains. Blue ranges present different feedstocks, grey ranges represent feedstocks + distance range from 500-17500km. Specific GHG of case studies are represented by coloured dots in the ranges. The black bar represents the base case supply chain, used throughout the research as a comparison.

Acronyms

ASTM	American Society for Testing and Materials
ALCA	Attributional Lifecycle Assessment
$CaCO_3$	Calcium Carbonate
CaO	Calcium Oxide
CH_4	Methane
CLCA	Consequential Lifecycle Assessment
CO_2	Carbon Dioxide
CO_2eq	Carbon Dioxide Equivalent
DLUC	Direct Land Use Change
DME	Di-methyl Ether
EC	European Commission
EU	European Union
FU	Functional Unit
FT	Fischer-Tropsch
GHG	Greenhouse Gas
GWP	Global Warming potential
H_2	Hydrogen
HEFA	Hydro processed Esters and Fatty Acids
HTL	Hydrothermal Liquefaction
ILUC	Indirect Land Use Change
IPCC	Intergovernmental Panel on Climate Change
JRC	(European Commission) Joint Research Centre
K_2O	Potassium Oxide
Kg	Kilogram
LCA	Life Cycle Assessment
LHV	Lower Heating Value
LUC	Land Use Change
MJ	Mega Joule
MC	Moisture Content
NG	Natural Gas
N	Nitrogen
N_2O	Nitrous Oxide
PEM (E)	Proton Exchange Membrane (Electrolyser)
Pyr	Pyrolysis
P_2O_5	Phosphorus Pentoxide
RED-I	Renewable Energy Directive
RED-II	Revised Renewable Energy Directive
RJF	Renewable Jet Fuel
SB	Sawdust Boiler
SHF	Separate Hydrolysis and Fermentation
SMR	Steam Methane Reforming
SOEC	Solid Oxide Electrolysis Cell
SRC	Short Rotation Coppice
SSF	Simultaneous Saccharification and Fermentation
TTW	Tank-to-Wheel
WB	Woodchip boiler
WTT	Well-to-tank
WTW	Well-to-Wheel

Contents

1 Introduction

1.1 Background

Since the start of the industrial revolution, greenhouse gas (GHG) levels have kept rising causing a net increase in global temperature. Ecosystems across the world are affected by the rise in temperature causing disturbances in wildlife, sea level rise and acidification and numerous other negative effects (Walther et al., 2002). Reducing the GHG emissions of fossil fuels is recognized as the main mitigation option for climate change, together with creating more GHG sinks. Governments across the world have committed themselves to international agreements like the Kyoto Protocol and later the Paris Agreement (COP21) to reduce fossil GHG emissions, aiming at keeping the global temperature rise below 2 °C until the end of this century (Britannica, 2019; United Nations Climate Change, 2015).

1.2 Biofuels and sustainability

Conventional and advanced biofuels are seen as a promising option to reduce GHG emissions in transport, while increasing diversity of the energy supply creating more energy security as well as creating rural development and job opportunities (Scarlat & Dallemand, 2011; Wicke, 2017). However multiple concerns are in place related to the sustainability of these biofuels, especially regarding the calculation of the GHG emission reduction and the associated Land Use Change (LUC) effects (van der Hilst et al., 2018). The high amount of feedstock possibilities and the large amount of conversion technologies together with the inclusion of Direct and Indirect Land Use Change (DLUC & ILUC) effects, can create large uncertainties in sustainability assessments (Scarlat & Dallemand, 2011; Searchinger et al., 1989; van der Hilst et al., 2018). A response to these concerns are biofuel certification schemes in which sustainability criteria are set to safeguard sustainable development. Multiple certification schemes exist, each specialised on a specific market, geographical area or part of the biofuel supply chain (Fritsche & Iriarte, 2014; Scarlat & Dallemand, 2011).

1.3 The Renewable Energy Directive (RED- I) & Revised RED II

Within Europe, the Renewable Energy Directive (RED-I) published by the European Commission (EC) set clear goals for EU member states regarding an overall policy for the production and promotion of renewable energy sources up to 2020 (European Parliament, 2009). In 2018 a revised directive (RED-II) was published with more ambitious and specific targets beyond 2020 increasing the overall renewable energy sources consumption to 32% by 2030. Additionally specific sub-targets for the transport sector were set, where 14% of road and rail transport should to be supplied from renewable energy (European Parliament, 2018). The RED II introduced five types of fuel categories, with three specifically aimed at biofuels with specific sub-targets and maximum contributions caps.

Biofuels produced from food-based crops (first generation biofuels), which have high ILUC risks need to be faced out by 2030. Biofuels produced from food-based crops with low ILUC risks have a maximum contribution cap of 7%. Biofuels made from feedstocks listed in the RED-II Annex IX part A[1] & B[2] are defined as advanced biofuels or second generation biofuels. These advanced biofuels produced from feedstocks listed in part A must have a minimum contribution of 3.5% by 2030, however they may be counted twice thus the actual minimum contribution is 1.75%. Additionally a 1.2 multiplier is also allowed when the fuels are used in marine and aviation industry making the actual contribution lower. Advanced biofuels made from feedstocks listed in part B may also be counted twice, but are capped at 1.7%.

[1] Includes algae, municipal waste, straw, manure, palm oil mill effluent, crude glycerine, bagasse, nut shells, husks, cobs from corn, forest residues and forest-based industry residues and other non-food lignocellulosic materials (European Parliament, 2018).

[2] Includes used cooking oil and animal fats (European Parliament, 2018).

1.4 Lifecycle greenhouse gas emissions

Biofuels produced from food-based feedstocks have mature technological performance and market penetration, while advanced biofuels are not commercialised to a significant market share. Main reasons are the technological, economical and legislative barriers and corresponding uncertainties for developing and implementing the advanced biofuels (IRENA, 2016). The specific targets set by the EC could help to reduce these uncertainties and stimulate the production of advanced biofuels. To contribute to the set targets, biofuels must proof compliance to several sustainability criteria related to GHG emissions and land use. One of the key sustainability criteria of biofuels is the lifecycle GHG emissions and the associated minimum GHG saving thresholds compared to the fossil fuel counterpart, which is set 65% reduction by 2023 (European Parliament, 2018; Khanna & Zilberman, 2017).

A lifecycle GHG assessment has been widely accepted by the scientific community as well as governments because it takes all emissions from feedstock until conversion and usage into account and can function as a clear and consistent assessment tool (Wiloso, Heijungs, & de Snoo, 2012). Although many advanced biofuels will create a carbon dept, meaning the absolute GHG emissions will at first increase, over the longer period this CO_2 is reabsorbed. Within the scientific community this defined as biogenic carbon. This carbon dept can cause climate effects in the short term, however due to the biogenic carbon characteristic this is not included within the RED-II and is therefore also excluded from this research (EU, 2018).

1.5 Problem definition & Research question

Many tools have been developed to calculate the GHG emissions of biofuels, for example to demonstrate compliance with the RED-II GHG saving criteria. However, most tools such as Biograce I are limited to first generation biofuel production systems used for road transport and use the calculation rules of the RED I (Biograce, 2015). With the implementation of the RED-II, new GHG calculation rules have been introduced as well as the necessity for the inclusion of the advanced biofuels and renewable fuels of non-biological origins for different end-markets including marine and aviation (European Parliament, 2018). Although various lifecycle GHG studies have been conducted for different advanced biofuel supply chains, they often differ in methodology regarding goal & scope, design assumptions, input data, type of impact assessment, functional unit (FU), dealing with multifunctionality, assumptions on DLUC & ILUC effects and the choice of a reference system (Hoefnagels, Smeets, & Faaij, 2010). The time scope and emission characterisation (global warming potential) can also be different across systems (Cherubini et al., 2009). For that reason they have the inability to use them as comparison across each other and can therefore mislead policy makers in their decisions (ISO, 2006; Khanna & Zilberman, 2017; Plevin, Delucchi, & Creutzig, 2014; Wiloso et al., 2012).

Applying the same methodology from the RED-II to all the supply chains will create a consistent comparison model which can be used to calculate GHG performances of relevant advanced biofuel production systems with spatial explicit variable feedstock characteristics, as will be done in the ADVANCEFUEL project (see section 1.6). The focus of this thesis was to deliver a dynamic model similar to Biograce-I, but instead focusing on the lifecycle GHG emissions of advanced biofuel production systems for road and aviation markets. The development of this dynamic model and applying it helped to answer the main research question which is formulated as:

"What are the lifecycle GHG emissions of relevant advanced biofuel production systems (feedstock – conversion combinations) for aviation and road markets and can they comply to the RED-II emission reduction threshold?

To answer this main question several sub-questions have been formulated:

- What are the total GHG emissions of the different production systems (feedstock-conversion combinations) and can they comply to the RED-II GHG emission saving threshold?
- What is the effect of changing the following variables on the total GHG emissions of the production systems and on the compliance of the RED-II emission saving threshold?
    - Different types of feedstock.
    - Different transportation distances & transportation modes.
    - Different types of pre-treatment (pelletisation).
    - Different hydrogen production technologies and their energy source.
- Within the possible range of feedstock-conversion combinations what are realistic case studies (feedstock type – location - conversion combination) and what are their total GHG emissions?
- What is the effect of using different methods of dealing with multifunctionality, including mass, energy and economic value allocation or using displacement theory on the GHG emissions

1.6 The ADVANCEFUEL project

This thesis will be conducted in the context of H2020 project ADVANCEFUEL, set up by multiple universities and research organisations (Uslu, Detz, & Mozaffarian, 2018). The main goal of the project is to facilitate market roll-out of advanced biofuels and other liquid renewable fuels in the transportation sector between 2020 and 2030 (Advance fuel project, 2018). This LCA GHG tool will add to Task 4.4.1, which is responsible for assessing the sustainability criteria GHG emission of the relevant advanced biofuel supply chains and will be linked to Task 4.3 that aims to develop spatial explicit environmental impacts of biomass feedstock supply in the European Union (EU). Together with the ADVANCEFUEL consortium the relevant conversion technologies and their produced products were selected based on a Technological Readiness Level (TRL) of four or higher, which can be seen in table 1. Additionally the process of syngas fermentation is added, which is currently not commercially available, but is included because it shows great potential in the near future (Daniell, Köpke, & Simpson, 2012). Also the process of ethanol upgrading to Renewable Jet Fuel (RJF) and the process of Hydrothermal Liquefaction (HTL) are included, because they both have sufficient high enough TRLs.

Table 1 - Relevant advanced biofuel conversion technologies (Papadokonstantakis, 2018; Papadokonstantakis & Johnsson, 2018)

Conversion process		TRL	Fuels produced
Gasification pathways	- Fischer Tropsch (FT) synthesis - Methanol synthesis - Di-methyl Ether (DME) synthesis - Syngas fermentation	4-8	- Diesel - Gasoline - RJF - Methanol - DME - Ethanol
Biochemical pathways	- Fermentation - Ethanol upgrading	6	- Ethanol - RJF
Thermochemical pathways	- Pyrolysis - Hydrothermal Liquefaction (HTL)	4-6	- Diesel - Gasoline - RJF - Heavy hydrocarbons

2 Theoretical background

2.1 LCA theory

The most common and international standardised Life Cycle Assessment (LCA) framework is the ISO14040:2006, where 4 phases are defined as the goal and scope definition, the inventory analysis, the impact assessment and the interpretation phase (ISO, 2006). The structure of the LCA can be seen figure 2. The theory behind each element will be described, however within section 3 of the methodology each element is coupled to the actual research with the corresponding calculation rules from the RED-II as well as the assumptions and practical considerations being made.

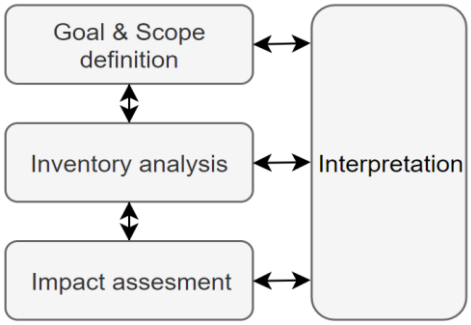

Figure 2 - Life Cycle Assessment framework (ISO, 2006)

2.1.1 Goal and scope

The first phase is defining the *goal and scope* of the LCA, where the system boundaries have to be set with regard to the goals of the research as well as the scope. Also with regard of the goal of the research, a fitting Functional Unit (FU) should be chosen. According to ISO:2006 the primary purpose of the FU is to provide a mathematical normalized reference to which all inputs and outputs can be expressed in. Another definition is that the FU is the quantification of the identified functions (the performance characteristics) of the products (Wiloso et al., 2012). Within fuel LCAs typical FUs include land area, mass or volume of input, mass or volume or energy of the end product, caloric value of the end product or distance travelled in a certain vehicle (Wiloso et al., 2012). It depends on the goal of the research what kind of FU should be used. For example, a FU like mass or volume would not be possible when electricity is included as a fuel. When comparing fuels like gasoline and electricity in the same type of vehicle, a FU in terms of 1-km driven would be best due to the vastly different drivetrain efficiencies. To compare the best use of liquid fuels, a FU in terms of 1 MJ would be best (Wiloso et al., 2012).

A next important element is how to deal with multifunctionally. The allocation method refers to the attribution of certain environmental burdens of multifunctional processes to the inputs and outputs (Wiloso et al., 2012). When processes have multiple inputs and outputs, the burden of the main products can be divided across the co-products or co-inputs. Different allocation methods exist varying from mass, volume, energy and costs allocation. Another type of dealing with multifunctionality is using the displacement theory, where all displaced emissions are accounted for. It should be noted that this can only be done when the main product has at least a 50% share (Chomkhamsri, Wolf, & Pant, 2011).

A last element that can vary, which is related to the method of dealing with co-products, is the type of LCA that is being performed. An Attributional LCA (ALCA) focusses on the analysis of environmental impact of a product, process or system (Rehl, Lansche, & Müller, 2012). This means that the emissions are allocated (based on mass, economic value or energy) to the main product and to the possible co-products. The Consequential LCA (CLCA) is focused on a macro scale, where the effect of the

introduction of a product or process on the system/market is analysed (Plevin et al., 2014; Rehl et al., 2012). In practical terms this means that the consequence is analysed, implying that displaced emissions can be calculated and possibly subtracted when the system is expanded. However other elements like indirect effects of the introduction of the biofuel on social elements or market dynamics should also be included making it difficult to assess.

2.1.2 Inventory analysis

The second phase is creating the *inventory* of all the processes within the system and quantifying the inputs and outputs of all the processes involved. All the decisions made in the first step are implemented regarding boundaries of the systems, dealing with multifunctionally and applying the FU. The main element of this step in the framework is therefore the data collection, where consistency across the data sources should be maximised and must be validated iteratively (ISO, 2006).

2.1.3 Impact assessment

2.1.3.1 Types of impact assessments

The third phase links all the process data from the previous steps to the possible environmental *impacts* that need to be assessed (ISO, 2006). Within LCA multiple environmental impacts can be assessed, the choice again depends on the goal an scope of the research. Environmental impacts can relate to GHG emissions, water use, land use, public health, biodiversity, eutrophication, acidification or photochemical ozone creation (Rehl et al., 2012). In practice this list can be extended, due to subcategories or combinations of impact assessments. Although this step follows the inventory analysis, the impact category needs to be clear due to the specific data required for the analysis.

2.1.3.1 Global Warming Potential (GWP)

For the assessment of the GHG emissions, which is the goal of this research, the Global Warming Potential or GWP is often used. The theory relies upon calculating the radiative forcing of different gasses over a set year timeframe compared to CO_2, thus creating the CO_2 equivalent (CO_2eq). The specific time horizon is often set at a 100 years, but can also be 20 or 500 year. The fourth Intergovernmental Panel on Climate Change (IPCC) assessment report (AR4) uses a GWP of 100 years in which the values for methane (CH_4) and nitrous oxide (N_2O) are given (International Panel Climate Change, 2016). The formula for the calculation of the GWP_{100} can be seen below, where GWP_{CH4} is set at 25 and GWP_{N2O} at 298.

$$CO_2\ eq = CO_2 + GWP_{CH4} * CH_4 + GWP_{N2O} * N_2O \quad (1)$$

2.1.4 Interpretation

The last phase is the *interpretation* in which the environmental impacts are compared and discussed to answer the research questions and make recommendations. Although the interpretation step takes place in all phases, it is especially important at the end of the research to assess the calculated impacts in a broader perspective and see what assumptions have led to the obtained results (ISO, 2006). This phase also contains the sensitivity analysis.

2.2 Land use change theory

2.2.1 DLUC & ILUC definition

When assessing the GHG footprint of the various advanced biofuels, a controversial element that can contribute significantly are the DLUC or ILUC effects that can occur. When land is being repurposed for other use, the carbon content or carbon stock of the land can change thus affecting the overall GHG performance of the produced biofuel (van der Hilst et al., 2018; Wicke, 2017). Figure 3 represents a simple visualisation of the DLUC and ILUC effects. DLUC causes the function of a piece of land to change to another function. An example would be to change the land from a food production function to a

biofuel production function. DLUC can also simply mean that another type of food or even another type of tree is produced, causing changes in carbon stock of the land. ILUC is often defined as the land use change that takes place elsewhere to still meet the demand for a certain good, which is often a food product. An example would be that due to the extra use of soybeans for biofuels, the demand for soybeans becomes higher thus increasing the commodity prices resulting in an expansion of soybean plantations on forest land (Wicke, 2017). Another example would be that a soybean plantation is replaced by a more economically attractive switchgrass plantation for biofuels, resulting in the same effect where other (forest) land will be sacrificed to meet the demand in soybeans (van der Hilst et al., 2018; Wicke, 2017).

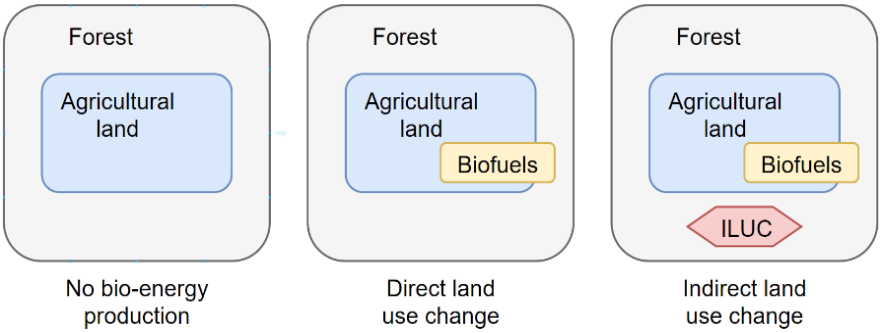

Figure 3- Schematic representation of Land Use Change principle (Wicke, 2017)

Calculating the DLUC can be done relatively simply by comparing the carbon balance of the current and the previous land. However this is also dependent on a timescale since DLUC can increase or decrease the carbon content of a piece of land over time. This is caused by carbon sequestration which increased the carbon stock or harvest which decreases the carbons stock (van der Hilst et al., 2018). ILUC is more complicated since it is also depended on many other factors such as the commodity prices of the feedstock, the demand of the feedstock and the price and demand of the product that is being displaced. Searchinger et al. (1989) was one of the first to calculate the GHG effect of the ILUC on corn based ethanol production. Due to the large ILUC effects, the ethanol production emitted more than the fossil based gasoline (Searchinger et al., 1989). This caused a heated debate on the accuracy and robustness of the analysis. Other authors modelled the same ethanol production system with significantly different results. Khanna & Zilberman (2017) describe that many types of models are used including computable general equilibrium models, dynamic programming models and partial equilibrium models to calculate the ILUC effects. Currently there is no consensus on the right method of calculating ILUC, therefore causing significant deviating results in literature (Khanna & Zilberman, 2017).

2.2.2 DLUC & ILUC in the RED-II

The RED-II only accounts for DLUC effects, which uses the change in carbon stock of the previous land (20 years before the current use) compared to the carbon stock of the current land. This change is averaged out over the period of 20 years to see what the yearly change in carbon stock is. A bonus of 29gCO_2eq/MJ biofuel can be given if the land was previously not in use for any function or if it is restored degraded land (European Parliament, 2018). To calculate the carbon stock multiple aspects are taken into account including the soil organic carbon (SOC) based on the type of soil, climate region and type of feedstock as well as the above and below ground carbon within dead or alive vegetation (European Commission, 2010).

The ILUC effects are not accounted for with a calculation within the RED-II. However as became clear from the introduction, certain policies are in place to face out feedstocks with high ILUC risks until

2030. Furthermore a contribution cap of 7% is set on feedstocks with low ILUC risks. The feedstocks within this research are not categorized as high ILUC feedstocks because they are mainly residues or co-products of other processes. Regarding the grasses like miscanthus or switchgrass or the SRC's like willow, poplar and eucalyptus, the amount of ILUC risks will strongly depend on the type of land being used. When marginal or unused lands are used these risk are lower compared to agricultural land use (Elbersen, 2019).

2.3 N_2O soil induced emissions theory

Using nitrogen as a fertilizer for crop management can affect the total GHG emission value significantly. As became clear from the GWP_{100}, the N_2O value has 295 times the radiative forcing effect compared to CO_2 thus having a significant effect on the total CO_2eq (see GWP_{100}). The RED-II asks member states to apply a method of standard N_2O field emissions from standard crops. Due to costs and complexity this is hard to measure for each specific crop and spatially specific location, therefore the IPCC (2006) developed a model which can be used to calculate the soil N_2O emissions (IPCC, 2006). The nitrogen (N) that is used as a fertilizer within managed crops can result in N_2O in the atmosphere via two different pathways: Directly from the N that is added or removed from the soil, together with the N that is found on crop residues that are left behind. Or it can be induced indirectly via volatilisation of N with the atmosphere resulting in NH_3 and NO_x escaping or leaching resulting in run-off of N (Edwards et al., 2019; IPCC, 2006). An important element in the calculation are the emission factors being used, which strongly depend on the type of fertilizer, the crop or feedstock used as well as the geographical location with the corresponding temperature and humidity (Edwards et al., 2019; IPCC, 2006).

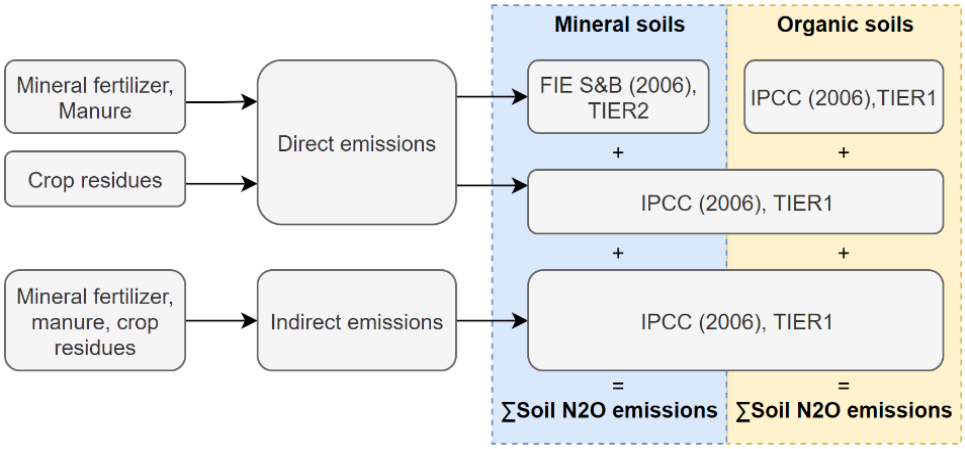

Figure 4- Schematic representation of required nitrogen calculation methods in RED-II (Edwards et al., 2019)

Figure 4 gives an overview of what Tier (measurement of accuracy of the method used) is required to cohere to the RED-II guidelines. As can be seen for each element only TIER1 of the IPCC (2006) should be used, except for fertilizer use on mineral soils where a statistical model from Stehfest and Bouwman (2006) should be used. This model provides crop and location specific emission factors thus creating a higher level of accuracy (Stehfest & Bouwman, 2006). For some feedstocks of this research these steps are not required, since they only apply for managed crops and not for residues.

3 Method

The first section of the method consist of specifying all the elements of the goal and scope definition of the LCA framework mentioned in the theory and tailor it to the specific needs and calculations rules of this research. Then within the second section, the inventory analysis, the included supply chains are described in detail together with the used data sources and the calculation methods. Lastly the impact assessment will describe the chosen supply chains for analysing the four variations as well as the chosen case studies to which a sensitivity analysis is performed.

3.1 The goal and scope

The goal and scope of this research is the lifecycle GHG emissions assessment for the production systems of the advanced biofuels listed in table 1. The fitting type of LCA to asses this goal was therefore an ALCA. The system boundary is the entire lifecycle of the supply chain taking all emissions into account of each phase in the lifecycle. As can be seen in figure 5, the supply chain consist of two main parts: the Well-to-Tank (WTT) and Tank-to-Wheel (TTW). This research takes all the steps from cultivating the feedstock, harvesting, pre-processing, transport, conversion and distribution (WTT) as well as the end use (TTW) into account. It should be noted that only emissions regarding 100% biofuel use are accounted for in the TTW phase, see section 3.2.5.

The geographical boundary for conversion systems and end-use is the EU, however feedstock cultivation and harvesting can be done on a global scale. The emission factor of the electricity mix is based upon the average electricity mix of the EU. All production systems are based on current performances of technologies, which are changed in the sensitivity analysis. The scope of emission characterisation is based upon the 100 year time horizon Global Warming Potential (GWP_{100}) of CH_4 & N_2O relative to CO_2 defined in the IPCC AR4 (see section 2.2.3.1). The formula that is used to calculate the lifecycle GHG emissions of the supply chains is defined in Annex V of RED-II as:

$$E = e_{ec} + e_l + e_p + e_{td} + e_u - e_{sca} - e_{css} - e_{ccr} \quad (2)$$

Where:

E = Total emissions from the use of the fuel
e_{ec} = Emissions from the extraction or cultivation of raw materials
e_l = Annualised emissions from carbon stock changes caused by land − use change
e_p = Emissions from processing
e_{td} = Emissions from transport and distribution
e_u = Emissions from the fuel in use
e_{sca} = Emission savings from soil carbon accumulation via improved agricultural management
e_{css} = Emission savings from CO_2 capture and geological storage
e_{ccr} = Emission savings from CO_2 capture and replacement

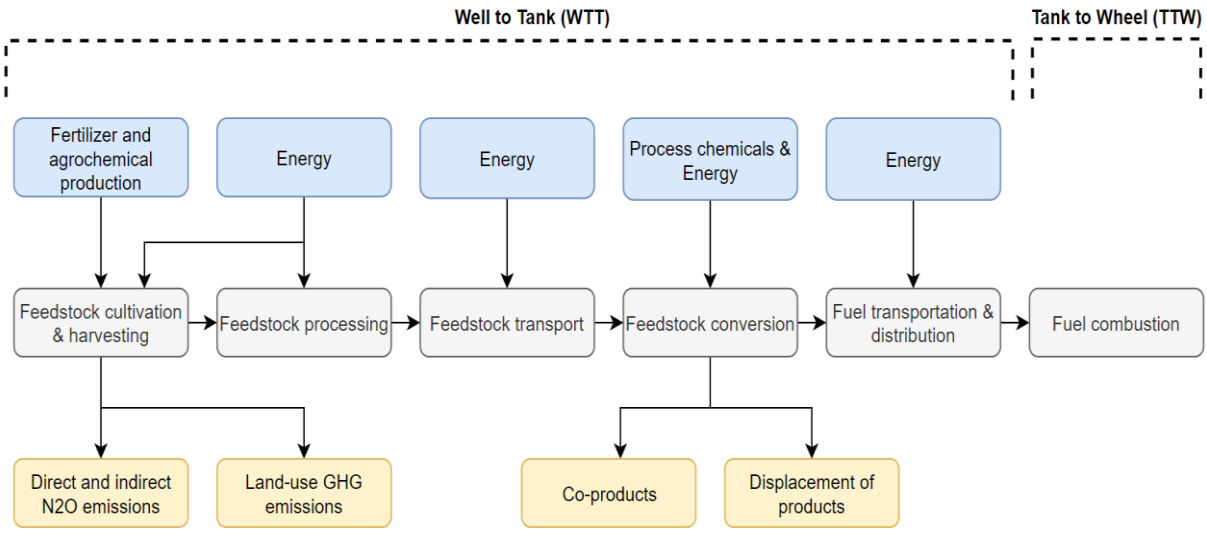

Figure 5 - General stages considered in biofuel LCA. Blue boxes are direct inputs of supply chain. Grey boxes is the supply chain itself. Yellow boxes contain indirect effects, the possible impacts and co-products. (Khanna & Zilberman, 2017)

3.1.1 The functional unit (FU)

From section 2.1.1 of the LCA theory it became clear that several FUs could be used within fuel LCAs, each having their advantages and disadvantages (Wiloso et al., 2012). The main goal of this research is calculating the lifecycle GHG emissions and the associated emission reduction threshold of the RED-II. The FU is therefore be line with the RED-II together with the considerations from section 2.2.1 resulting in the final FU which is defined as gCO_2 eq/$MJ_{endproduct}$ (European Parliament, 2018).

3.1.2 The allocation

From section 2.1.1 of the LCA theory it became clear that there are several methods to deal with multifunctionality. The ISO14040 (2006) includes clear procedures: Avoid allocation if possible with the use of system expansion or divide into subprocesses. However the RED-II uses energy allocation instead of system expansion (European Parliament, 2018; Wiloso et al., 2012). Therefore the allocation method is based upon energy content, which is also in line with the ALCA. Within the sensitivity analysis also mass and economic value allocation are included as well as the consequential system expansion method.

3.2 The inventory analysis

The inventory analysis, in which all the data was collected, follows the same order as formula 2 from the RED-II method. The included elements of the supply chains are described in detail at the corresponding parts of the formula. This means that the included feedstocks are described in the cultivation & extraction (e_{ec}) part of the formula and the included conversion processes and reactor types are described in the processing (e_p) part of the formula. Next to the description of the feedstocks and conversion processes, the calculation methods are given.

3.2.1 Cultivation & extraction of feedstocks

The first sign E_{ec} of formula 2 covers all the emissions related to the cultivation and extraction of the feedstocks, excluding the carbon stock changes caused by LUC effects. The included feedstocks, which are all made from lignocellulosic material, can be seen in table 2. However they all differ in terms of composition of carbon content, moisture content (MC) and locations from where they are harvested. As can be seen from table 2, the included feedstocks can also be pre-processed into different appearances like woodchips, bales and pellets, depending on the feedstock type. This will be elaborated further in feedstock processing section 3.2.3.1.

Table 2 - Included feedstocks and their physical appearances (Giuntoli et al., 2017; Koçar & Civaş, 2013)

Type of feedstock	***Woodchip (50%MC)***	***Woodchip (30%MC)***	***Grasses (30%MC)/ Bales (13.5%MC)***	***Pellets (10%MC)***
Forest residues				
Short Rotation Crops (SRC) eucalyptus				
SRC poplar With Fertilizer (WF)				
SRC poplar Without Fertilizer (WOF)				
SRC willow				
Stem wood				
Bagasse				
Switchgrass				
Miscanthus				
Industry residues				
Agricultural residues				
Straw				

For the calculation of this first step the following elements were collected per feedstock, with the corresponding values in table 12 of appendix B:

- Yield of the feedstock (kg/ha/y)
- Lower heating value (LHV_{dry}) of the feedstock (MJ/Kg_{dry})
- Amount of synthetic and natural N-fertilizer (Kg/ha/y)
- Amount of Cao fertilizer (Kg/ha/y)
- Amount of K_2O fertilizer (Kg/ha/y)
- Amount of P_2O_5 fertilizer (Kg/ha/y)
- Amount of pesticides (Kg/ha/y)
- Amount of field CO_2 emissions (acidification) (Kg/ha/y)
- Amount of seeding materials (Kg/ha/y)
- Amount of field N_2O emissions (Kg/ha/y)
- Amount of diesel use for machinery during harvesting (MJ/ha/y)

For all the elements above the values were obtained per feedstock, which could then be converted to kg required per MJ fuel obtained (kg cultivation products/MJ fuel)[3]. To obtain the actual emissions of each of these elements in terms of gCO_2eq/ha or gCO_2eq/MJ of fuel produced, the values were multiplied with a standardized emission factor which can be found in table 17 of the appendix E. Within the report of Edwards et al. (2019) an extensive analysis for the production of each of these elements is given, with a finalised emission factor. This is based on the amount of energy like diesel, coal and electricity being used together with other material inputs that are required for the production of these fertilizers, pesticides and seeding materials. The emission factors are also based on EU averages, where the amounts produced per geographical location and required transport distances effects are accounted for (Edwards et al., 2019).

The field N_2O emissions which are dependent on the amount of N-fertilizer used and the chosen emissions factors, which in turn are dependent on multiple other factors (see section 2.3), can be calculated with the dynamic tool developed by Bio-grace-I which is added in the dynamic model. With

[3] It should be noted that multiple steps take place between cultivation and final fuel conversion (pre-processing, drying, transport, pelletising etc.) resulting in many efficiency (mass) losses. For each individual step an efficiency is applied which add up to a cumulative efficiency. The cumulative efficiency is therefore applied to correct all losses up into the supply chain until the cultivation, to obtain the value Kg cultivation products /MJ fuel.

the use of the formulas found in appendix A, a user is also able to perform the calculations for a specific case in the future to gain a higher level of accuracy in the model. However in this research the standard values depending on the type of feedstocks from the report of Giuntoli et al. (2017) are used as can be seen in table 12 of the appendix B. Standardized values of the field CO_2 emissions are also added based on the same standardized values from Giuntoli et al. (2017).

All the cultivation elements, except for the diesel use during feedstock collection, can be obsolete when the feedstocks are residues. This means that no agricultural management is applied and that therefore only emissions during diesel use of feedstock collection can be allocated to the feedstock production.

3.2.2 Direct land use change (DLUC)

The second sign E_l represent the change in carbon stock due to DLUC. Section 2.4 of the theory explained that the calculation depends on multiple factors like soil type, type of land, climate region, type of feedstock and above and below ground vegetation which can be dead or alive (European Commission, 2010). Because these values strongly depend upon the geographic location, the feedstocks in question and the temporal situation, it was chosen to not include this in the model with actual values. However the dynamic tool developed by Biograce-I was added within the dynamic model based on these calculations, to enable a user to perform the calculations for a specific case in the future. The used formulas are also included appendix C.

3.2.3 Processing

The third sign E_p represents the emissions related to all the processing steps within the supply chain. This research breaks it down into four parts: First, the feedstock processing accounting for all processing steps from the fresh feedstock into woodchips, bales and/or pellets. Second, the feedstock conversion method, where a general method is given to calculate the emissions regarding the feedstock conversion into the fuels. Third, a detailed description of the included feedstock conversion technologies and the used reactors with their efficiencies. Fourth, a description of the included hydrogen (H_2) production technologies and their energy source.

3.2.3.1 Feedstock processing

Woodchips are generally processed directly during the harvest step of the feedstocks. During this step the raw material is cut and collected from the ground and chipped, after which they are often dried at the roadside to reduce the MC from 50% to 30%. The roadside drying causes a dry matter loss of 5% resulting in an indirect increase of feedstock requirement up in the supply chain[3] (Giuntoli et al., 2017). The only emissions that are allocated to the processing of the woodchips, is the diesel use of the machinery of the harvesting and the extra fresh feedstock required due to losses during drying. However forest residues also require an additional chipping step due to vastly different mix raw material. The data collection of the woodchip production uses values from Giuntoli et al. (2017), which can be seen in table 24 and 25 of appendix I. It should be noted that these values are corrected for in the actual dynamic model with upstream and downstream alterations and efficiency loses[3]. The feedstocks included for woodchips are: Forest residues, SRC willow, SRC eucalyptus, SRC poplar, stem wood and industry residues (see table 2).

Wood pellets production have additional steps next to the collection phase, because they also require auxiliary services like heat and electricity for the drying and pelletising of the fresh feedstock. Depending on the LHV_{dry} and the MC of the fresh feedstocks, the amount of heat required was calculated with formula 3. All the feedstocks, except for industry residues since this is sawdust, needed to dry from 50%MC to 10%MC. The required heat for the drying is provided by a natural gas (NG) boiler, a woodchip boiler (WB) or a sawdust boiler (SB). The efficiencies of the boilers can be found in table

22 of appendix H. The additional amount of woodchips required for the WB or SB were calculated using formula 4. The total emissions of the processing of these feedstocks is therefore directly related to the amount of diesel and electricity use for the pelletisation machine and the amount of NG or woodchips for the drying of the feedstock. All input data used can be seen in table 24 and 25 of appendix I.

Next to the feedstocks described above, also bagasse, straw, miscanthus, switchgrass and agricultural residues are included to produce pellets (see table 2). Bagasse is mainly produced in Brazil and is a residue of sugarcane production. The heat required for pelletisation is provided by a bagasse pellet boiler. Emissions of bagasse pelletization thus only accounts for the electricity use of the pellet mill (Jonker et al., 2015). The other feedstocks resemble the characteristics of grasses instead of wood. Therefore they use another processing method including bailing of the wet feedstock, which is left to dry to reduce the MC of 30% to 13.5% after which they are pelletised to reduce the MC of 13.5% to 10%. The total emission of the processing of these feedstocks is related to the diesel and electricity use of the bailing machine together with the electricity use of the pelletisation machine. All input data used can be seen in table 24 and 25 of appendix I.

$$Heat\ required\ = \left(\left(\frac{(1-MC@drybiomass)}{(1-MC@wetbiomass)} - 1\right) * 3.96\right)/(\text{LHV@drybiomass} * (1 - (\text{MCdrybiomass}/100)) \quad (3)$$

$$Additional\ feedstock\ (MJ/MJpellets = (Heat\ required * 1.01)/(Boiler\ efficiency - heat\ required) \quad (4)$$

3.2.3.2 Feedstock conversion method

The included feedstock conversion processes with the used efficiencies are described in detail in the next section. This section will provide a general calculation method which is applied to all conversion processes. The calculation of the conversion processes and the corresponding emissions are based upon four main factors:

- The efficiency of the reactor ($MJ_{feedstock}$ /MJ_{fuel}) or ($\sum MW_{out}$ / $\sum MW_{in}$) or (LHV_{out}/LHV_{in})
- The amount of energy needed (MJ_{fuel} / $MJ_{fuel\ produced}$)
- The amount of process chemicals required ($Kg_{chemicals}$ / $MJ_{fuel\ produced}$)
- The amount of co-products produced ($MJ_{co\text{-}products\ produced}$ / $MJ_{fuel\ produced}$)

Actual process diagrams of conversion plants are often too detailed or they differ from each other in terms of capacity, type of feedstock, MC of the feedstocks, products and co-products produced or other specific (sub) processes, causing the comparison between reactors to be difficult or resulting in a wide variety of performance characteristics. Therefore the processes were only analysed as a whole. In practice this means that not a mass and energy balance was made for each specific sub-process within the whole conversion process, but only a net energy balance covering all inputs and outputs of the process as a whole with the corresponding amounts.

The first step was identifying the efficiency of the reactors, which was done by calculating the total input and output in Kg, MW, LHV_{dry}, HHV_{dry} or a combination of these. Then the inputs and co-products produced where calibrated to the main output (1MJ of the chosen fuel) and multiplied with the corresponding emission factors from the feedstock production phase. Because all feedstocks are coupled to all the included conversion processes an assumption had to be made regarding the change in conversion efficiency which is dependent on the type of feedstock.

For each type of process a different correction method was applied. For the gasification and synthesis processes, the LHV is corrected for the MC as well as the energy required for vaporizing the moisture within the feedstocks. This can be seen in formula 5 and 6, where the LHV is first corrected for the MC and within the latter the LHV is corrected for the vaporizing energy. All LHVs of the feedstocks can be found in table 19 of appendix F. For the biochemical processes as well as HTL, the MC does not affect

the reactor efficiency, because it is based on a wet conversion process. The only correction factor is the LHV_{dry} of the feedstocks which represents the amount of carbon available for conversion. It should be noted that the conversion chemicals for the biochemical conversion are also made specific per type of feedstock. For the thermochemical pyrolysis the feedstocks are again corrected for the LHV_{dry}, but the entire drying step is also calculated separately. This is done because pyrolysis requires a very low MC before entering the reactor.

$$LHV_{dry} = LHV_{wet} * MC \quad (5)$$

$$LHV_{dry\ corrected} = LHV_{dry} - 2.442 * MC \quad \text{(Nieuwlaar, 2017)} \quad (6)$$

The emission factors for the production of the chemicals and catalysts required for the conversion processes are based upon the reports of Edwards et al. (2019) and the Greenhouse Gases, Regulated Emissions, and Energy Use in Transportation (GREET) model developed by the Argonne National Laboratory (2018a). These values can be found in table 18 of appendix E. The last element included the fuel requirements like electricity, diesel, hydrogen and ethanol use for the whole process, which are also calibrated to the main output and multiplied with the emission factors of table 13 & 16 from appendix D. Per type of pathway all the conversion emissions are summed to create a total emissions value. The total emissions are allocated to the main fuel based on energy allocation (see formula 7), however within the sensitivity analysis they were also allocated based on mass and market value or accounted for with the displacement method (see formula 8, 9 and 10 respectively). The input values for the mass allocation as well as the market value allocation can be found in table 14 & 15 of appendix E respectively.

$$Energy\ allocation = All\ emission\ of\ the\ process\ * \left(\frac{energy\ main\ product}{energy\ main\ product + energy\ co\ products\ produced}\right) \quad (7)$$

$$Mass\ allocation = All\ emission\ of\ the\ process\ * \left(\frac{mass\ main\ product}{mass\ main\ product + mass\ co\ products\ produced}\right) \quad (8)$$

$$Economic\ allocation = All\ emission\ of\ the\ process\ * \left(\frac{energy\ main\ product * price\ main\ product}{energy\ main\ product * price\ main\ product + energy\ co\ products\ produced * price\ co\ products}\right) \quad (9)$$

$$Displacement = All\ emisson\ of\ the\ process - all\ emission\ that\ are\ displaced\ by\ co\ products\ produced \quad (10)$$

3.2.3.3 Included feedstock conversion processes and their efficiencies

The included feedstock conversion processes are divided into 3 types, where each process is subdivided to produce specific fuels as output. The description of in the feedstock conversion processes follows the same order as table 1, which is again presented below as table 3.

Table 3 - Relevant advanced biofuel conversion technologies (Papadokonstantakis, 2018; Papadokonstantakis & Johnsson, 2018)

Conversion process		TRL	Fuels produced
Gasification pathways	- Fischer Tropsch (FT) synthesis - Methanol synthesis - Di-methyl Ether (DME) synthesis - Syngas fermentation	5-8	- Diesel - Gasoline - RJF - Methanol - DME - Ethanol
Biochemical pathways	- Fermentation - Ethanol upgrading	6	- Ethanol - RJF
Thermochemical pathways	- Pyrolysis - Hydrothermal Liquefaction (HTL)	4-6	- Diesel - Gasoline - RJF - Heavy hydrocarbons

3.2.3.3.1 Gasification pathways

For the gasification process, the ADVANCEFUEL project selected pathways between TRL 5-8. The lower part of the range is caused due to the syngas production technologies. The actual synthesis of the advanced biofuels is responsible for the higher part of the TRL range (Papadokonstantakis, 2018). In addition the process of syngas fermentation is also included, because it shows great potential for the near future (Daniell et al., 2012). First the gasification of the lignocellulosic biomass into syngas (CO & H_2) is explained, after which the various subsequent processes of syngas into liquid synthesis to produce the final products diesel, gasoline, RJF, methanol, DME and ethanol are explained.

The gasification process

There are multiple configuration options to gasifier the lignocellulosic feedstocks into syngas. The configuration type is often determined by the heating configuration which can be direct or indirect and the gasification agent which can be air, steam or a pulverized solid (Tijmensen, Faaij, Hamelinck, & van Hardeveld, 2002). Direct gasification implies that the heat is provided directly within the gasification reactor from combustion of the char and the produced syngas. Indirect gasification (see figure 6) implies that part of the gasification agent is removed together with char, to combust outside the gasification reactor after which the heated gasification agent is brought back to provide heat for the process itself. The type of gasification agent, as well as the type of heating solution have an effect on the syngas composition (H2/CO ratio) and the contaminants like H_2S, NH_3, dust and alkalis (Tijmensen et al., 2002).

Within the gasification process the biomass is heated without air to make charcoal, tar gasses and liquids. The tar gasses and liquids are heated to a high temperature with addition of O_2 and are partly combusted to produce the heat to crack the molecules into H_2 and CO and to produce and increase the amounts of H_2O and CO_2 and other gasses. The last step of reduction converts the highly reactive hot charcoal with the present H_2O and CO_2 to produce extra H_2 and CO (ALL Power Labs, 2019). Then cleaning and conditioning the syngas consists of separating the solid particles and removing the ammonia and sulfer (Hofbauer, Rauch, & Ripfel-Nitsche, 2007). With the use of the water shift reaction the ratio of H_2 & CO can be adjusted for the subsequent gas to liquid synthesis reactions.

The Fisher Tropsch (FT) reactor

The first synthesis option is the Fischer Tropsch (FT) reaction where using a catalytic chemical reaction causes the syngas to convert to hydrocarbons of various molecular lengths. Often the catalyst is iron or cobalt (Tijmensen et al., 2002). The optimal stochiometric ratio for the conversion of H_2 & CO is 2:1 (Iglesias Gonzalez, Kraushaar-Czarnetzki, & Schaub, 2011). The main product is often an FT-wax, naphtha and a distillate. Dependent on the temperature, the catalyst, the pressure and the CO/H_2 ratio, the amounts of the final products can be changed. Within figure 6 it can be seen that for each of final products a different reaction takes place. Both naphtha and the distillate are hydrotreated with the earlier formed H_2 gas to produce gasoline, diesel or RJF. The FT-wax is cracked to also produce gasoline, diesel or RJF. The wax cracking conditions can affect the ratio between the desired output. Since the reaction of FT synthesis is highly exothermic (see formula 11), excess heat can be used for pre-heating the syngas and for steam production, which in turn can provide electricity. Since electricity is also a valuable product output some reactors try to optimize the balance between FT-liquids and power production, while other configurations aim to maximize the fuel production and exclude power production (Tijmensen et al., 2002).

$$CO + 2H_2 = -CH_2- + H_2O \qquad \Delta H = - \text{ kJ/mol} \qquad (11)$$

Although the produced dynamic model included eight different case studies of FT reactors, all having different conversion efficiencies and ratios of produced products, only one was used to create a fair

comparison across the different fuels. The chosen reactor is the PTL 400, combined with a two staged Carbo V gasifier based on the research of van Vliet, Faaij, & Turkenburg (2009). The MC of the feedstock used is 10%, however with the use of formula 6, other feedstocks could also be calculated. The PTL 400 and all other included reactors produce a net surplus of electricity. The required H_2 is produced from the syngas using the water gas shift reaction. It should be noted that the reactors only include diesel and gasoline as produced products, however a 25%/75% split was put on the diesel output, to produce 25% RJF ranged hydrocarbons and 75% diesel ranged hydrocarbons. According to De Jong et al. (2017), this should not impose additional emissions due to the already included distillation step. All included reactors and their efficiencies relative to the main produced product can be found in table 26 of the appendix J.1.

The Methanol reactor

Another product that can be made from syngas is methanol. According to Lücking (2017) the most common technology for the production of methanol is the low pressure catalytic reaction (Lücking, 2017). The catalyst being used is Copper-Zinc Oxide with Aluminium Oxide or Chromium(III) Oxide (Hannula & Kurkela, 2013; Lücking, 2017). These catalysts allows for high selectivity (the amount of desired product against by-products) which reaches 99.9%. The current efficiency of commercial methanol synthesis rectors is 25% per pass conversion, which can be increased to 60% when the products and off-gases are recycled back multiple times to the synthesis reactor (Hannula & Kurkela, 2013). From reaction 12 it becomes clear that the basic reaction is exothermic, thus resulting in excess heat which can be used for pre-heating the syngas and for power production.

$$CO + 2H_2 = CH_3OH \quad \Delta H\ 298K,5MPa = -90.1\ kJ/mol \tag{12}$$

Within the produced dynamic model three different case studies with different configurations were included, which all described an integrated process of gasification and fuel synthesis. To create a fair comparison across the produced fuels, only one reactor was chosen for the calculations, which was based on Hannula & Kurkela (2013). They describe a pressurised fluidised-bed steam/O2-blown gasification reactor followed by a methanol synthesis reactor, which had a 61% energy efficiency based on the main produced product. The heat is internally produced and excess heat is converted to electricity creating a net surplus. The used feedstock was based on forest residues 30%, which is corrected to other feedstocks and MC using formula 5 and 6. The efficiencies of all the reactors can be found in table 27 of the appendix J.1.

The Di-methyl Ether (DME) reactor

The methanol itself is used as a final product, however with the use of subsequent dehydration (see formula 13) of methanol in the presence of a catalyst, DME is made (National Energy technology Laboratory, 2019). Commercially this two-step process is most common, where the methanol is first produced after which the dehydration step takes place (Hannula & Kurkela, 2013). More modern catalysts can perform reaction 12 & 13 simultaneously, however this is currently not commercially available (Hannula & Kurkela, 2013).

$$2CH_3OH = CH_3OCH_3 + H_2O\ \Delta H\ 298K,5MPa = -20.003\ kJ/mol \tag{13}$$

Just as the methanol synthesis, the produced dynamic model included three different case studies with different configurations, which can be found in table 27 of the appendix J.1. The chosen reactor for the calculations was based on Hannula & Kurkela (2013). The same pressurised fluidised-bed steam/O2-blown gasification reactor is used followed by a DME synthesis reactor, which had a 60% energy efficiency based on the main produced product. The heat is also internally produced and excess heat

is converted to electricity creating a net surplus. The used feedstock was also based on forest residues 30%, which is corrected to other feedstocks and MC using formula 5 and 6.

Ethanol reactor

The last product which can be made from syngas is ethanol. This is technically a combination of the thermo-catalytically produced syngas and the biochemical fermentation of the syngas into ethanol. According to Karatzos, Mcmillan, & Saddler (2014) some autotrophic micro-organisms can use CO and CO_2 as carbon sources and the CO and H_2 as energy sources for the conversion. Compared to the biochemical fermentation of sugar into ethanol, this new technique has in theory, a higher yield. This is mainly because within the biochemical conversion only the C5 and C6 sugars are used and the lignin is excluded, whereas the useable carbon content from gasification is higher because the lignin is included in the process resulting in a higher overall yield (Karatzos et al., 2014). Heat that is required during the fermentation step is derived from either the syngas conversion or from syngas combustion.

The used reactor for the dynamic model was based upon the model from the Argonne National Laboratory (2018a). They specify a different conversion efficiency based on the MC of the feedstock. To account for efficiency changes of different feedstocks, the difference in LHV per feedstock type was used for correction. The final reactor efficiencies can be found in table 28 with the corresponding conversion chemicals in table 29 both in the appendix J.1.

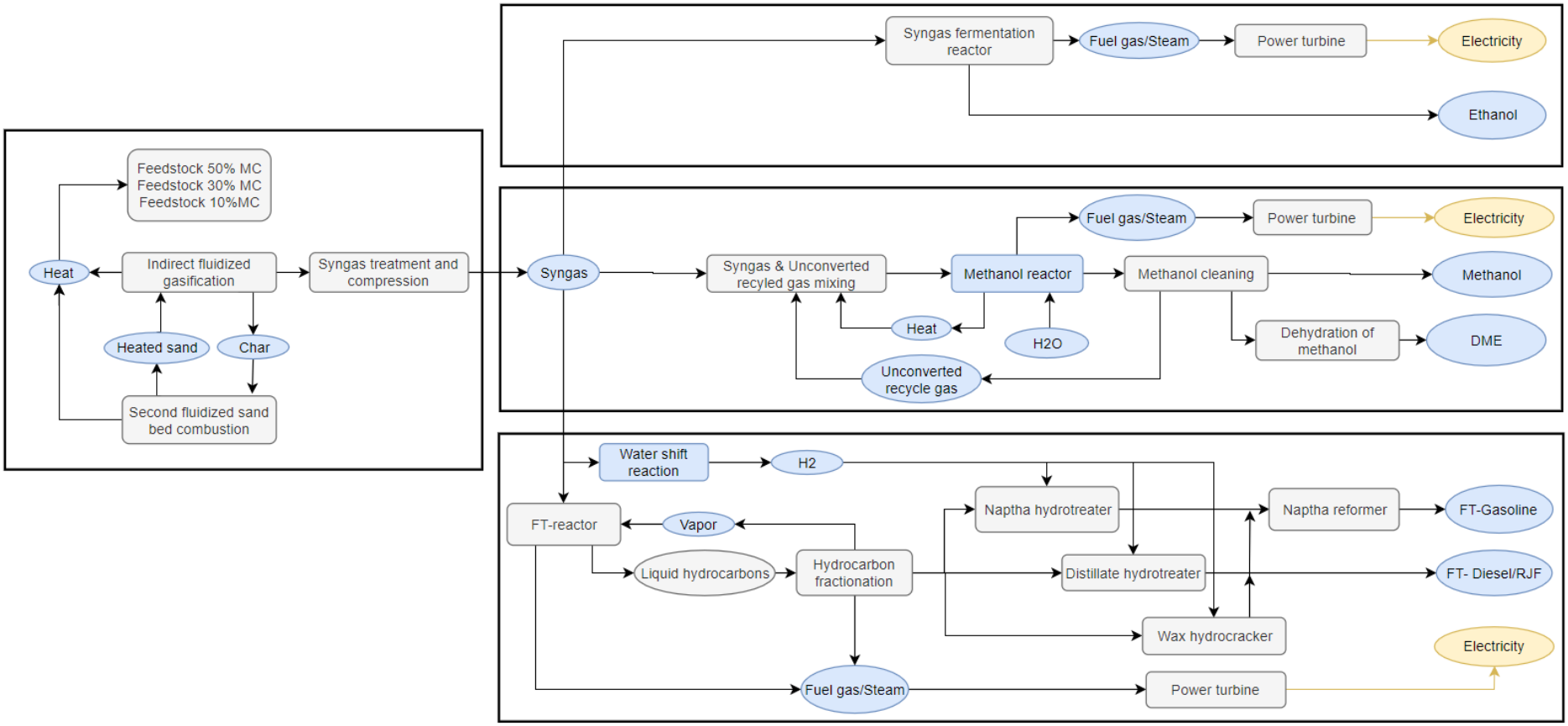

Figure 6 – Schematic representation of syngas production with the additional subsequent fuel synthesis processes (Hannula & Kurkela, 2013; Lücking, 2017; Tijmensen et al., 2002)

3.2.3.3.2 Biochemical pathways

The biochemical pathways that are included in the ADVANCEFUEL project typically have a TRL of 6, where the final product is ethanol. Although the fermentation of sugars into ethanol has a TRL of 8-9, the pre-treatment steps to produce the fermentable sugars from the lignocellulosic material takes up large amounts of energy and chemicals resulting in a lower TRL (Papadokonstantakis, 2018). A subsequent process can also take place in which the produced ethanol itself can be upgraded with the use of H_2 to produce RJF. Since this process is similar to the already existing fossil fuel refineries, the TRL is 8-9 (Karatzos et al., 2014). First the main conversion process to ethanol is explained followed by the subsequent ethanol upgrading process.

Ethanol production

Although the final product is the same, the conversion process often differs in terms of pre-treatment method and type of hydrolysis and fermentation configuration. All pre-treatment methods are done to separate the complex structure of cellulose, hemicellulose and lignin. Zabed et al. (2016) describes various pre-treatment methods, however due to the complexity only pre-treatment technologies given in table 4 with their TRL are included in this research. The mechanical pre-treatment is done to produce feedstock with a lower MC and a higher energy density, which will be done depending on the distance between the feedstock source and the factory gate. Dilute acid or steam explosion however are necessary pre-treatment steps, because they create significant increases in the conversion efficiency. Based on this, two main production routes are included which can be seen in figure 7.

Table 4- TRL of pre-treatment technologies (Papadokonstantakis, 2018; Papadokonstantakis & Johnsson, 2018)

Pre-treatment technologies	**TRL**
Physical Methods	
Mechanical chipping, grinding, milling	8-9
Drying, pelletisation	9
Chemical Methods	
Dilute acid pre-treatment	5-7
Physicochemical methods	
Steam explosion	6-8

After pre-treatment a detoxification step is required due to the generation of by-products during the pre-treatment. These by-products can act as inhibitors for the enzymes and fermenting micro-organism within the subsequent steps. By-products include sugar acids, formic acid, acetic acid, levulinic acid and furfural. These inhibitors are reduced by various approaches including the addition of chemicals, enzymatic treatment or extraction (Nanda, A. Kozinski, & K. Dalai, 2015; Nanda, Mohammad, & Reddy, 2014; Zabed, Sahu, Boyce, & Faruq, 2016).

Within the hydrolysis step the cellulose and hemicellulose are hydrolysed and converted to fermentable sugars. Cellulose mainly consists of glucan which is converted to glucose and hemicellulose consist mainly of xylan and is converted xylose. This can be done via acid hydrolysis which requires either a low or high temperature and pressure depending on the concentration of the acids. The hydrolysis can also be enzymatic, in which micro-organisms produce enzymes that hydrolyse the glucan and xylan. For this research only enzymatic hydrolysis is included. Next to the type of hydrolysis, the configuration related to the fermentation can also differ. Two main types are separate hydrolysis and fermentation (SHF) or simultaneous saccharification and fermentation (SSF) (Papadokonstantakis & Johnsson, 2018). The prior configuration often has a lower conversion efficiency compared to the latter, due to higher glucose accumulation and thus enzyme inhibition. The use of the SSF configuration can create another benefit of reducing equipment costs

(Papadokonstantakis & Johnsson, 2018). This research includes the configuration of the Argonne National Laboratory (2018a), which uses SSF with dilute acid pre-treatment, while Wang, Littlewood, & Murphy (2013) uses SHF with steam explosion. Both configurations are included within this research ((Nanda et al., 2015; Papadokonstantakis & Johnsson, 2018; Zabed et al., 2016).

After the hydrolysis, the glucose and xylose are fermented to produce the ethanol. The most common method is the submerged fermentation, in which water acts as a medium in which the micro-organisms can ferment the sugars. The last step is the broth distillation, where the alcohol is evaporated and distilled (Nanda et al., 2015; Zabed et al., 2016). The fermentation reactions equations 14 until 17 are shown below.

$C_6H_{12}O_6$ (Glucose) = $2C_2H_5OH + 2CO_2$ (14)

$3C_5H_{10}O_5$ (Xylose, arabinose) = $5C_2H_5OH + 5CO_2$ (15)

$C_{12}H_{22}O_{11}$ (Cellobiose) + $H_2O = 5C_2H_5OH + 5CO_2$ (16)

$3C_{10}H_{18}O_9$ (Xylobiose) + $3\ H_2O = 5C_2H_5OH + 5CO_2$ (17)

The total process requires heat for the pre-treatment steps as well as the hydrolysis, fermentation, and broth distillation. This heat can either be provided by NG boilers, however within the used case studies, the separated lignin is combusted and is used to fuel the various conversion processes and to produce a surplus of electricity (Argonne National Laboratory, 2018a; Mu, Seager, Rao, & Zhao, 2010; M. Q. Wang et al., 2011). The case study from the Argonne National Laboratory (2018a) used multiple conversion efficiencies based on the LHV_{dry} of the different feedstocks. The required conversion chemicals were also specified based on the type of feedstock. The case study of M. Q. Wang et al. (2011) was based upon straw as feedstock. The conversion efficiency correction to other feedstocks was based upon the LHV_{dry} of the feedstocks. Both reactor efficiencies can be found in table 30 and 33 of the appendix J.2. The conversion chemicals can be found in table 32 and 34 of appendix J.2.

Ethanol upgrading to RJF

Although the ethanol upgrading to RJF is a thermochemical process and not a biochemical production process, because it uses the biochemically derived ethanol as a feedstock, it can be thought of as a hybrid production route. Karatzos, Mcmillan, & Saddler (2014) describe that the process is relative simple due to resemblance of the already existing refinery technologies including dehydration, oligomerization and hydrogenation as seen in figure 8. The first step removes the water from the ethanol, after which the oligomerization process synthesises the long chain molecules. With the use of H_2, the large molecules are separated as well as the removal of double bonds in the last step (Antonissen, 2016). The main challenge lies in making the process economically viable due to the usage of electricity and hydrogen, making it an energy intensive process. The included external H_2 production technologies and their corresponding energy sources are explained in section 3.2.3.4. Within this research the ethanol upgrading to RJF is seen as a subsequent upgrading process of the dilute acid pre-treatment and fermentation of ethanol. This process of ethanol production is used because it is currently most common and economic feasibly (Nanda et al., 2014). The used reactor is based upon De Jong et al. (2017), which used the model developed by the Argonne National Laboratory (2018a). The upgrading efficiency can be found in table 35 of the appendix J.2.

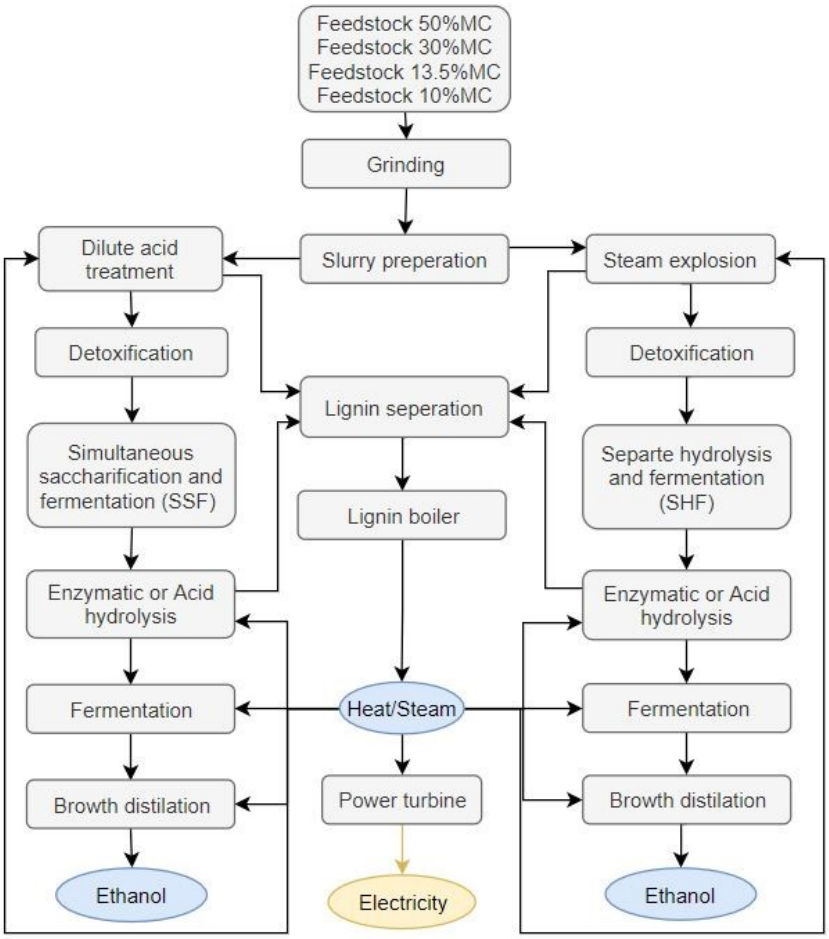

Figure 7 – Schematic representation of biochemical pathways (Nanda et al., 2014; Zabed et al., 2016)

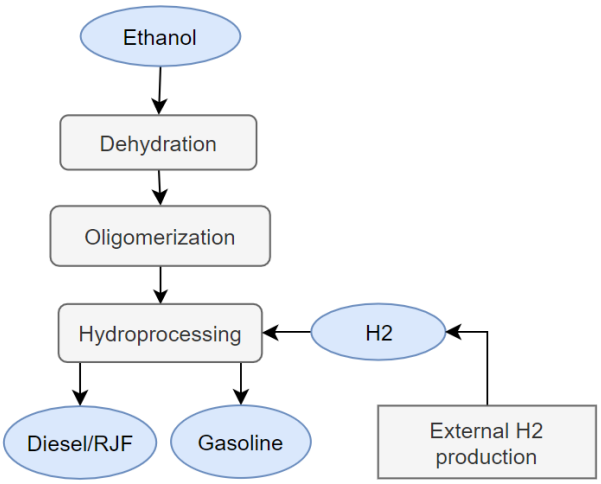

Figure 8 – Schematic representation of ethanol upgrading to RJF (Karatzos et al., 2014)

3.2.3.3.3 Thermochemical pathways

The included thermochemical conversion process based on the ADVANCEFUEL project is pyrolysis, which has a TRL of 4-6. The conversion process into pyrolysis oil has a TRL of 6, however the upgrading process into gasoline, diesel, RJF has a lower TRL of 4-5 due to the high contamination and high viscosity of the oil (Papadokonstantakis, 2018). Another thermochemical conversion process, which is not included in the ADVANCEFUEL project, is HTL. This conversion technology has a TRL of 4-6 due to the high feedstock flexibility and a lower and less intensive energy upgrading process (Castello, Haider, & Rosendahl, 2019). Both conversion processes are similar to a certain extent, however due to specific MC requirements of different feedstocks as well as the MC and oxygen levels of the final bio-oil produced, they are explained separately.

Thermochemical pyrolysis

Thermochemical pyrolysis is defined by Kan, Strezov, & Evans (2016) as: " The thermal decomposition of the biomass organic matrix in non-oxidising atmospheres resulting in liquid bio-oil, solid biochar, and non-condensable gas products''. Parameters during the pyrolysis like heating rate and residence time results in different ratios between the aforementioned intermediate products. Flash- and fast-pyrolysis, which uses a fast heating rate and low residence time, result in a high yield of bioliquids and a low yield of char (Kan et al., 2016). Slow or conventional pyrolysis, with a longer residence time and a lower heating rate, results in mainly biochar and less bioliquids. For the production of the fuels included in this research fast pyrolysis is the preferred choice because of the high bio-liquid ratio (Kan et al., 2016).

The production process can be seen in figure 9 and is based upon Tews et al. (2014). It is essential that the MC of the feedstock is low (10%wt) before entering the pyrolysis reactor, due to the negative effect of moisture on the heating value of the produced bio-oil. Even with a low MC of 10%, the bio-oil produced has a MC just below 30% (Karatzos et al., 2014). Another problem is the high oxygen content of 30%. The high concentration of both is eliminated during the hydrodeoxygenation step. Next to the bio-oil, also solid biochar is produced which is removed from the reactor and is fed into a char boiler to provide heat for the drying of the feedstock. The off-gases from the pyrolysis reactor can be used for drying of the feedstock and for H_2 production which is needed for the subsequent hydrodeoxygenation and hydrocracking step. In figure 9 the H_2 is produced internally from the off-gases, however another option is using the off-gases for power production resulting in a net surplus of electricity and producing the H_2 externally which can be seen in figure 10. Regardless of the aforementioned configurations, the same bio-oil is produced which needs to be upgraded using a hydrodeoxygenation step for oxygen removal to less than 2% and a hydrocracking step with H_2 to create the desired lengths of the final products (Antonissen, 2016; Kan et al., 2016; Tews et al., 2014). Based on the amount of H_2 introduced together with the temperature and pressure, the ratios of the final products can be altered.

The included reactors within the produced dynamic model, are based upon the case study of Tews et al. (2014) or De Jong et al. (2017). To create a consistent comparison between the fuels, the case study described by Tews et al. (2014) is used for the results, which describes a configuration with internal H_2 production and wet feedstock as input. Because the H_2 production takes up a large share of energy, a second configuration of external H_2 production was added, just as figure 10, to identify the effect on the total GHG emission value. The electricity input of the H_2 reformer was subtracted from the total electricity use and the total amount of off-gasses was used to drive a steam turbine for electricity production. Because the described reactor only used 30% MC as feedstock, a third configuration was added with the exclusion of the pre-treatment technology. This was assessed by using all the extra heat normally being back-channelled to the dryer, instead used in the same steam turbine for extra

electricity generation. The electricity generator efficiency can be found in table 23 of appendix H. The external H_2 can be produced with the technologies and their corresponding energy source described in section 3.2.3.4. The correction of reactor efficiency for different feedstocks is based on the corresponding LHV_{dry} of the feedstocks. The difference in MC is corrected for with the inclusion or exclusion of the pre-drying step. Just as the FT reactor the used case study only included diesel and gasoline as produced products, however the same 25%/75% split was put on the diesel output, to produce 25% RJF and 75% diesel ranged hydrocarbons. All conversion efficiencies, relative to the main produced product, of the different configurations can be found in table 36 of appendix J.3.

Hydrothermal liquefaction (HTL)

HTL also produces bio-oil just as pyrolysis, however the bio-oil produced has a lower O_2 content of 5-20% compared to the 30% of pyrolysis. Another difference is the MC of the feedstock which can be up to 50% (Karatzos et al., 2014). The process starts with high pressure water injection to produce a slurry, after which it is pressurised and heated up to start the HTL reaction. The off-gasses can be used to provide heat for the HTL process. Just as the pyrolysis process, H_2 can either be produced integrated with the use of the off-gasses or produced externally. The process diagrams can be seen in figure 6 and 7 respectively. In both figures the same bio-oil is produced which only needs hydrocracking with H_2 to create the desired lengths of final products and needs little or no hydrodeoxygenation due to already low oxygen content. The result of this effect is a lower requirement of H_2 in the upgrading process compared to pyrolysis, making the process overall more efficient (Karatzos et al., 2014; Tews et al., 2014).

The included reactors within the produced dynamic model, are based upon the case study of Tews et al. (2014) or De Jong et al. (2017). Again to create a consistent comparison between the fuels, the case study described by Tews et al. (2014) is used for the results. This configuration is based upon using wet feedstock and internal H_2 production. Therefore the same second configuration as within the pyrolysis process was calculated, in which the energy for internal H_2 production was used for electricity production and the H_2 production was made an external process. The external H_2 can again be produced with the technologies and their corresponding energy source described in section 3.2.3.4. The pre-treatment drying step could not be excluded since HTL relies upon wet feedstock. Again the correction of reactor efficiency for different feedstocks is based on the corresponding LHV_{dry} of the feedstocks. Just as within the pyrolysis reactor 25%/75% split was put on the diesel output to produce 25% RJF ranged hydrocarbons and 75% diesel ranges hydrocarbons. All conversion efficiencies, relative to the main produced product, of the different configurations can be found in table 37 of appendix J.3.

3.2.3.4 External hydrogen production

The processes of ethanol upgrading, pyrolysis and HTL have configurations in which externally produced H_2 is required. Since H_2 production is an energy intensive process, the type of production method and the corresponding energy source can greatly affect the total GHG emission value of the conversion processes. Most common H_2 production method is Steam Methane Reforming (SMR), where NG is reacted with steam to produce syngas. Additional H_2 is formed with the water shift reaction (Mehmeti, Angelis-Dimakis, Arampatzis, McPhail, & Ulgiati, 2018). Electrolysis is another method, which uses electricity and water to split the water molecules into H_2 and O_2. Different kinds are Proton Exchange Membrane electrolysers (PEM) or Solid Oxide Electrolysis Cells (SOEC) (Mehmeti et al., 2018). These are currently the most common industrialized electrolysers, with the latter having an overall higher efficiency (Mehmeti et al., 2018). Both fossil and renewable electricity configurations are included as energy source for the electrolysers. The emission factors of the H_2 production energy sources can be found in table 21 of appendix H.

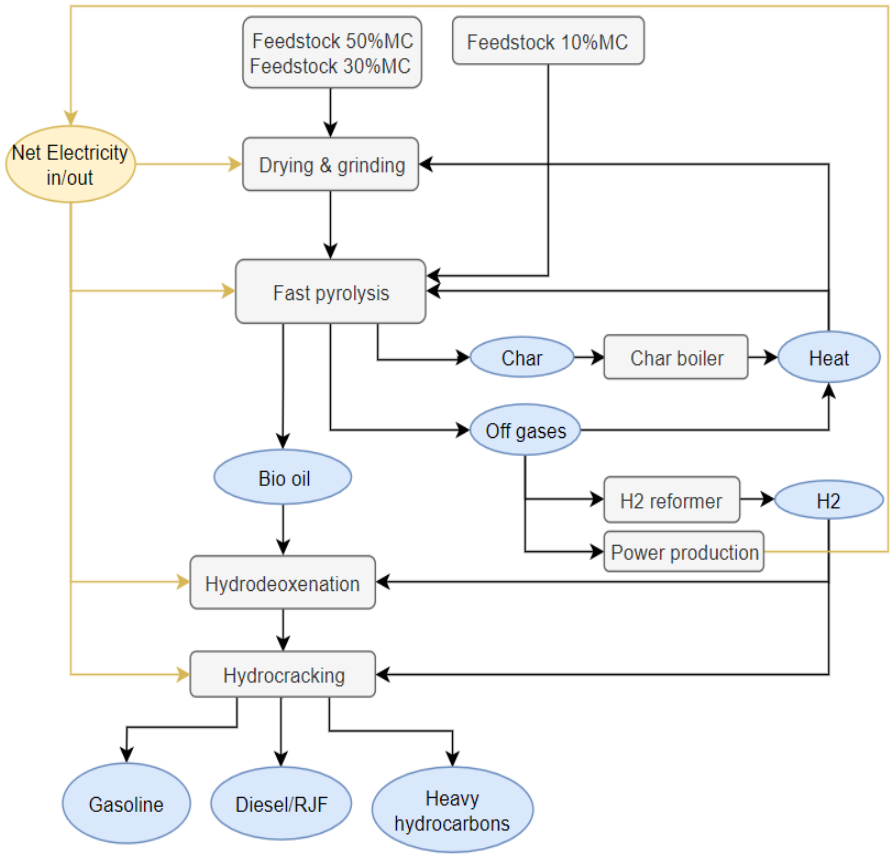

Figure 9 – Schematic representation of thermochemical pyrolysis with internal hydrogen Production (Antonissen, 2016; Kan et al., 2016; Karatzos et al., 2014; Tews et al., 2014)

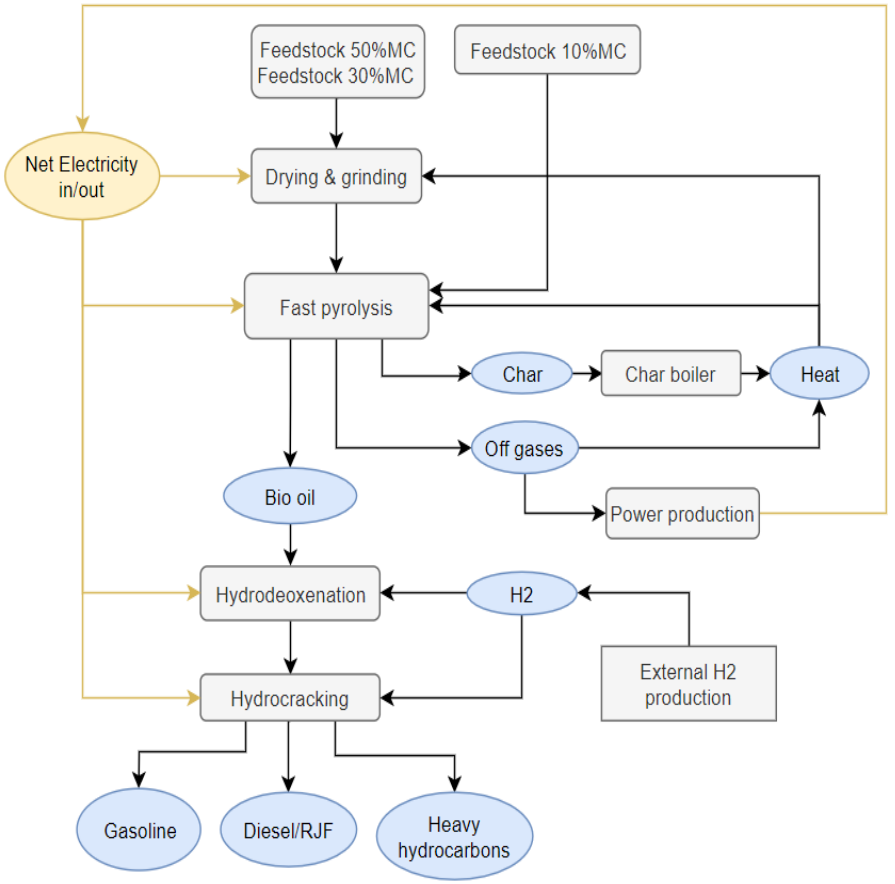

Figure 10 - Schematic representation of thermochemical pyrolysis with external hydrogen production (Antonissen, 2016; Kan et al., 2016; Karatzos et al., 2014; Tews et al., 2014)

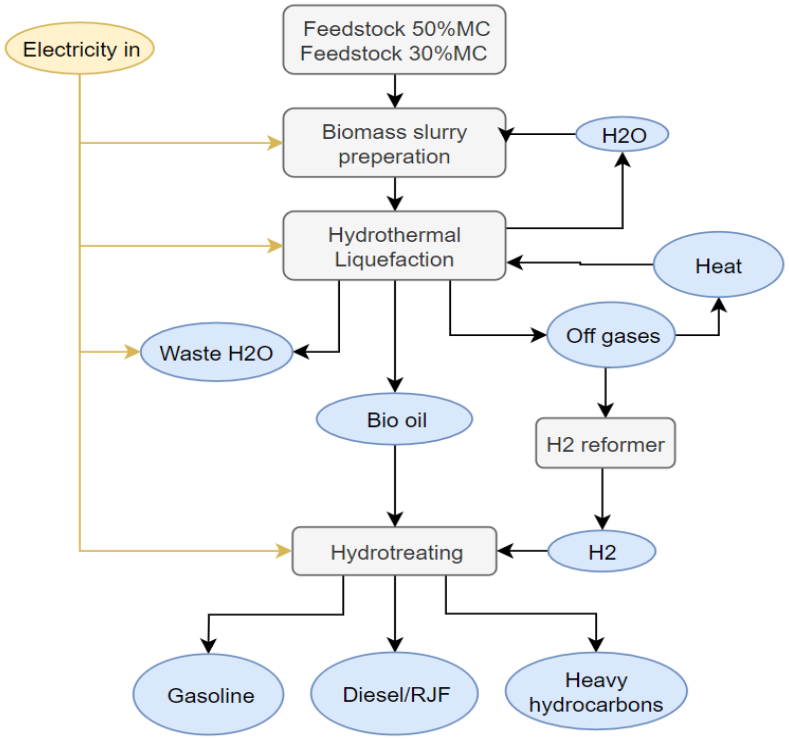

Figure 11 - Schematic representation of hydrothermal liquefaction (HTL) with internal hydrogen production (Antonissen, 2016; Kan et al., 2016; Karatzos et al., 2014; Tews et al., 2014)

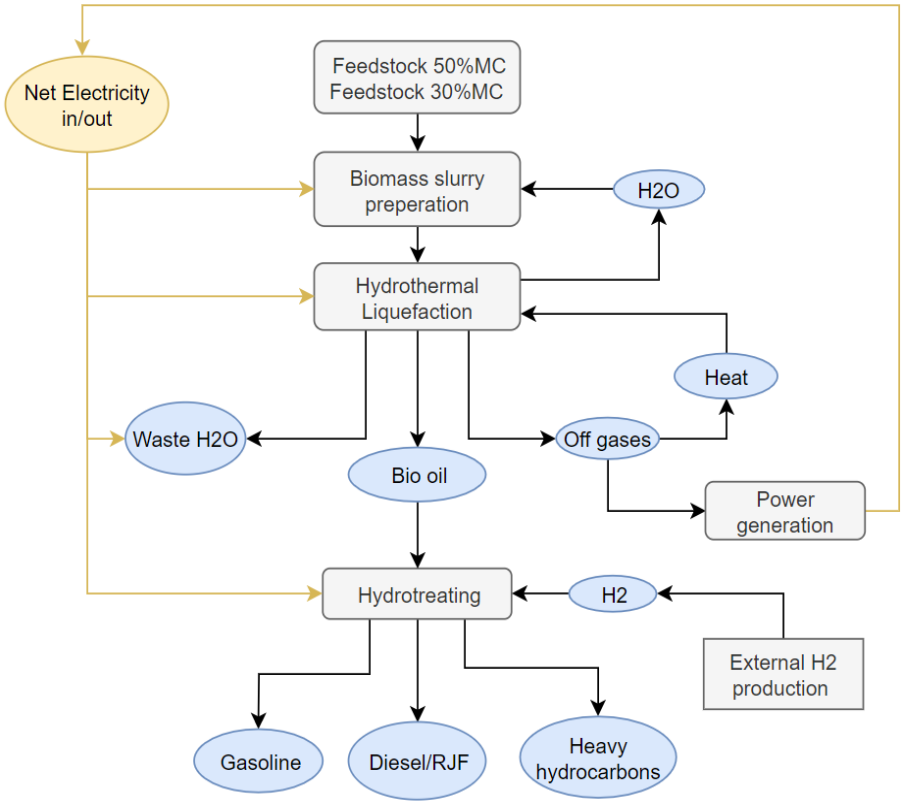

Figure 12 - Schematic representation of hydrothermal liquefaction (HTL) with external hydrogen production (Antonissen, 2016; Kan et al., 2016; Karatzos et al., 2014; Tews et al., 2014)

3.2.4 Transport and distribution

The fourth sign e_{td} represent the emissions allocated to the transport and distribution. These emission take place between the cultivation and extraction of the feedstocks and between or after the multiple processing steps. The amount of emissions allocated to the transport relies upon the type of transport, the type of feedstock that is being transported and the distance covered. For each vehicle the fuel use is calculated in terms of energy per tonne load travelled over 1 km (MJ/t*km). The value also accounts for the empty return journey of the vehicle thus increasing the fuel use per tonne of cargo, as can be seen in formula 18.

$$Fuel\ use\ \left(\frac{MJ}{t*km}\right) = \frac{\left(\frac{Fuel\ use\left(\frac{L}{100km}\right)}{100}\right)*Energy\ desity\ \left(\frac{MJ}{L}\right)}{Payload\ (t)} * 2 \quad (18)$$

Multiplying the fuel use with the corresponding emission factors related to the used transport mode, results in the total emissions per tonne cargo per km or $gCO_2eq/t*km$. Then using formula 19 the total emissions per $MJ_{product}$ can calculated.

$$Emissions\ \left(\frac{gCO2eq}{MJproduct}\right) = (Fuel\ use * Payload * Distance)/(Actual\ payload * LHVproduct * 1000 * (1 - MCproduct)) \quad (19)$$

Most of the data collection was based upon the report of Edwards et al. (2019) and Giuntoli et al. (2017) as well as the existing Biograce 1 & 2 databases. The report of Giuntoli et al. (2017) made extensive calculations regarding the maritime transportation ships, using the second and third report made by the International Maritime Organization to account for averages of fuel usage between different regions of the world and accounting for partial or full load capacity on the return journey (Buhaug et al., 2009; IMO, 2015). The used values can be found in table 20 of appendix G.

The chosen distances from cultivation until the conversion plant gate are chosen in line with the report of Giuntoli et al. (2017) having four grades of distances. Table 5 displays the distances of the woodchip production and table 6 the distances travelled for the wood pellet production. The 500 km distance represent European supply chains, whereas the 2500km, 10000km or 17500 represent global supply chains. Depending on the MC and the density of the feedstock, the right type of transportation mode is chosen, for example a truck for pellets or a truck for woodchips. After the conversion plant the fuel is distributed which can be seen in table 7.

Table 5- Standardized transport distances of woodchip production pathways and their characteristics (Giuntoli et al., 2017)

Woodchips transportation distance	Woodchip truck	Pellet truck	Diesel train	Supramax woodchips Ship	Location
500km	500 km				Intra EU
2500km	250 km			2000 km	Russia
10000km	200 km			8000 km	Brazil
17500km	200 km		750 km	16500 km	Western Canada

Table 6 - Standardized transport distances of woodchip production pathways and their characteristics (Giuntoli et al., 2017)

Wood pellets transportation distance	Woodchip truck	Pellet truck	Diesel train	Supramax wood pellets Ship	Location
500km	50 km	500 km			Intra EU
2500km	50 km	250 km		2000 km	Russia
10000km	50 km	200 km		8000 km	Brazil
17500km	50 km		750 km	16500 km	Western Canada

Table 7- Fuel distribution characteristics

Fuel distribution transportation distance	Truck (Truck for liquids)	Truck	Train	Ship	Location
Local (50km)	50 km				Local use

3.2.5 Fuel in use

The fifth sign e_u represents the emissions allocated towards the fuel in use. First the different fossil based fuels for road and aviation market are shortly elaborated and how the corresponding advanced biofuels can be introduced and implemented as drop-in fuels or alternatively, if slight modification to the engines have to be made, after which the possible emissions due to implementation can be calculated.

3.2.5.1 Road fuels blending possibilities

Road transport is currently dominated worldwide by gasoline and diesel, both derived from petroleum fuel oil. Within the (EC, 1998)b specific fuel standards for the petroleum derived gasoline and diesel have been set, primarily based on the methods from the American Society for Testing and Materials (ASTM). Because of a change in composition of biochemical or synthetically produced biofuels, certain caps on blending ratios have to be set to account for differences of injection and combustion properties as well as safety and health aspects (Kampman et al., 2013).

Therefore looking at gasoline, maximum amounts of blending with ethanol are in place, to which most types of gasoline cannot exceed 5-15% volume. These fuels are classified as E5 or E10 or E15 gasoline, where the E-number reflects the percentage of ethanol blending. Kampman et al. (2013) concluded that higher blend ratios of E20 or E30 are possible for Europe, however the vehicles themselves need to be altered. The synthetically produced gasoline from the gasification process or the thermochemical process can also be blended up to 30% (Kampman et al., 2013). The blending of diesel with biocomponents like Fatty Acid Methyl Esters (FAME), excluded from this research, is currently possible up to 7%. Hydrotreated vegetable oil (HVO), also excluded from this research, can be added up to 30% making B30 (Kampman et al., 2013). The blending capacity of 30% is also applicable for the synthetically produced diesel made from the gasification or the thermochemical processes.

Flexible fuel vehicles can increase the blending ratios with gasoline to a point where E85 and E100 (85% ethanol or 100% ethanol) are possible for spark ignition vehicles and M85 (85% methanol blended with 15% diesel) or M100 (100% methanol) for compression ignition engines (Kampman et al., 2013). Next to methanol, the diesel can also blended with ethanol up to 15%. Another 100% replacing fuel for diesel is DME (Kampman et al., 2013; Papadokonstantakis & Johnsson, 2018). Next to flexible fuel vehicles it also possible to modify the vehicles so that they can cope with 100% synthetic produced fuels however it is likely that blending the fuels will be the first step, since full modification is not likely to happen due to large complexity of retrofitting the current road fleet (Kampman et al., 2013).

3.2.5.2 Aviation fuel blending opportunities

The aviation transport sector is currently dominated by fossil based kerosene. The RJF can be blended into the fossil based kerosene, however to which extent depends on the conversion process. The produced RJF needs to be certified by the ASTM. The main reasons for strong regulations regarding the blending of RJF is the high amount of technical and safety requirements of the fuels. Some examples are low freezing point, low sulphur, water and oxygen content (SkyNRG, 2019). Currently RJF from FT, ethanol upgrading, Direct sugars to hydrocarbons (DSHC), Hydrotreated esters and fatty acids (HEFA) and Synthesized iso-paraffins (SIP) are ASTM certified. The RJF from pyrolysis and HTL are currently under review (De Jong et al., 2017; SkyNRG, 2019).

Table 8- ASTM certified RJF's and allowed blending ratio's (De Jong et al., 2017; SkyNRG, 2019)

Type of conversion	Max blend ratio
Fischer-Tropsch (FT)	50%
Ethanol upgrading	50%
Direct sugars to Hydrocarbons (DSHC)	50%
Hydrotreated esters and fatty acids (HEFA)	50%
Synthesized iso-paraffins (SIP)	10%

3.2.5.3 Emission calculations based on blending ratios

From the previous two sections it becomes clear that multiple blending ratios occur depending on the end market as well as the type of fuel and vehicle used. This means that dependent on these factors the emissions due to the fuel in use can differ greatly. However the FU was chosen to be gCO2eq/MJ of advanced biofuel produced, therefore the actual emissions caused by the fossil fuel part of the blended fuel mix are automatically excluded from the calculation. Additionally the emissions causes by the biofuel part of the blended fuel are categorized as biogenic carbon, which can therefore be counted as zero. This means that within the produced dynamic model, the fuel in the use phase or TTW phase is always zero.

3.2.6 Emission savings due to improved agricultural management.

The sixth sign e_{sca} allocates possible emission savings from carbon accumulation within the soil due to improved agricultural management. The improved agricultural management is a part of the LUC calculations, because it assesses the carbon stock changes within the soil over time. The difference is that within this section, the type of feedstock stays the same and only the SOC is calculated. Within the LUC section next to the SOC, the changes in vegetation (below and above ground, dead and alive) are also calculated. When the LUC effects are added within the dynamic model, this section becomes obsolete. For the same reason described in the LUC section, no actual emissions will be added or subtracted due to the high dependence on varying input values.

3.2.7 Emission savings due to CO_2 capture and storage

The seventh sign e_{cc} represent the allocation of emission savings due to CO_2 capture and storage. This means that carbon that is captured during cultivation, transport or processing that has not been accounted for within the phase itself, can reduce the total GHG emissions of the fuel. When more biogenic carbon is captured (during the combustion phase for example), compared to the total GHG emissions, a net negative GHG emission value is possible. This research does not account for CO_2 capture however it is possible to include actual values in the produced dynamic model.

3.2.8 Emission savings due to CO_2 capture and replacement

The last sign e_{ccr} represents the allocation of emissions savings due to CO_2 capture and replacement. The CO_2 can be used within the industry for many purposes. In a reference situation the CO_2 would be produced using fossil fuels. The savings are due to the fact that CO_2 produced that originates from biogenic biomass does not create additional emissions, whereas the CO_2 produced from fossil fuels does. This research does not account for CO_2 capture and replacement however it possible to include actual values in the produced dynamic model.

3.3 Impact assessment

The impact assessment combines all data from the inventory assessment to create the final impact category GHG emissions. Within this research the impact category GHG emissions was assessed using the standard GWP_{100} defined by the IPCC fourth report, which is in line with the RED-II (European Parliament, 2018; International Panel Climate Change, 2016). The formula and explanation can be found in section 2.2.3.1 of the theory. The GWP of each of the phases of the inventory analysis is summed up to create a total GHG emission value for each of the chosen supply chains. As stated before, the total GHG emissions are allocated to the main product produced based on energy allocation.

3.3.1 The digital appendix & chosen supply chains

This research focusses on multiple feedstocks and multiple conversion technologies which both have multiple sub-categories of choice each. This resulted in a large variety of possible supply chains. Within figure 26 of the appendix K a schematic representation is given of the possible choices and sub-choices within each phase. It was found that there were many different options of creating complete supply chains. A digital appendix was therefore created, in which the total GHG emissions based on energy allocation, mass allocation, economic value allocation and the displacement method of all possible combinations were calculated.

Within the digital appendix all supply chains can be analysed in detail with the use of filtering on a certain feedstock, MC, transportation distance, conversion process or a type of fuel produced. Although the digital appendix contains a large data set, it is hard to analyse what important variables make up the total GHG emission, thus making the research questions hard to answer. To accommodate this problem and to provide clear answers with visual results to the research questions, only a small amount of supply chains was analysed.

The first step was to provide a range of the final GHG emissions of the included conversion processes. This was done by using the best performing feedstock (with the lowest emission value) compared to the worst performing feedstock. Additionally the lowest transportation distance was added together with the highest transportation distance, which combined created a final emission range to which all specific supply chains would fall into. It should be noted that different reactors case studies as well pelletisation upstream in the supply chain were excluded from this range.

To break down this range, several variables were altered to find the effect of each. The alteration of each variable induced a change in the final GHG emissions, which in turn directly relates to the research questions. The following effects were analysed:

- The effect of different feedstocks (Forest residues 30%MC, SRC eucalyptus 30%MC, SRC Poplar WF 30%MC and Miscanthus 13.5%MC) on the same distance of 500km.
- The effect of different transport distances (500km, 2500km, 10000km and 175000km) on the same feedstock (Forest residues 30%MC).
- The effect of the same feedstock (Forest residues 10%MC pelletized upstream in the supply chain) on different transport distances (500km, 2500km, 10000km and 175000km).
- The effect of using different H_2 production technologies and their energy sources (Internal biomass gasification, SMR, PEM electrolyser and SOEC using EU average electricity mix or renewable electricity) on one feedstock (forest residues 30%MC) on the same distance of 500km.

The feedstock forest residues 30%MC transported over 500km was chosen as a standardized supply chain (as baseline) to analyse all the other effects and to create a fair comparison across the results. A substantiation for this choice was that most case studies used for the conversion reactors used forest residues as feedstock input, therefore making it a reliable feedstock in terms of conversion efficiency. All effects of the four variables were analysed and described in a separate section, in which all the different fuels produced were compared across each other. Additionally the comparison to the fossil fuel counterpart was made as well as the 65% GHG emission reduction thresholds defined in the RED-II.

3.3.2 Case studies

Next to the analysis of the different variables behind the GHG emissions described above, which only focused on a standardized feedstock and standardized distances, a second results section focusses on applying supply chains to the real world with the use of four realistic case studies.

The conversion plant is situated in the harbour of Rotterdam, since this could be a strategic place due to easy accessibility for biomass supply as well as distribution of the biofuels. West Canada was chosen for the international supply of forest residues, because currently they already provide a large share of wood pellets for the co-firing power plants within the Netherlands (PricewaterhouseCoopers et al., 2017). Additionally Canada has a high share of forest residues that is exported annually (1.06MToe/y)[4] with a high certainty that this will continue until 2030, due to the large availability and rising domestic production market (PricewaterhouseCoopers et al., 2017). The export of biomass from the south east of the United States (US) is significant (4.11MToe/y), however it is expected to reduce between 2020-2030 due to the rise in demand of domestic biomass use . However the export of commercial thinning's and forest residues into pulpgrade stemwood will likely still continue due to the large availability (PricewaterhouseCoopers et al., 2017). The third international supply chain is based bagasse, which currently is only exported on a large scale (0.37Mtoe/y) from Brazil (PricewaterhouseCoopers et al., 2017). The last supply chain is European, where various countries could be chosen. Bretagne in France was chosen due to the already existing SRC willow plantation (Dimitriou & Rutz, 2015). The feedstocks and the locations with corresponding distances and transportation modes can be seen in table 9. The electricity mix and corresponding emission factors are based on the location on which the activity takes place, which can be found in table 16 of appendix D.

Table 9- Chosen studies and their characteristics

Case studies	Cultivation location	Port	Woodchip truck	Pellet truck	Diesel train	Supramax wood pellets Ship	Processing location	Distribution	Source
1a. Forest residues 30%MC from west Canada	British Columbia	Vancouver	100km		500km	16038km	Rotterdam	50km	(PricewaterhouseCoopers et al., 2017)
1b. Forest residues 10%MC from west Canada	British Columbia	Vancouver	50km	50km	500km	16038km	Rotterdam	50km	
2a. Pulpgrade stemwood 30%MC from south east US.	Mississippi	New Orleans	250km			8785km	Rotterdam	50km	
2b.Pulpgrade stemwood 10%MC from south east US	Mississippi	New Orleans	50km	200km		8785km	Rotterdam	50km	
3. Bagasse 10%MC from Brazil	Near Santos	Santos		364km		10056km	Rotterdam	50km	
4.a SRC willow 30%MC from Bretagne France	Bretagne France		300km		300km		Rotterdam	50km	(Dimitriou & Rutz, 2015)
4b. SRC willow 10%MC from Bretagne France	Bretagne France		50km	250km	300km		Rotterdam	50km	

[4] MToe stands for millions of tons of oil equivalent, which converts to $4.1868*10^{16}$ J or 41868 PJ (Engineering ToolBox, 2003)

3.3.3 The sensitivity analysis

The last section of the results is the sensitivity analysis, which consists of two separate parts. The first part assessed the effect of using different methods of dealing with multifunctionality. The second part assessed the effect of changing important input variables of the case studies including reactor efficiency, nitrogen use and H_2 production energy source.

3.3.3.1. Impact of different methods of dealing with multifunctionality

As described before, the RED-II calculation methods rely on using an ALCA with energy allocation to account for multiple product outputs. Although this research also based all assessments on energy allocation, the impact of applying other allocation methods were also assessed including mass and economic value allocation. Additionally the consequential displacement theory was assed, however only the displaced emissions are accounted for with the exclusion of other indirect effects like social development or market dynamics. The formulas used were described in section 3.2.3.2 . Due to the complexity, these methods are only applied to the standardized supply chain of 3.1.1 which consists of forest residues 30%MC transported over 500km.

3.3.3.2 Impact of reactor efficiency, nitrogen use and hydrogen energy source

This part of the sensitivity analysis acts as a robustness test of important input variables on the results of the case studies. Several variables could affect the total GHG emissions of the case studies. However this part analysed the input values that have high uncertainty or that could affect the total GHG emissions with a significant amount. The analysis was applied to case study 1b, 2a, 3 and 4a. It was chosen to see what the effect was on changing the values of three different elements: The nitrogen use during cultivation, the H_2 production energy source and the conversion efficiency of the reactors. The change in feedstock does not apply, since the case studies have fixed feedstocks. The change in transportation distance also does not apply, since the distances are fixed in the case studies.

Within table 10 a lower pessimistic value and a higher optimistic value of the reactor efficiencies are given. Most reactor efficiencies are likely to increase in the future, therefore making the upper value higher than the lower value compared to the baseline. This is substantiated by the likelihood of the technological development of a chosen conversion process. For the fertilizer use, an assumption was made to see what the effect was of +/- 20% use. The change in H_2 production energy source is based on the included production processes and their corresponding fuels as described in section 3.2.3.4.

Table 10-Input values for sensitivity analysis

		Reactor efficiency		**Fertilizer use**		**Source**
Diesel & Gasoline & RJF	FT	76%	129%	80%	120%	(Antonissen, 2016; De Jong et al., 2017)
	HTL H2 in	71%	142%	80%	120%	
	HTL H2 ex	71%	142%	80%	120%	
	Pyr H2 in	71%	161%	80%	120%	
	Pyr H2 ex	71%	161%	80%	120%	
DME	Gas & Synth.	84%	116%	80%	120%	(Hannula & Kurkela, 2013)
Met.	Gas & Synth.	84%	116%	80%	120%	
Ethanol	Steam exp.	85%	115%	80%	120%	(Mu et al., 2010; L. Wang et al., 2013)¦
	Dil. Acid	85%	115%	80%	120%	
	Gas & Ferm.	70%	130%	80%	120%	(Argonne National Laboratory, 2018b)
RJF	EtOh Upgr.	95%	105%	80%	120%	(Antonissen, 2016; De Jong et al., 2017)

4 Results

The results section consists of three part, the first part presents the results of the four variables regarding the effect of feedstock types and feedstock supply chains, the effect of transportation distance, the effect pelletization and the type of H_2 production energy source. The second part presents the results of the case studies. The third part presents the results of the sensitivity analysis in which the impact of using different methods of dealing with multifunctionally is assed as well as the effect of changing reactor efficiency, nitrogen use and H_2 production source on the case studies.

4.1 GHG lifecycle emissions of different advanced biofuel supply chains

Figure 13 represent the possible range of the total GHG emissions of the selected advanced biofuel supply chains following the RED-II calculation method. The ranges are results of possible variations in feedstock types, feedstock supply chains and transportation distances. It can clearly be seen that most supply chains can reach the RED-II GHG saving threshold, except the process of pyrolysis with SMR made H_2. Generally, if the used feedstock is a residue and supplied from local sources, the final GHG emission is low (see base case figure 13). The GHG emissions increase when dedicated energy crops are used as feedstocks or when the transportation distance is increased. Also feedstock pre-treatments like pelletisation can increase or decrease the GHG emissions. Although each of these elements is described within the upcoming sections, a first finding can already be made based on figure 13.

The FT fuels, DME and methanol all have the possibility to have a very low emission value (< 8 CO_2eq/MJ fuel) reaching the RED-II threshold with ease. This is mainly due to their high conversion efficiency and no additional external H_2 consumption requirements. All fuels produced with HTL (Bio H_2 and SMR H_2), pyrolysis with bio H_2, all ethanol production process and ethanol upgrading to RJF reach the RED-II threshold, where the lowest emission value of these processes are between 12 and 25 gCO_2eq/MJ fuel. As stated pyrolysis with SMR H_2 production cannot reach the threshold having the lowest emission value >36g CO_2eq/MJ of fuel.

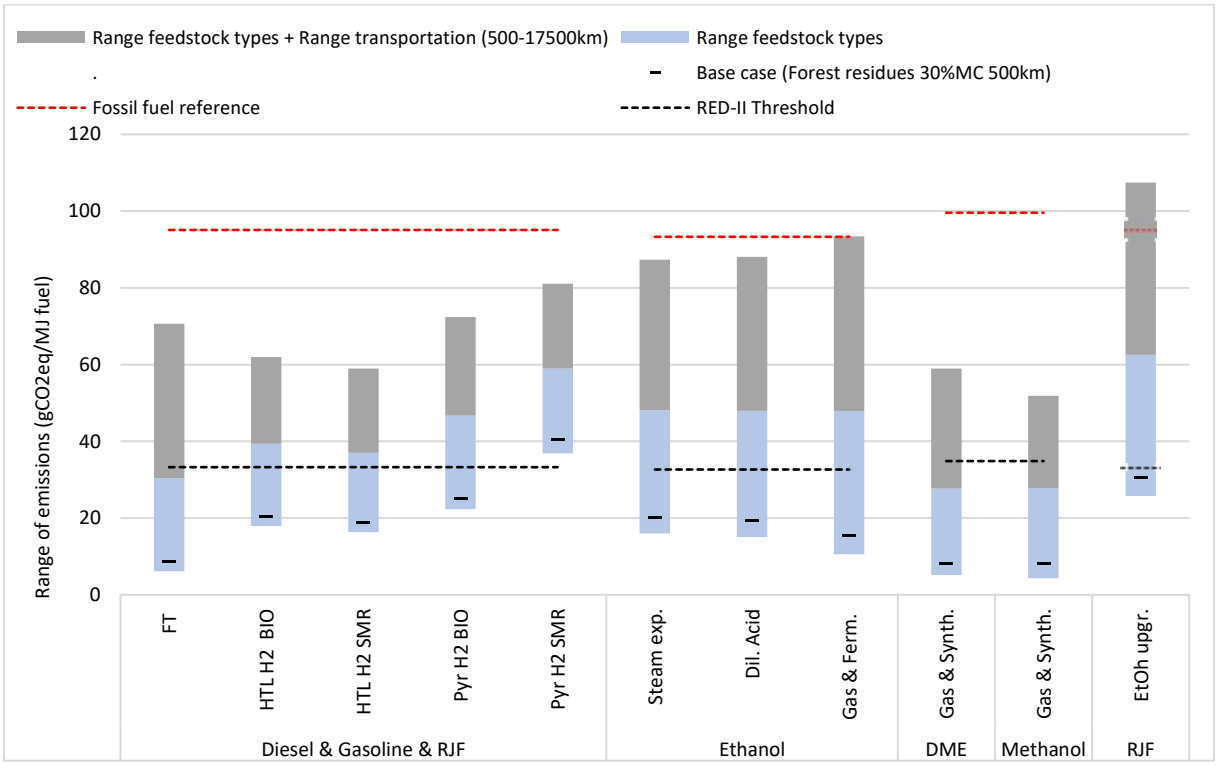

Figure 13-Total GHG emissions of advanced biofuel supply chains. Blue ranges present different feedstocks, grey ranges represent feedstocks + distance range from 500-17500km.

4.1.1 The effect of feedstock types and feedstock supply chains

Figure 14 shows the total GHG emissions of four selected feedstock types supplied from 500km. It shows that primary forest residues have the lowest GHG emissions for all processes, followed by SRC poplar (WF), miscanthus and lastly SRC eucalyptus. The effect of the difference in upstream emissions of feedstock production increases the final sum of emissions when the reactor has a low conversion efficiency or when the final emission value is mainly caused by feedstock emissions instead of the conversion chemicals, the H_2 or the electricity consumption. It can be seen that forest residues always reaches the RED-II threshold. Poplar WF also shows compliance for most fuels, except for pyrolysis with SMR made H_2 and ethanol upgrading to RJF. Miscanthus shows the same compliance of fuels to the RED-II threshold, only with the additional exclusion of pyrolysis with internal biomass gasification made H_2. SRC eucalyptus only shows compliance for the FT-fuels, DME and methanol.

The main observation is that, next to the residues, dedicated energy crops can often show compliance to the RED-II criteria. Differences in GHG emissions are caused by the difference in LHV_{dry} of the feedstocks together with the MC, which affect the allocated emissions to the transportation phase. The second reason is the cultivation phase, in which dedicated energy crops have allocated emissions due to agricultural inputs like nitrogen and pesticide use. This means that forest residues, which require no cultivation, have the best performance, followed by the dedicated energy crops, poplar, miscanthus and eucalyptus where the order describes the performance of the cultivation phase.

Figure 14- Total GHG emissions of four selected feedstocks, supplied from 500km. Within figure 27 of appendix L all GHG emissions for each of the feedstocks over multiple distances are given, which follow the same order of GHG emissions as presented here.

4.1.2 Feedstock transportation distance

The performance of the transportation phase depends on the LHV_{dry}, the MC, the type of transportation mode and fuel efficiency of the transportation mode. To create a consistent comparison for all processes, the same transportation modes and distances from table 5 are used for each process. The results are shown in figure 15, where the impact of four feedstock transportation distances of forest residues 30%MC are given. The total GHG emissions double or quadruple when the distance is increased from 500km to 17500km causing all fuels, except for DME and methanol to exceed the RED-II threshold. To show compliance the transportation distance should not exceed 2500km for pyrolysis with H_2 bio, all ethanol production processes and ethanol upgrading to RJF. The FT fuels and HTL show compliance to the threshold when the distance is increased up to 10000km.

Note that the pathways where the feedstock performance is the main contributor to the final emission value, result in an increased rise between the distances relative to the lowest distance. This can be seen for FT fuels compared to the pathways in which additional factors like H_2, conversion chemicals or electricity use contribute to the final emission value like HTL and pyrolysis and the biochemical pathways.

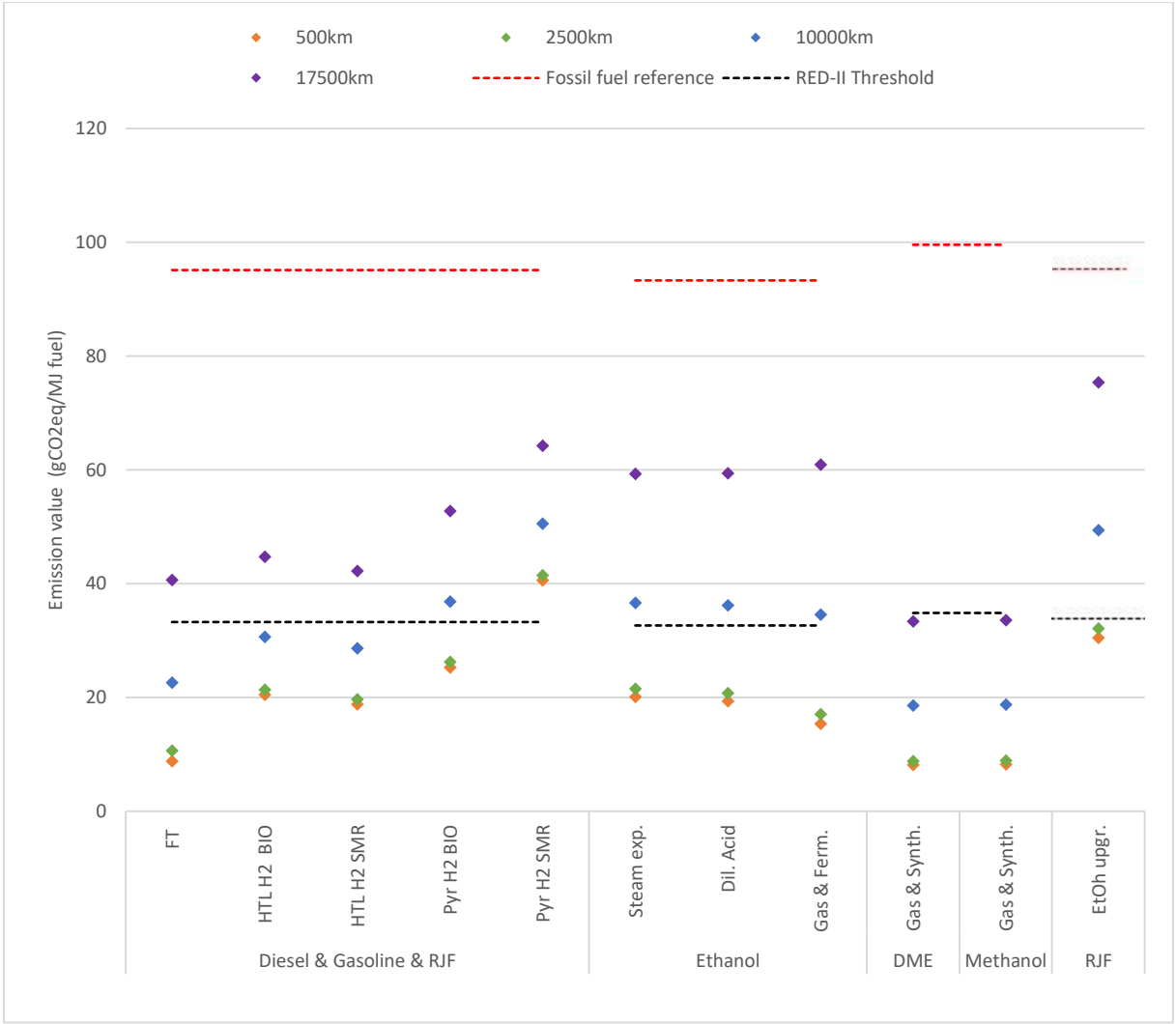

Figure 15- GHG emissions of forest residues 30%MC compared over different distances. Within figure 27 of appendix L all GHG emissions of forest residues over multiple distances are given, which follow the same order of GHG emissions as presented here.

4.1.3.The effect of feedstock pelletization

Energy requirements and associated GHG emissions can be reduced by upstream pre-treatment such as drying and densification (pelletization). A lower MC and increased density cause lower emissions during transportation due to less water being transported and a higher mass of dried feedstock per volume which is often the limiting factor in transportation modes. The positive effect of pelletization is increased when the transportation distance is increased, since the emission are reduced per km. Emissions can also be reduced downstream at the reactor, when the feedstock is already dried. This is the case for the gasification processes and especially pyrolysis, where already dried feedstock increases the reactor efficiency or results in exclusion of a separate drying step. Note that the biochemical processes and HTL require wet feedstocks, therefore do not benefit from already dried feedstock. Because drying and pelletising is done in the biomass supply area with the use of either a NG fired or biomass fuelled boiler and requires electricity from the local grid (e.g. for grinding and pelletization) it causes an increase in GHG emissions upstream. Whether the effect of pelletization upstream in the supply has a positive effect on the total GHG emissions therefore depends on the additional emissions caused by the pellet mill compared to the reduced emissions during transportation and reduced emissions caused by a possible increase in reactor efficiency when drying at the refinery is avoided.

To show these effects, figure 15 and 16 can be compared, where the first depicts the GHG emissions of forest residues without pelletization and the latter depicts the GHG emissions of forest residues with pelletization upstream in the supply chain. For all processes pelletization is effective when the transportation distance is 17500km and a biomass boiler is used. When a NG boiler is used in the pellet mill, pelletization is not effective for any produced fuel. For FT fuels, pyrolysis fuels with H_2 from SMR and gasification & fermentation into ethanol, pelletization is also effective when the transportation distance is 10000km and a biomass boiler is used. For pyrolysis fuels with H_2 from biomass, the upstream pelletization is already effective when the distance is 2500km and a biomass boiler is used. This last effect is primarily caused due to the additional electricity generation when the drying step is excluded before the reactor.

A main finding is that pelletizing using a NG boiler is never effective, regardless of the transportation distance. Pelletising using a biomass boiler is effective for all fuels however the distance should be 17500km. Pelletizing can be effective for shorter distances when the reactor efficiency improves like FT fuels and gasification & fermentation into ethanol or when the drying step before the reactor can be excluded in the case of pyrolysis.

The process of pelletization can therefore also result in showing compliance to the RED-II threshold for longer transportation distances. This is the case for FT fuels with 17500km or pyrolysis with H_2 made from biomass with 1000km, which both show compliance when pelletization up in the supply chain is used.

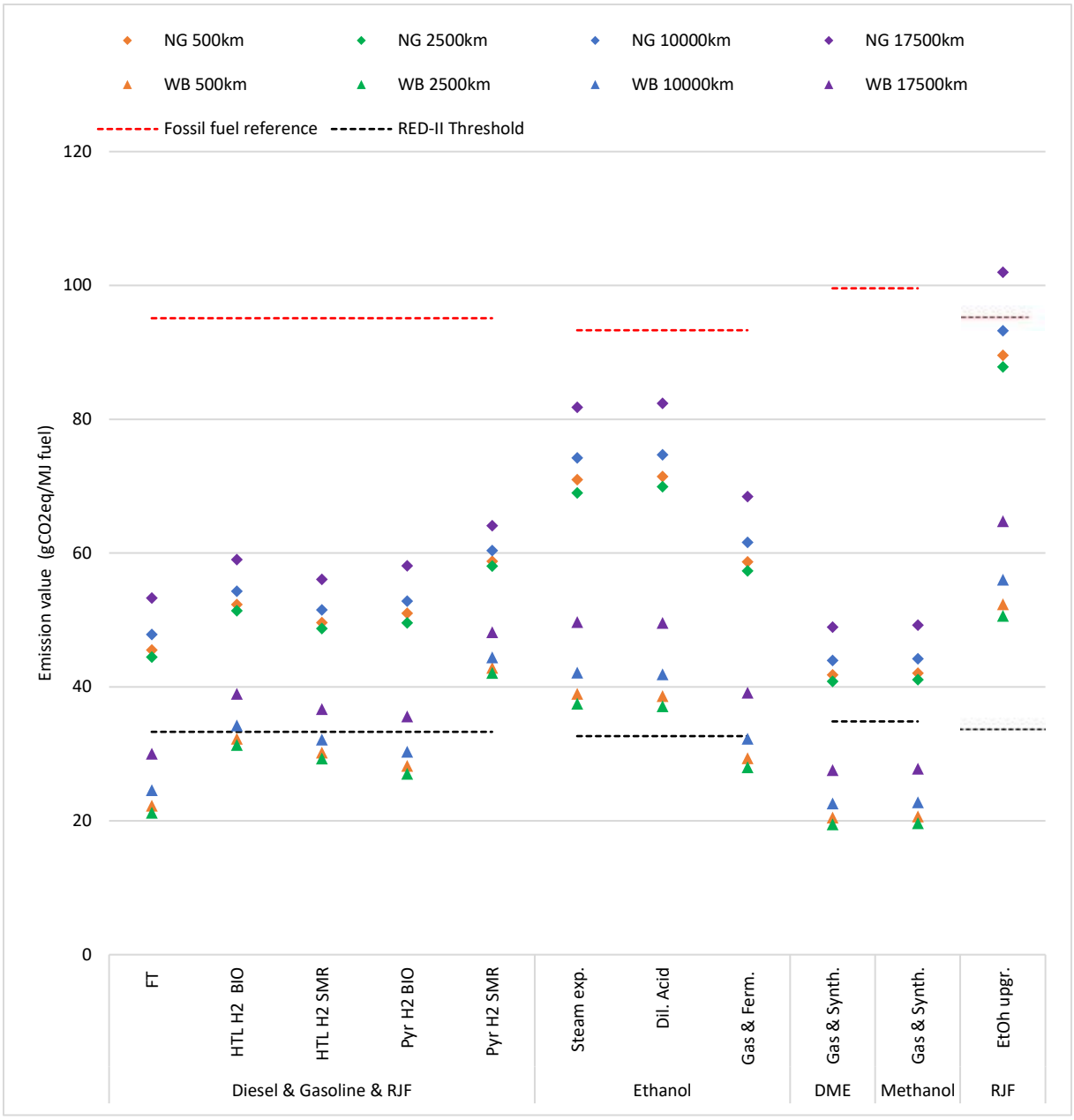

Figure 16- GHG emissions of pelletized forest residues 10%MC compared over different distances and pellet boiler used.

4.1.4 Hydrogen production energy source (Fossil vs renewable)

The H_2 production source can significantly change the GHG emissions of the supply chains and affect the compliance to the RED-II threshold. The included H_2 production processes and their corresponding energy sources were described in section 3.2.3.4. Figure 17 shows the effect of using these different processes and their energy source.

The results show that HTL with SMR made H_2, has a lower GHG emission value compared to HTL with H_2 made from biomass. This can occur, because the internal gasification of biomass also requires additional electricity, whereas the external SMR made H_2 causes the process to produce its own (surplus) of electricity. When using renewably produced H_2, the GHG emissions reduces to almost half. H_2 from the SOEC using EU average electricity mix significantly increases the GHG emission. When using a PEM electrolyser combined with the EU average electricity mix, the GHG emission increases to point where the RED-II threshold is not reached anymore.

The pyrolysis process shows the same order of GHG emissions of external H_2 production technologies, however because pyrolysis has a more H_2 intensive upgrading process these differences are enlarged. A result is also that the internal biomass gasification made H_2 has a lower emission value, compared to the external SMR, SOEC and PEM electrolysers made H_2. This is because the increased emissions from electricity use with internal biomass gasification are overcompensated for the additional emissions due to external H_2 production from SMR. The large H_2 consumption results in the fact that SMR, SOEC and PEM all do not reach the RED-II threshold. Only renewably produced H_2 results in showing compliance with the RED-II emission savings threshold.

When looking at the ethanol upgrading to RJF, it can be seen that the differences between the H_2 production sources are relatively low, due to the low amount of H_2 required. Although the effect is not large, using a SOEC and PEM electrolyser still results in showing non-compliance to the threshold.

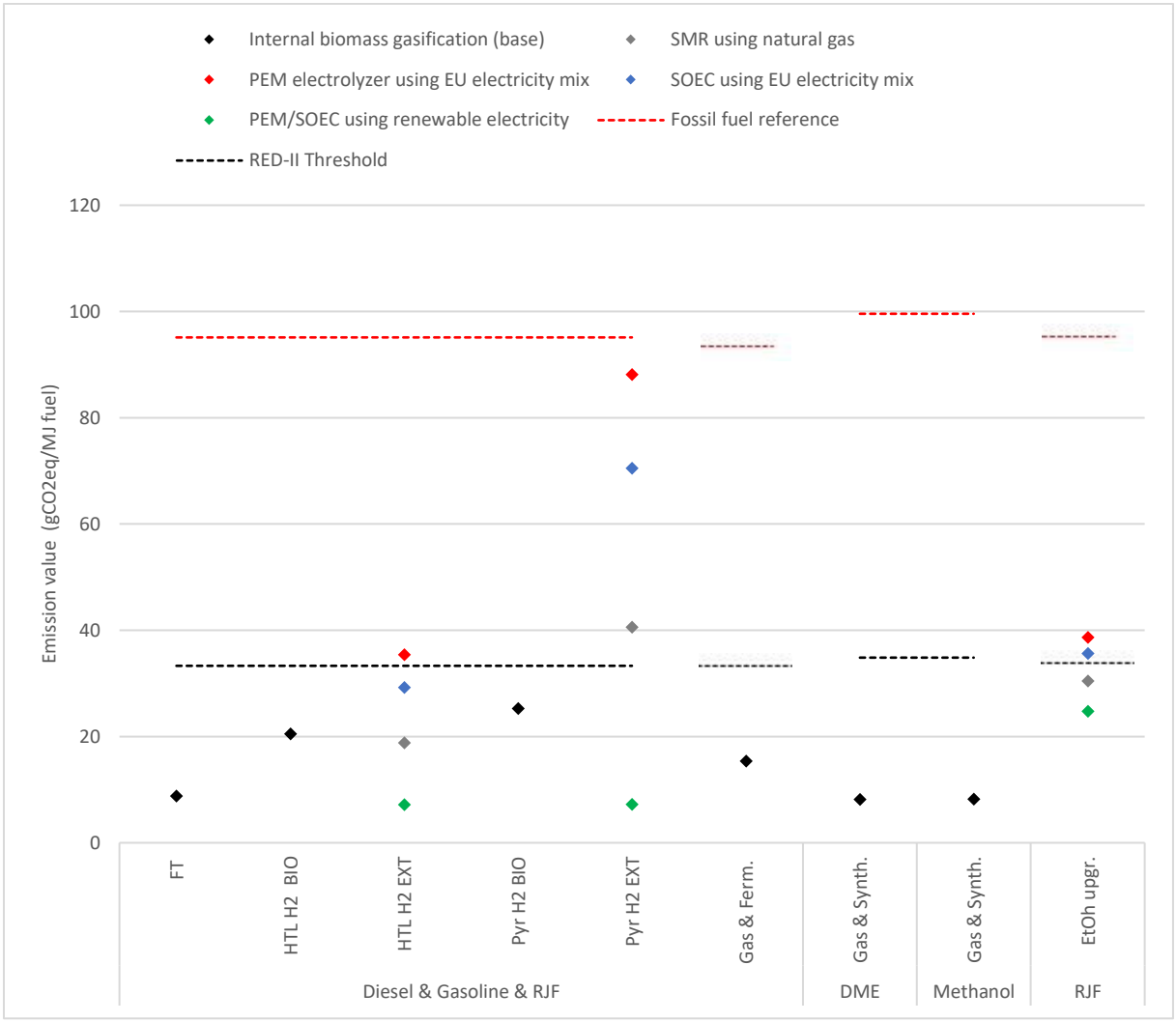

Figure 17- GHG emissions of forest residues 30% using different H_2 production processes and their corresponding energy sources over 500km transportation distance.

4.2 The case studies

Figure 18, depicts the total GHG emissions of the case studies 1a, 2b, 3 and 4b. The case studies 1b, 2a and 4a were also calculated, however they performed worse than their counterpart, therefore they were excluded. The effect of feedstock type, transportation distance and pelletisation can all be seen within the figure.

The FT fuels, DME and methanol always reach the RED-II threshold with SRC willow as feedstock from France having the lowest emissions followed by bagasse from Brazil, forest residues from Canada and lastly pulp grade stem wood from the US. The reason for the relative low emissions of the pellets from Canada and Brazil is the low electricity emission factor that is used. From section 4.1.3 it became clear that pelletisation for large distances is effective, this is enforced in these cases due to the low emissions caused by the pellet mill. Additionally the processes that benefit from already dried feedstock before conversion, like pyrolysis, profit even more.

Looking at ethanol production, bagasse or SRC willow should be used when using the biochemical fermentation processes. Syngas fermentation into ethanol also reaches the threshold when forest residues are used. Looking at the HTL fuels all case studies reach the threshold. Within the pyrolysis process the threshold is reached when H_2 is produced internally using biomass gasification, except when stemwood from the US is used. The pyrolysis fuels using SMR H_2 production and ethanol upgrading into RJF, never reach the RED-II threshold.

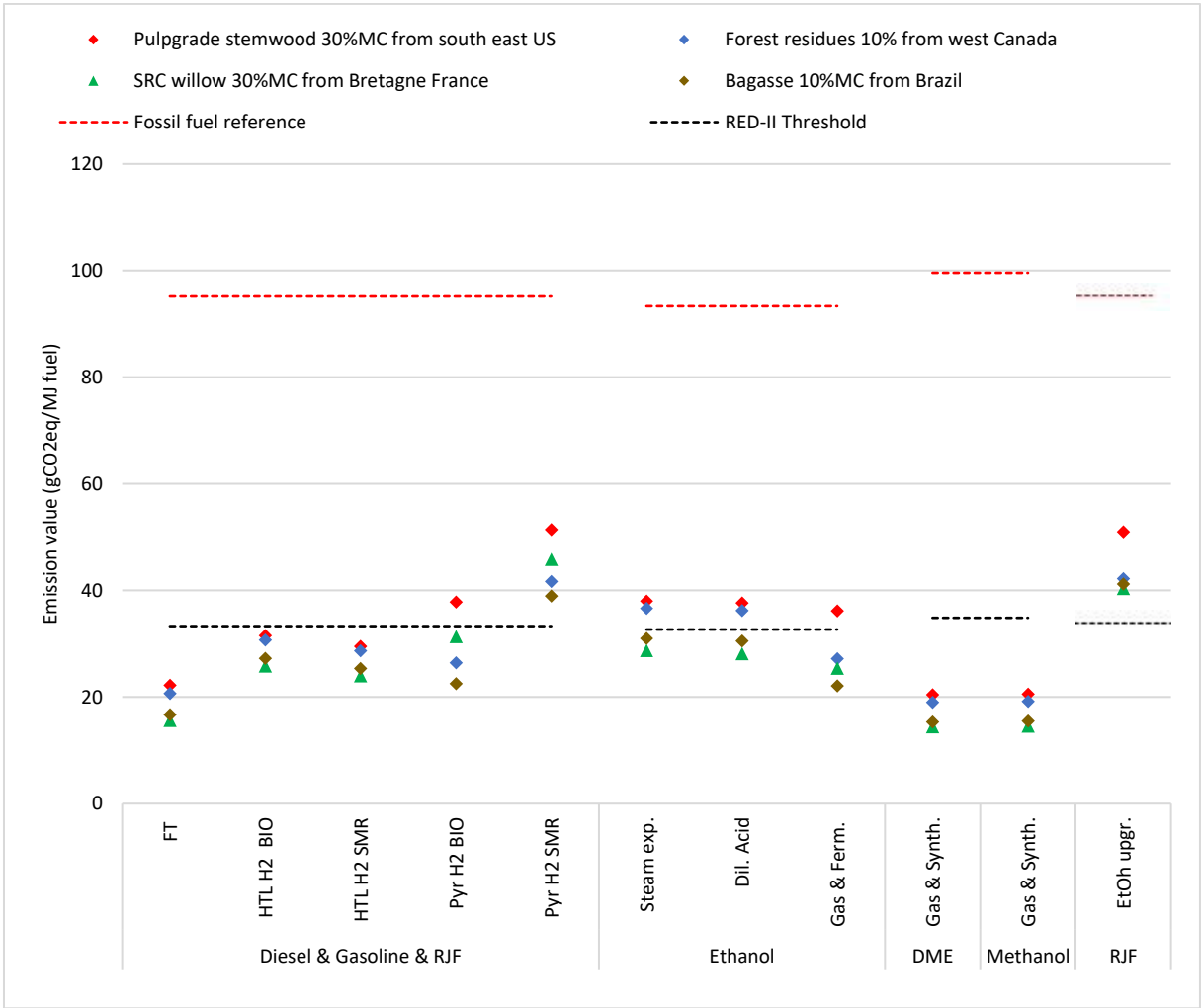

Figure 18 - GHG emissions of the different case studies, with location specific feedstock, electricity use and transportation distance.

4.3 The sensitivity analysis

The first section of the sensitivity analysis shows the impact of the applying different methods of dealing with multifunctionality on the standardized supply chain. The second part shows the impact of changing the reactor efficiency, nitrogen use and H_2 energy source on the case studies.

4.3.1 The impact of different methods of dealing with multifunctionality

Figure 19 shows the impact of four chosen methods of dealing with multifunctionally on the standardized supply chain of forest residues. The energy and mass allocation methods are close to each other for most production processes. A difference between these two allocation methods occurs when large amounts of electricity are co-produced compared to the main output. Since the produced electricity has no mass, more emission are allocated towards the fuels that do have mass, resulting in increased GHG emissions of the main fuel. This can clearly be seen in the pyrolysis processes with SMR made H_2. Differences can be enlarged when the LHV of the produced co-products are different. A lower LHV_{dry} of the main produced fuel, for example diesel in the process of pyrolysis compared to the higher LHV_{dry} of the co-product gasoline, causes a larger difference compared to the energy allocation.

Looking at the GHG emissions of the displacement method or system expansion, the differences are significantly larger. As described in the LCA theory, the displacement method can only be applied when the main product consists of 50% of the total output. Therefore some processes are excluded for this method. As can be seen, FT diesel and pyrolysis into gasoline have negative emission values. This occurs when a large amount of co-products is produced which have a cumulative larger displaced GHG emissions than the total GHG emissions of the whole supply chain. Especially the conversion processes which produce high amounts of electricity, which has a high emission factor, can create a large amounts of displaced emissions.

Looking at the economic allocation, the GHG emissions are often lower than the energy allocation. The main reason being is the higher price of electricity compared to the fuels, resulting in a higher share of emissions allocated to the co-produced electricity. In cases like HTL into gasoline, where H_2 is produced from biomass gasification, no excess electricity is produced. When combined with a high price of the main product produced of gasoline, results in a high share of emissions allocated to the main product. Cases where the main fuel produced has a low economic value like RJF, results in the finding that very little emissions are allocated to this fuel, causing significantly lower GHG emissions compared to the energy allocation. It should be noted that the economic value of the products strongly depends the taxes that are put on the products instead of the actual production price.

Although the RED-II calculations method uses energy allocation, it can clearly be seen that using other methods could significantly alter the GHG performances of the produced fuels and change the compliance to the emission reduction threshold. Especially the consequential displacement theory creates distorted results due to the different ratios of product outputs with vastly different emission factors.

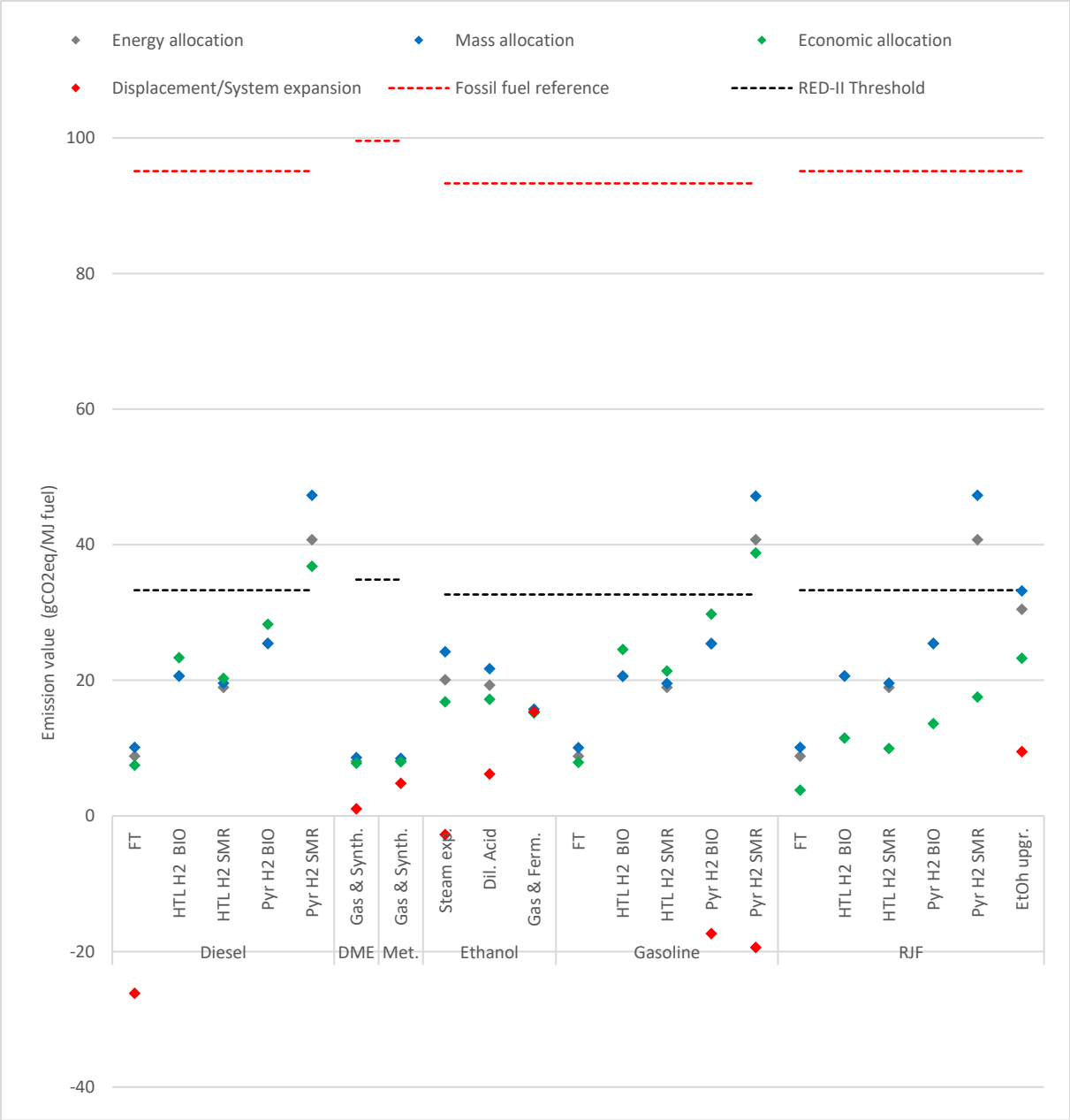

Figure 19 - GHG emissions of forest residues 30%MC using different multifunctionality methods over 500km transportation distance.

4.3.2 The impact of reactor efficiency, nitrogen use and hydrogen energy source

Figure 20 until 23 represent the effect of changing the reactor efficiency, the nitrogen usage during cultivation and the H_2 energy source on the different case studies. The red bars (R) give the range of the reactor efficiency, the blue bars (H_2) give the range of the H_2 energy source, the green bars (N) give the range of the nitrogen usage during cultivation and lastly the grey bars (T) give the total summation of the aforementioned ranges.

Analysing the sensitivity of case study 1a (forest residues 10%MC from Canada), it can be seen that large ranges are possible, resulting in the possibility for pyrolysis with SMR made H_2 and biochemically produced ethanol to reach the RED-II threshold when the optimistic reactor efficiencies are used. Additionally for the cases where H_2 is produced with renewable electricity, like pyrolysis and HTL, the GHG emissions can reduce even more. The combination of an optimistic reactor efficiency combined with renewably produced H_2 in these cases results in having the best GHG performance of all the

processes. However not all processes benefit the same amount from the sensitivity analysis, as seen in the process of ethanol upgrading into RJF which does not reach the threshold, even with optimistic input values.

The sensitivity analysis of case 2b (pulpgrade stemwood 30%MC from the US), follows the same ranges as case 1a, only with higher base emissions. This causes the biochemically produced ethanol to not reach the threshold with optimistic reactor efficiencies. Within the pyrolysis process the H_2 needs to be made renewable, since only using an optimistic reactor efficiency does not result in showing compliance to the threshold.

The sensitivity analysis of case 3 (Bagasse 10%MC from Brazil), also follows the same ranges as the previous two, however because the base emission are even lower than case 1a, all processes can reach the threshold. Where ethanol upgrading to RJF could not reach the threshold in case 1a and case 2b, it can reach the threshold within case 3 on the condition that renewable H_2 is used.

The sensitivity analysis of case 4b (SRC willow 30%MC from France) also adds the uncertainty of the nitrogen use. As can be seen, this does not affect the total GHG emissions significantly, mainly because the nitrogen use was responsible for a relatively low amount of emission compared to the total emissions. The nitrogen can reduce the total GHG emissions of this case study, however the main reductions are still induced by using renewable H_2 and increasing the reactor efficiency. Again all processes could reach the threshold using optimistic values.

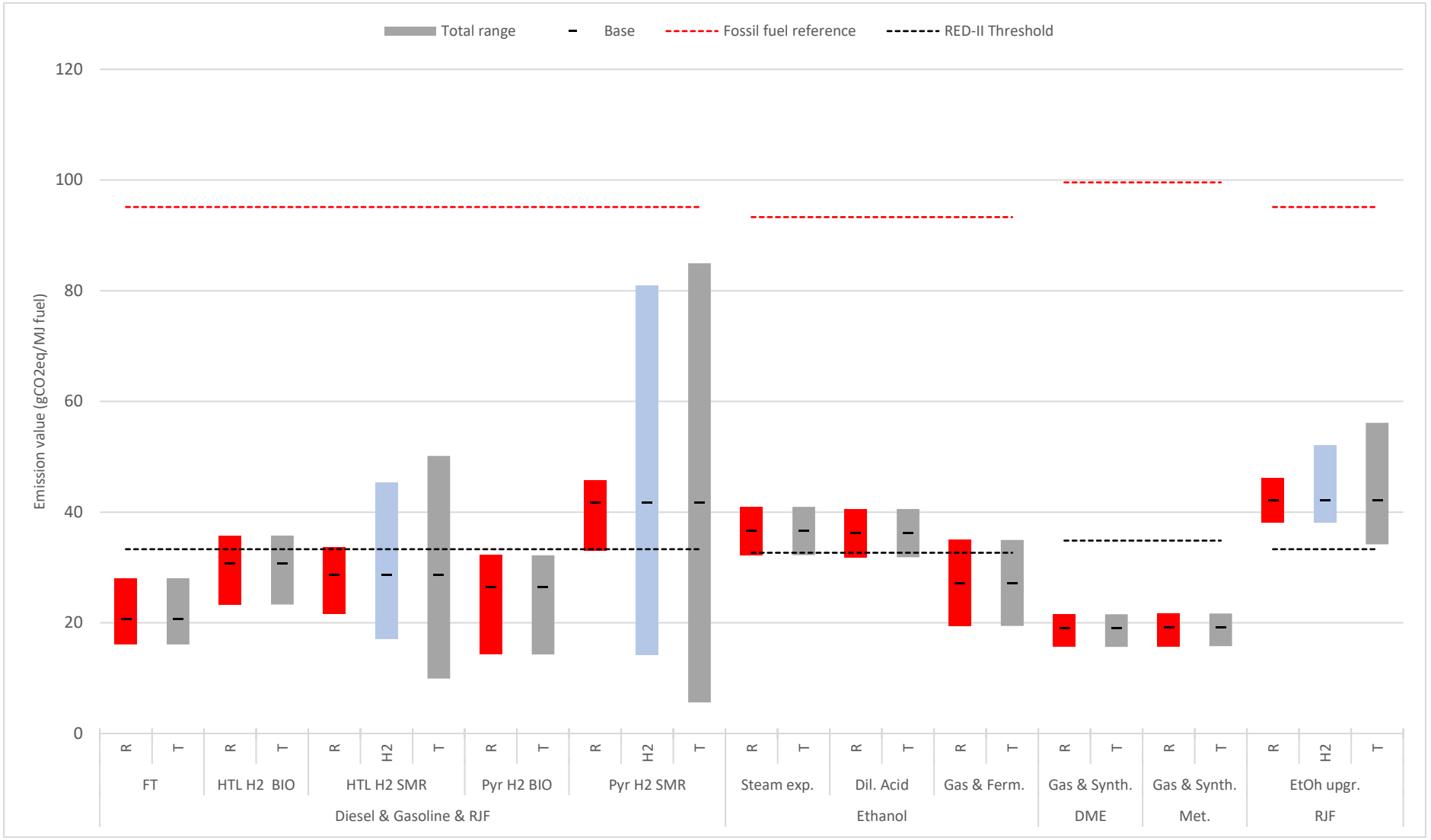

Figure 20- GHG emissions sensitivity of Case study 1a (Forest residues 10%MC from Canada)

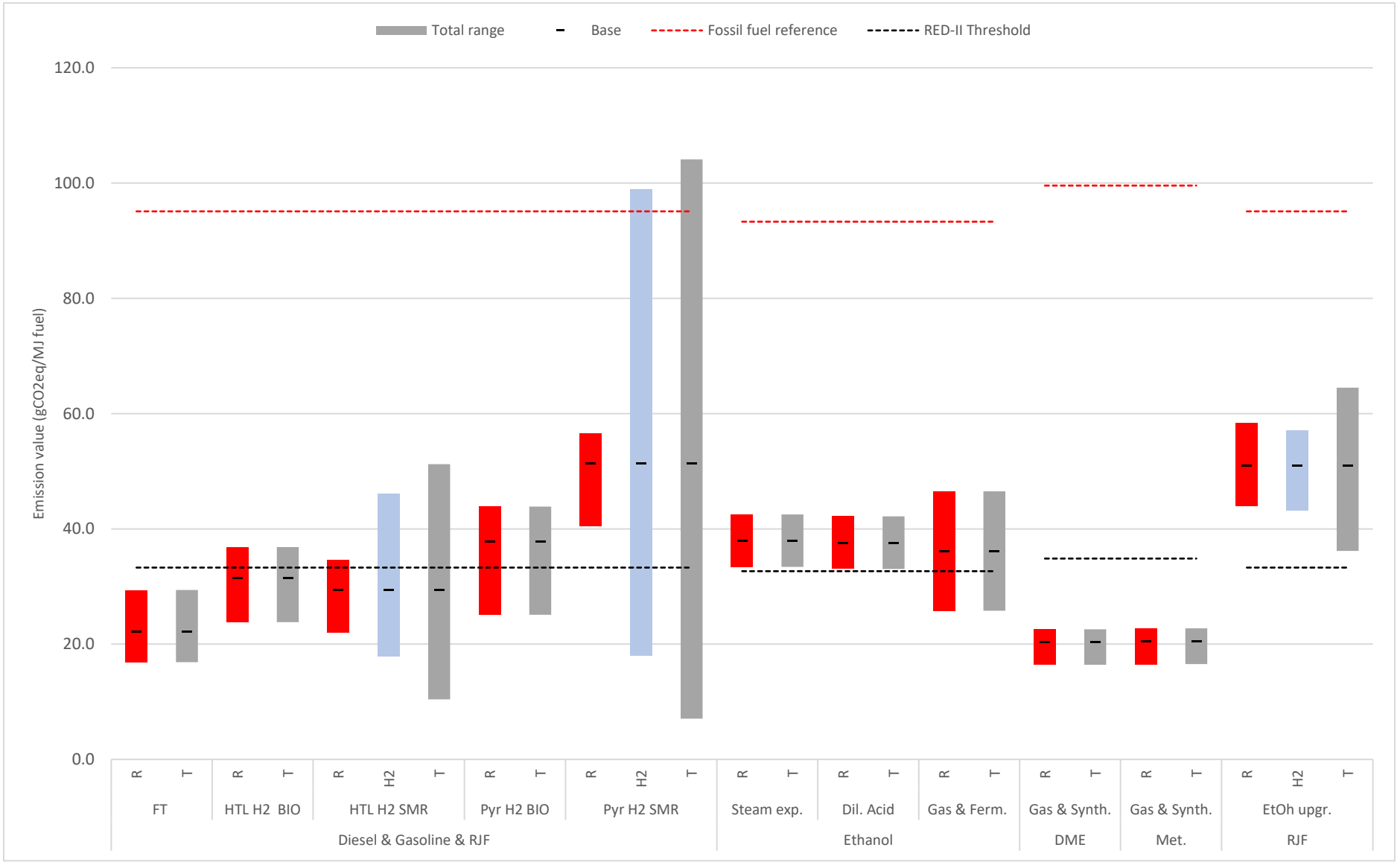

Figure 21- GHG emissions sensitivity of Case study 2b (Pulpgrade stemwood 30%MC from the US)

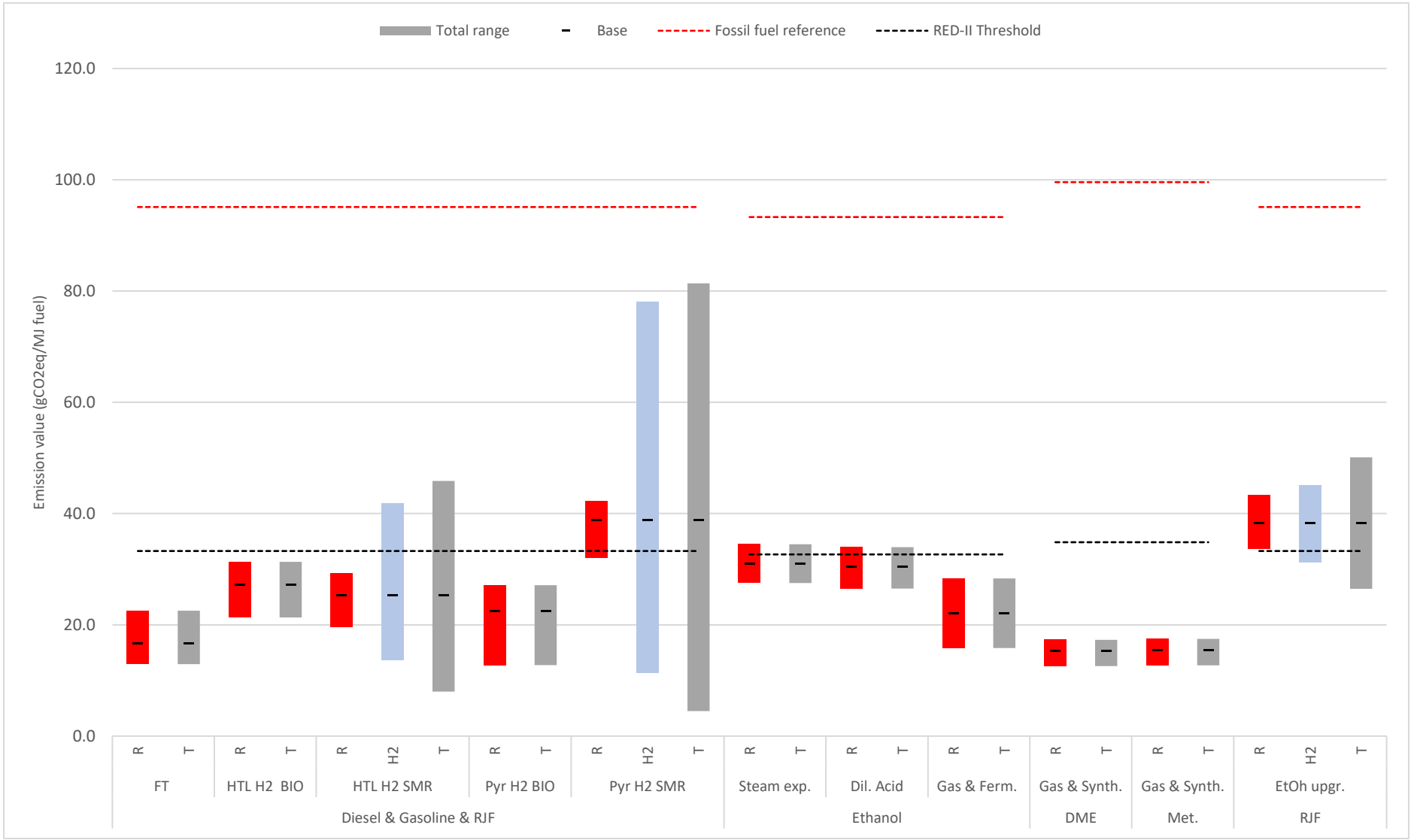

Figure 22- GHG emissions sensitivity of Case study 3 (Bagasse 10%MC from Brazil)

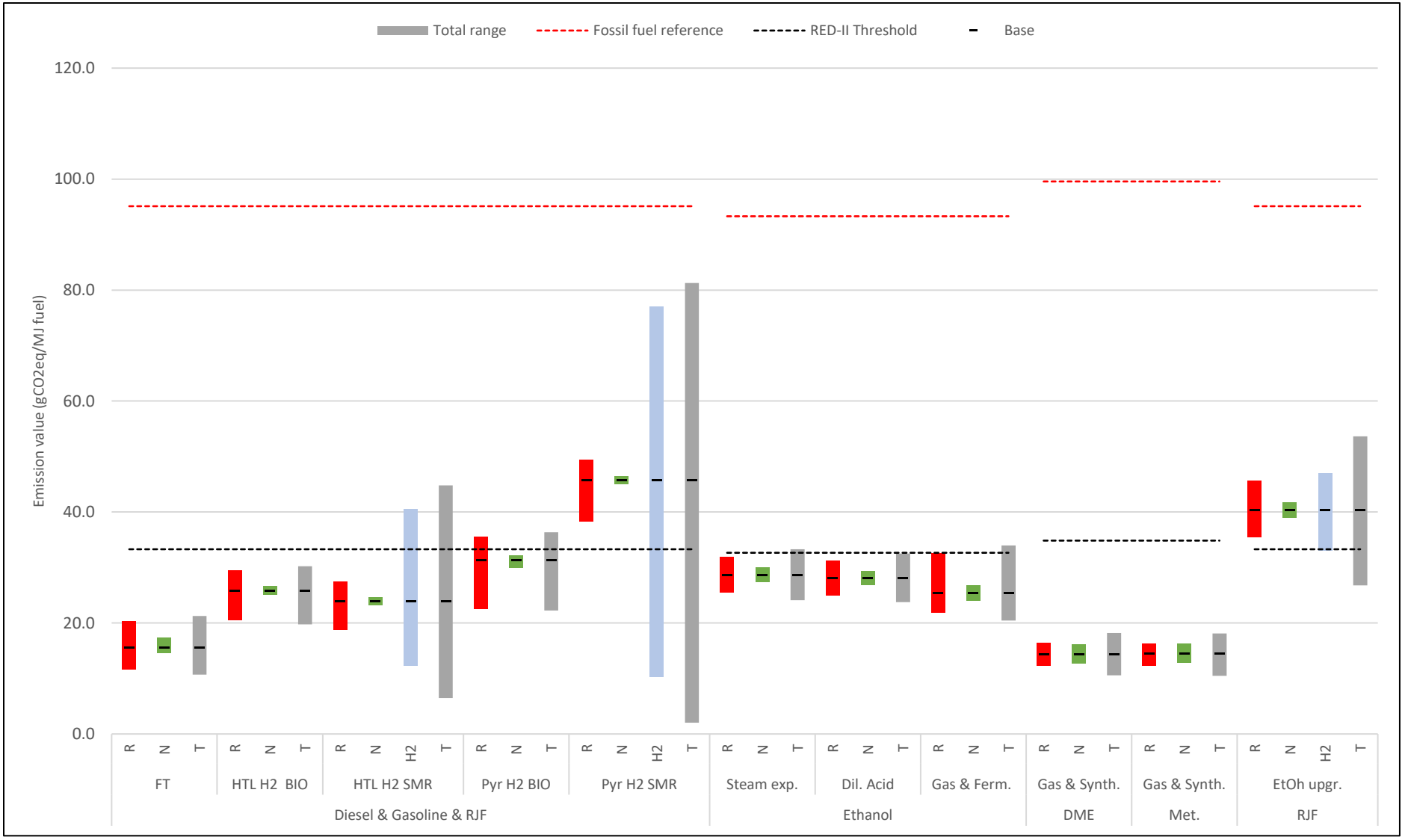

Figure 23- GHG emissions sensitivity of Case study 4b (SRC Willow 30%MC from France)

5 Discussion

The introduction of the advanced biofuels in road and aviation markets create opportunities to reduce GHG emissions caused by current fossil fuel use. The conducted research created a consistent lifecycle GHG emission comparison of various advanced biofuels supply chains and the possible emissions reduction potentials compared to their fossil fuel counterpart. Before the conclusions can be drawn, all phases of the LCA method will be discussed with their corresponding data inputs and assumptions that were made. Additionally the result and the comparison to literature are discussed as well as possible future research.

5.1 Goal and Scope

The goal and scope of the research was to assess the GHG performance of the various international and European supply chains for the production of advanced biofuels. The aspects regarding the choice of scope and related FU as well as the type of LCA and related method of dealing with multifunctionality are discussed.

5.1.1 Functional Unit

The scope of the research was chosen to include all phases of the lifecycle from cultivation until the use phase of the fuel, however because the FU was set to be gCO_2eq/MJ and not be gCO_2eq/km transported, the actual use phase of the fuels could induce deviations in the results. An example would be that implementing the biofuels would change the efficiencies of the vehicles, therefore affecting the GHG performance. Blending of the biofuels with fossil based fuels could also induce differences in GHG performance, due to the changes in compositions which creates alterations in fuel efficiency as well as an increase the CO_2 emissions when accounting for the fossil based fuel fraction. Another example of changes in GHG performance would be when a comparison is made with electric vehicles, which have a significantly higher TTW efficiency. This effect is also present when comparing RJF to diesel, where an entirely different transportation mode is used with a different fuel economy. The scope of this research did not account for the calculation of the actual implementation within vehicles and therefore possible differences in efficiencies and related blending ratios. Extending the scope to the implementation within different transportation modes and analysing the CO_2 reduction per km transported could make the research more realistic.

5.1.2.Type of LCA and method of dealing with multifunctionality

The chosen type of LCA within this research was an Attributional LCA (ALCA). Most LCAs used for databases and published studies within literature use this type, however Plevin et al. (2014) argues that certain shortcomings are inevitable. An ALCA uses all energy and material flows of a process along the biofuel supply chain and allocates the environmental burdens towards the produced outputs in a static manner with the use of average input values (Plevin et al., 2014). The result is that it is hard to identify the effect of the implementation of a biofuel on the system as whole, which tends to be more dynamic. When using a Consequential LCA (CLCA) the consequence of a implementation of the biofuel can be assessed, accounting for other indirect effects like displaced activities or even social development and market dynamics (Plevin et al., 2014; Rehl et al., 2012).

As described before ISO recommends to expand the system resulting in a LCA that tends to be consequential, however the RED-II used an energy allocation method therefore creating an ALCA (European Parliament, 2018; ISO, 2006). Within the first part of the sensitivity analysis, the different allocation methods of mass, energy, economic value and the ‘consequential’ LCA method of displacement theory were applied. It should be noted that only the displaced emissions are accounted for in this method, excluding the aforementioned other indirect effects that also occur.

It became clear that the chosen method could affect the results significantly. Literature is not united on a 'best' method, because each one has their strengths and weaknesses (Agostini, Giuntoli, Marelli, & Amaducci, 2019; Wiloso et al., 2012). Where economic allocation gives the opportunities to compare products regardless of their use through economic value, it is subjectable to fluctuations in price and taxes on top of the production costs. To avoid this, mass allocation could be applied where the physical relations between the produced products are applied bringing less uncertainty, however including products with no mass like electricity create an inaccurate way of representation of the results. The chosen energy allocation eliminates this problem, however this methods assumes that all products have the same 'value' if they contain energy although in reality they can be less valuable. Therefore theoretically the consequential displacement theory is the most accurate because it represents the actual production of multiple products and accounts for indirect avoided activities. However within this research it created distorted results when the main product was less than 50% share of the produced goods. Also the actual implementation of this method with additional indirect effects often results in a complex LCA with many assumptions being made.

5.1.3 Biogenic carbon and carbon neutrality

The used LCA defined all carbon from biomass sources to be biogenic carbon which is set to be zero. The reason behind this, would be the sequestration of carbon in biomass over time, which in turn is brought back in the atmosphere using various pathways including decomposition, direct combustion or through processing it into biofuels or other materials with a possible subsequent combustion step (Junginger, 2018; van der Hilst et al., 2018). The carbon is essentially reused over a period of time, without creating a net increase in the system. However the recycling time of the carbon circle as well as the reference point (counterfactual land use/ counterfactual fossil fuel use), can affect the calculation of the carbon within the atmosphere at a specific timepoint. A carbon dept can therefore be induced, however the assumption is made that eventually this carbon is sequestered back creating a net zero change (Junginger, 2018; van der Hilst et al., 2018). The additional carbon reduction into the atmosphere can be the reduced fossil based fuels use or the additional carbon stock of a piece of land that was previously not in use for carbon sequestration creating additional carbon stock.

5.2 Inventory input data and uncertainty

The inventory phase was the largest part of the research, due to the identification of all the included processes and their characteristic along the various supply chains. The used data as well as the assumptions made for the feedstock supply, conversion processes with the related end use markets are discussed.

5.2.1 Feedstock supply

The primary data sources used for the feedstock production chains were based on the reports of Edwards et al. (2019) and Giuntoli et al. (2017) made for the European Joint Research Centre (JRC). The JRC is a collaborative consortium for advising the EU, therefore it can be thought of as a reliable and representative data source for the calculation of GHG emission values. Because the dynamic model could be used to give insight in the possible supply chains that are eligible for support and can contribute to the advanced biofuel targets within the RED-II, the corresponding calculation methods should be used. These methods require the use of EU average input values related to emissions factors of the electricity mix, the production of conversion chemicals, the production of agricultural chemicals and pesticides as well as the use of different transportation modes. They are all calculated on a basis in which the value represents an average and relative correct representative for the EU. The use of average values instead of specific data is also in line with the chosen ALCA method instead of CLCA as described by the ILCD handbook (Chomkhamsri et al., 2011). An implication of the use of average values would be the lack of specificity. An example would be that although feedstocks were sometimes

transported from Brazil or Canada which have a low carbon electricity mix, the used electricity mix would still be based on the EU average. This could induce differences on the total GHG emissions as was shown in the case studies. This effect is also at play when specific countries within the EU are used for feedstock production or conversion processes, because within the EU large fluctuations of electricity emissions factors also exist. However, next to the RED-II calculation rules, the choice of using EU averages was made to create a coherent approach in which the different elements throughout section 4.1 could be identified separately, by the means of changing only one key variable at once.

A second input data assumption aimed at the exclusion of location specific calculated N_2O induced soil emissions and effects of DLUC and ILUC. Because N_2O field emissions are highly reliant on spatially explicit locations, they were only added in the model as a dynamic tool. However standardized average values from Giuntoli et al. (2017) were used to account for additional emissions. This is also the case for the effects of DLUC. They too are highly reliant on the location, combined with the specific timeframe of the land being used compared to the previous land as described in 5.1.3. Because calculation of DLUC and especially ILUC are still very controversial and are depended on specific input parameters, these were excluded from the research (Khanna & Zilberman, 2017). The implication of the exclusion of specific N_2O emissions is dealt with in the sensitivity analysis, which showed that the N_2O induced emissions are only a fraction of the total GHG emissions and thus do not induce a significant limitation. The implication of the exclusion of DLUC and ILUC could have a significant effect on the total GHG emissions, however due to the uncertainty in the calculation, excluding it will likely induce less uncertainty.

5.2.2 Conversion processes

The aforementioned input values are robust and validated, however they often only apply to the feedstock production, pre-processing and transportation phases. The second data inquiry aimed at the conversion processes, which can be considered less robust due to the complexity of the processes or due to the lack of specific data. The used studies for the conversion processes are often based upon small commercial scale case studies or they are only performed in a controlled laboratory environment making the accurateness of the reactor efficiencies less realistic.

Although conversion processes like gasification into FT products for road markets have been documented extensively, they often differ in assumptions made and produced output, resulting in different efficiencies across different sources. The level of detail of the studies is also either very complicated, due to the use of ex-ante engineering estimates based on process modelling software such as Aspen Plus or contrary, to simplified in which only a conversion efficiency based on a LHV with no specification of MC is given (Aspentech, 2019). As can be seen in table 26 and 27 of appendix J.1, multiple types of reactors from different sources were used in the model for the gasification and synthesis into diesel, gasoline, DME and methanol for road markets to check consistency across literature and to make the reactor efficiencies more reliable. It was found that there is a large consistency between FT products where reactor efficiencies are almost the same across literature implying high reliability and validation. The synthesis of DME and methanol can differ slightly more due to the choice of the wanted outputs, creating differences in GHG performance. However within the sensitivity analysis it was found that the effect does not create significant absolute changes due to the already low GHG emission value.

Regarding the biochemical processes, the efficiency differences between reactor types were minimal. The induced data reliability is however caused by different amounts or combinations of pre-treatment and conversion chemicals, which can create large GHG emissions differences. This also relates directly to the GHG performance of ethanol upgrading into RJF. Within the sensitivity analysis it was found that

both processes are minimally affected by reactor efficiency changes, however the H_2 production energy source in the ethanol upgrading process had a more substantial impact on the performance.

Other conversion processes like pyrolysis and HTL, which are relatively new, have little available data on actual case studies or conversion plants. In the case of this research the case study of Tews et al. (2014) was used, where the difference in dried and pre-dried feedstocks as well as internal biomass gasification or external SMR H_2 production was calculated using the energy balances. It could be questioned if this theoretical approach of calculating these new configurations based on several assumptions regarding H_2 production energy source and including or excluding the drying step of feedstocks is actually technically achievable (Antonissen, 2016; De Jong et al., 2017). It was however chosen to include these configurations, because they create insight in the differences that can occur when changing these important elements on the total GHG emissions. Within the sensitivity analysis it was found that both the uncertainty in reactor efficiency as well as the H_2 production energy source could create significant changes in GHG performance.

All the data from the included conversion processes were based upon one type of feedstock with a specific MC, which in this research was often forest residues 30%MC. Because all feedstock-conversion combinations were included, a correction of the conversion efficiencies based on the differences in LHV_{dry} of the feedstocks was made. To account for differences in MC either the drying step before the reactor was included or excluded, or a corrected LHV_{dry} based upon the evaporation energy of water was calculated using the method of Nieuwlaar (2017). Although the conversion efficiencies are corrected for energy content and MC, it should be noted that feedstocks are also different regarding other chemical consistencies like lignin content, ash content, nitrogen content and chlorine content which can all affect the feedstock-conversion favourability and conversion efficiency with the related changes in GHG performance. Another related limitation is that the feedstocks are often not corrected for emissions related to the grinding the feedstocks. This means that sometimes the grinding emissions are being counted within the feedstock production step and in the pre-treatment step just before the conversion. Although this step could easily be made separate in the model, the used literature often did not suffice in the specific grinding energy, making it an inevitable limitation.

5.2.3 End-use markets

The aforementioned conversion processes were used for the products of road markets, however they were also used for the production of fuel for the aviation markets, the RJF. The main data sources used were (Antonissen, 2016; De Jong et al., 2017) who also used FT, HTL and pyrolysis for the calculation of the lifecycle GHG emissions. A large assumption made within their research as well as this research is setting the production performance of RJF the same to the production performance of diesel. They argue that due to the lack of data for RJF production, it is a common method in literature to use diesel as reference fuel and applying a split on the diesel output to create RJF (Antonissen, 2016; De Jong et al., 2017). This argumentation is validated within literature because the extra generated emissions for further upgrading to RJF are minimal and therefore would not induce significant additional GHG emissions (A. Elgowainy, J. Han, M. Wang, N. Carter, R. Stratton, J. Hileman, A. Malwitz, 2012).

Next to the inclusion of the advanced biofuels for road and aviation markets, the intention was to also include the maritime fuels in the research design. The heavy hydrocarbons or bio-oil made in the processes of HTL and pyrolysis could be upgraded with the use of mild hydrogenation (Geraedts, 2018). The leading company called Good fuels suggest that this upgrading process could create a sweet spot between lower upgrading production costs compared to diesel, gasoline and RJF, while creating exclusive use for the heavy maritime engines eliminating competition (Geraedts, 2018). However due to the lack of actual case studies on this process, this could not be calculated accurately enough and was therefore excluded from the results.

5.3 Impact assessment

The impact category was chosen to be the GWP_{100}. More extensive LCA's also include other impact categories like water use, land use, public health, biodiversity, eutrophication, acidification or photochemical ozone creation (Rehl et al., 2012). Including these impact categories could affect the results significantly, however this would require very (location) specific data inquiries, making the inventory analysis more complicated, which could increase the uncertainty of the obtained results.

5.4 Interpretation phase

The last part of the research was analysing and interpreting the results. The results and comparison to literature as well as contribution, practical implications and future research are discussed.

5.4.1 Results & comparison of results with literature

All fuels considered for road and aviation markets within this research, show a decrease in lifecycle GHG emission values compared to their fossil fuel counterpart. A main finding was that the GHG performance is dependent on many variables in the supply chain design. The specific results showed that the gasification and synthesis into methanol, DME, and FT fuels all have good GHG performance, having significantly lower GHG emissions compared to the fossil fuel counterpart and often reach the RED-II emission saving threshold. Ethanol production pathways showed that the new syngas fermentation conversion creates the lowest GHG emissions, followed by the dilute acid or steam explosion pre-treatment with the subsequent fermentations steps. Other new technologies like pyrolysis and HTL also show good GHG performance, however H_2 production should preferably be made renewable since this is a main GHG contributor. In the sensitivity analysis is was found that changing the method of dealing with co-product can significantly alter the GHG performances. Additionally the sensitivity analysis showed that further technological improvement regarding reactor efficiency, next to making H_2 renewable, could significantly reduce the GHG emission values.

A comparison between the calculated results and results from literature can be seen in table 11. Although the results of each of the produced fuels within this research could be compared to each other, due to the consistent method and input variables, it is hard to compare it to literature. Because of the many types of assumptions that lie at the core of a LCA and the chosen elements that make up the biofuels supply chains, certain deviations are to be expected. It should be noted that the results of literature are not calibrated or corrected to better match the supply chain configuration of this research. The comparison only serves the purpose of showing whether the results are reliable and possible compared to literature.

Comparing the FT fuels, DME and methanol taken from Edwards et al. (2013) to the results of this research, a deviation of ≈3gCO2/MJ fuel can be seen. Although the same method of co-product treatment is used as well as the use of waste wood (forest residues) as feedstock, the feedstock transportation distance is lower, which likely causes the deviation. Comparing the HTL and pyrolysis based on Tews et al. (2014), larger deviations can be seen of ≈7.5 gCO2/MJ fuel produced. Again the same feedstock and method of co-product is used. The differences are caused by different configurations upstream in the supply chain where pre-treatment and transportation are different compared to this research. Comparing the results of ethanol production, both processes have the same emission value as literature described by Edwards et al. (2013) and Olofsson et al. (2017) for the dilute acid pre-treatment process and Kumar & Murthy (2012) for the steam explosion pre-treatment into ethanol. A comparative results for syngas fermentation could not be found. The last comparison of ethanol upgrading into RJF was based upon Pierobon, Eastin, & Ganguly (2018), which showed a deviation of ≈-3.5 gCO2/MJ fuel using mass allocation or ≈+3.5 gCO2/MJ using system expansion. Again the biomass supply chain configuration is different compared to this research, as well as using other

methods of dealing with co-products. All results are relatively close to the values reported within literature, therefore making the results realistic and plausible.

Table 11 – Comparison with literature

Fuel	Process	Results literature (gCO2eq/MJ fuel)	Own results (gCO2eq/MJ fuel	Co-product treatment	Feedstock	Source
Diesel & Gasoline & RJF	FT	5	8.8	Energy allocation	Waste wood	(Edwards et al., 2013)
	HTL H_2 BIO	27.2	20.5	Energy allocation	Forest residues	(Tews et al., 2014)
	Pyr H_2 BIO	33.8	25.3	Energy allocation	Forest residues	(Tews et al., 2014)
Ethanol	Steam exp.	20	20.1	Economic value allocation	Straw, grasses	(Kumar & Murthy, 2012)
	Dil. Acid	16.3[1]-20[2]	19.3	Energy allocation	Waste wood	(Edwards et al., 2013[2]; Olofsson et al., 2017[1])
DME	Gas & Synth.	5	8.1	Energy allocation	Waste wood	(Edwards et al., 2013)
Methanol	Gas & Synth.	5	8.2	Energy allocation	Waste wood	(Edwards et al., 2013)
RJF	EtOh upgr.	26.9[1] 34[2]	30.5	Mass allocation[1] System expansion[2]	Forest residues	(Pierobon et al., 2018)

5.4.2 Contribution to literature, practical implications and future research.

The contribution of this research is the consistent comparison between the performance of different advanced biofuel production systems based on the RED-II calculation methods. Supply chains often differ in terms of configuration, input variables, feedstocks, method of dealing with multifunctionality and many other factors. Although very strict rules have to followed within the RED-II for the contribution of biofuels to the set targets, many research assumptions and supply chain configurations still have to be chosen. With the use of the created dynamic model these types of variables can easily be changed to directly see the effect of certain improvements along the production chain and to calculate the GHG performance of the produced biofuels. Additionally, the GHG performance of specific cases with spatially explicit biomass supply chains can easily be calculated.

Although this research showed the possible ranges of GHG performance caused by the many variables, a recommendation for future research could be made regarding the implementation of increased specificity of calculation methods and development of consistent databases with corresponding consistent assumptions. Especially regarding the conversion processes, standardized values could significantly simplify calculations for future research. This could reduce the uncertainty of GHG performances and create increased security for the production of advanced biofuels.

Other future research could also focus on a more realistic and practical comparison indicator of CO_2 mitigation costs. A future study could calculate the total costs of each of the production pathways with certain selected configurations, which in combination with this study, could be used to calculate the cost per gCO_2eq avoided. Because the model is set up to be dynamic, calculating the wide variety of configuration options is made easily, where the direct effect of an improvement of the lifecycle GHG emissions can be compared to a possible increase in cost. The model could therefore also be used for policy makers and other environmental agencies to make a techno-economic analysis in which multiple scenarios of fuel production mixes could be calculated and compared across each other. Putting the CO_2 mitigation costs in a broader perspective and comparing it with other technologies like electrification of the road and aviation industry, could influence policy makers to create economic incentives for certain technologies.

6 Conclusion

To reduce GHG emissions of transport, the RED-II has set up clear goals and production caps for producing biofuels, to increase sustainability and to decrease uncertainty related to production. Advanced biofuels are therefore likely to develop in the period 2020-2030 as a result of the sub-target set by the RED-II, which states biofuels listed in part A of Annex IX need to contribute 3.5% of the total road transport sector by the end of 2030. To contribute to these targets, the advanced biofuels must show compliance to the set GHG emission reduction threshold of 65% in 2023 compared to the fossil fuel counterpart. This research therefore assessed the lifecycle GHG emissions of advanced biofuel production systems for road and aviation markets, using the LCA theory developed by ISO (2006) combined with the calculation rules of the RED-II. Using a dynamic spatially explicit model, the GHG emissions of synthetic/bio-diesel, -gasoline, -methanol, -DME, -ethanol and -RJF using various conversion processes with 13 different feedstocks were calculated.

Due to the high number of possible feedstock-conversion combinations, only a selection was used to compare GHG performance of the produced fuels. To this selection, four important variables including feedstock type, transport distance, pelletisation and the H_2 energy source were changed to analyse the effect on the GHG performance. Additionally four case studies were assessed, representing realistic spatially explicit supply chains. A sensitivity analysis was applied to these case studies as well the impact of changing the method of dealing with multifunctionally.

The total possible range of GHG emissions of all possible supply chains are large. The selected supply chain for the analysis of the GHG performance, based on forest residues with 500km transportation distance, is at the bottom part of this range. It was found that the best performing processes are gasification and synthesis into methanol and DME (≈8.1gCO_2eq/MJ), closely followed by the FT fuels (≈8.8gCO_2eq/MJ). The GHG performance of ethanol production depends on the process, where syngas fermentation performs better compared to biochemical fermentation (≈15/20g CO_2eq/MJ respectively). HTL fuels made with H_2 from SMR perform better than with internal biomass gasification made H_2 (≈18.8/20.5gCO_2eq/MJ respectively). Pyrolysis fuels with internal biomass gasification for H_2 requirements performed worse than HTL (≈25gCO2eq/MJ). Then ethanol upgrading to RJF follows (≈30 gCO_2eq/MJ) with the worst performing process of pyrolysis with SMR made H_2 coming in last (≈41 g CO_2eq/MJ). All produced fuels show compliance to the RED-II emission saving threshold, except the pyrolysis fuels using SMR made H_2. Changing the four important variables on the selected supply chain, created significant differences in GHG performance of the fuels and induced compliance to the RED-II saving threshold.

Using dedicated energy crops instead of residues can triple the feedstock production GHG emissions, due to fertilizer and pesticide use. Higher feedstock production emissions especially affects conversion processes where the total emissions are mainly caused by the feedstock production and not by the requirements of auxiliary services like H_2, conversion chemicals or electricity usage. This is therefore mainly important for gasification and synthesis processes and less important for HTL, pyrolysis or ethanol production.

Increasing the transportation distance increases the GHG emissions, where the difference between an European supply chain of 500km compared to an international supply chain of 17500km can double or quadruple the GHG emissions. Changing the transportation mode from truck to ship, which has a lower fuel consumption, can limit the rise of these emissions. A higher feedstock energy density per mass and volume also limits transportation emissions.

Pelletising upstream in the supply chain reduces transportation emissions, due to higher energy density and lower MC as well as an increased reactor efficiency for the thermochemical processes

which require dry feedstock. However due to the additional emissions allocated to the pellet mill, pelletising is only effective for large transportation distances of 17500km. Pelletising is effective for shorter distances (10000km or 2500 km) when the increased reactor efficiency outweighs the pellet mill emissions. This is the case for the FT fuels and pyrolysis and not for HTL or biochemical fermentation which require wet feedstocks.

Changing the H_2 production energy source from fossil to renewable increases the GHG performance. Pyrolysis requires the largest amount of H_2 compared to HTL and ethanol upgrading to RJF, causing significant differences in GHG performance between renewable generated H_2 and fossil based H_2 production. Using a PEM electrolyser using fossil based electricity could double the GHG emissions compared to SMR produced H_2. Using renewable generated H_2 decreases the GHG emissions to a quarter of SMR, making it the best performing conversion process. For HTL and ATJ this range is less, however it can still cause changes in compliance to the RED-II.

The results of the four case studies with spatially explicit supply chains, showed that SRC willow 30%MC from France or baggage 10%MC from Brazil had the lowest GHG emissions, dependent on the process type. Forest residues 10%MC from Canada follow, with pulpgrade stemwood30%MC from the US having the worst GHG performance. The low electricity emission factor used for pelletisation in Brazil and Canada resulted in an increased GHG performance of these feedstocks. However the long transportation distance from Canada still causes the GHG performance to be second to last. Pulpgrade stemwood scores the lowest, due the high MC of 30% combined with the large distance transported. Almost all case studies showed compliance to the RED-II threshold independent of the conversion process. Ethanol upgrading to RJF and pyrolysis with SMR made H_2 never show compliance.

The first part of the sensitivity analysis showed that changing the method of dealing with multifunctionality significantly changes the GHG performance of the standardized supply chain. Changing from energy to mass allocation generally increases the GHG emission, due to not allocating emissions toward electricity production. Changing to economic value allocation decreases GHG emissions due to the high economic value of electricity, therefore reducing the allocated emissions for the main fuels produced. Using system expansion and accounting for displaced emissions also reduced the emissions, even to a negative point. This was caused by the high emission factor of electricity compared to the main fuel produced.

The second part of the sensitivity analysis, showed that using an optimistic reactor efficiency for certain case studies can result in showing compliance to the RED-II thresholds. This is case for the biochemical ethanol processes using forest residues from Canada. Using renewably made H_2 can also significantly reduce the GHG emissions, where even pyrolysis shows compliance to RED-II threshold independent of the case study. Using renewably made H_2 in ethanol upgrading to RJF with bagasse or SRC willow as feedstock will reduce the GHG emissions enough to also show compliance.

The results of this study confirms that, although advanced biofuels reduce GHG emissions compared to fossil based fuels in transport, many important variables can affect the GHG performance resulting in large possible ranges of these production systems. Some conversion processes have better performance than others, however the total GHG performance of the production systems also heavily depends on the supply chain design (feedstock & transportation) as well as the design of the system itself (H_2 source and pre-treatment technology). Additionally the performance is strongly dependent on the method of dealing with co-products, which can completely alter the results.

In the context of accelerating the implementation of advanced biofuels, uncertainty in these types GHG calculations should be reduced. Consistent types of detailed calculation methods with corresponding databases, with globally accepted assumptions could reduce these uncertainties.

Future research could additionally include a cost assessment, in which CO_2 abatement costs per process can be assessed, making a comparison to other technologies possible. Additionally this creates a more realistic policy decision indicator for advising or creating a future strategy regarding technical development and implementation.

7 References

A. Elgowainy, J. Han, M. Wang, N. Carter, R. Stratton, J. Hileman, A. Malwitz, S. B. (2012). Life Cycle Analysis of Alternative Aviation Fuels in GREET.

Advance fuel project. (2018). *Facilitating market roll-out of RESfuels in the transport sector to 2030 and beyond Participant*.

Agostini, A., Giuntoli, J., Marelli, L., & Amaducci, S. (2019). Flaws in the interpretation phase of bioenergy LCA fuel the debate and mislead policymakers. *The International Journal of Life Cycle Assessment*. https://doi.org/10.1007/s11367-019-01654-2

ALL Power Labs. (2019). The Five Processes of Gasification - ALL Power Labs. Retrieved May 7, 2019, from http://www.allpowerlabs.com/gasification-explained

Antonissen, K. (2016). Greenhouse gas performance of renewable jet fuel : a comparison of conversion pathways ., (May), 1–79.

ANWB. (2019). Dieselprijzen Europa | Bekijk het actuele overzicht | ANWB. Retrieved November 5, 2019, from https://www.anwb.nl/vakantie/reisvoorbereiding/brandstofprijzen-europa

Argonne National Laboratory. (2018a). Greet.excel.

Argonne National Laboratory. (2018b). GREET.net : The Greenhouse Gases, Regulated Emissions, and Energy Use in Transportation Model.

Aspentech. (2019). Aspen Plus. Retrieved from https://www.aspentech.com/en/about-aspentech

Biograce. (2015). The BioGrace GHG calculation tool: a recognised voluntary scheme. Retrieved from https://www.biograce.net/home

Britannica. (2019). Paris Agreement | Summary & Facts | Britannica.com. Retrieved May 15, 2019, from https://www.britannica.com/topic/Paris-Agreement-2015

Buhaug, Ø., Corbett, J. J., Endresen, Ø., Eyring, V., Faber, J., Hanayama, S., … Yoshida, K. (2009). *Second IMO GHG*. Retrieved from http://www.imo.org/en/OurWork/Environment/PollutionPrevention/AirPollution/Documents/SecondIMOGHGStudy2009.pdf

Castello, D., Haider, M. S., & Rosendahl, L. A. (2019). Catalytic upgrading of hydrothermal liquefaction biocrudes: Different challenges for different feedstocks. *Renewable Energy*, *141*, 420–430. https://doi.org/10.1016/j.renene.2019.04.003

Cherubini, F., Bird, N. D., Cowie, A., Jungmeier, G., Schlamadinger, B., & Woess-Gallasch, S. (2009). Energy-and greenhouse gas-based LCA of biofuel and bioenergy systems: Key issues, ranges and recommendations, *53*, 434–447. https://doi.org/10.1016/j.resconrec.2009.03.013

Chomkhamsri, K., Wolf, M.-A., & Pant, R. (2011). International Reference Life Cycle Data System (ILCD) Handbook: Review Schemes for Life Cycle Assessment. In *Towards Life Cycle Sustainability Management* (pp. 107–117). https://doi.org/10.1007/978-94-007-1899-9_11

Daniell, J., Köpke, M., & Simpson, S. D. (2012). *Commercial biomass syngas fermentation*. *Energies* (Vol. 5). https://doi.org/10.3390/en5125372

De Jong, S., Antonissen, K., Hoefnagels, R., Lonza, L., Wang, M., Faaij, A., & Junginger, M. (2017). Life-cycle analysis of greenhouse gas emissions from renewable jet fuel production. *Biotechnology for Biofuels*, *10*(1), 1–18. https://doi.org/10.1186/s13068-017-0739-7

Dimitriou, I., & Rutz, D. (2015). Sustainable Short Rotation Coppice. *© 2015 by WIP Renewable*

Energies, Munich, Germany. Retrieved from https://www.srcplus.eu/images/Handbook_SRCplus.pdf

EC. (1998). *DIRECTIVE 98/70/EC OF THE EUROPEAN PARLIAMENT AND OF THE COUNCIL of 13 October 1998 relating to the quality of petrol and diesel fuels and amending Council Directive 93/12/EEC*. Retrieved from https://eur-lex.europa.eu/resource.html?uri=cellar:9cdbfc9b-d814-4e9e-b05d-49dbb7c97ba1.0008.02/DOC_1&format=PDF

Edwards, R., Hass, H., Larivé, J.-F., Lonza, L., Mass, H., Rickeard, D., … Weindorf, W. (2013). WELL-TO-TANK (WTT) Report. Appendix 1 - Version 4a - Conversion factors and fuel properties WELL-TO-WHEELS. *Joint Research Center of the EU (JRC): Ispra, Italy*, 1–133. https://doi.org/10.2790/95629

Edwards, R., O'Connell, A., Padella, M., Giuntoli, J., Koeble, R., Bulgheroni, C., … Lonza. (2019). *Definition of input data to assess GHG default emissions from biofuels in EU legislation, Version 1c*. https://doi.org/ISBN 978-92-79-66185-3, doi:10.2760/284718, JRC104483

Elbersen, B. (2019). MSc course Biobased Economy :, (February).

Engineering ToolBox. (2003). Fuels - Higher and Lower Calorific Values. Retrieved August 22, 2019, from https://www.engineeringtoolbox.com/fuels-higher-calorific-values-d_169.html

EU. (2018). Directive (EU) 2018/2001 of the European Parliament and of the Council on the promotion of the use of energy from renewable sources. *Official Journal of the European Union*, (L 328), 82–209. Retrieved from https://eur-lex.europa.eu/legal-content/EN/TXT/PDF/?uri=CELEX:32018L2001&from=EN

European Commission. (2010). *Guidelines for the calculation of land carbon stocks for the purpose of Annex V to Directive 2009/28/EC*. *Official Journal of the European Union* (Vol. 17). Retrieved from https://eur-lex.europa.eu/LexUriServ/LexUriServ.do?uri=OJ:L:2010:151:0019:0041:EN:PDF

European Parliament. (2009). Renewable Energy Directive 2009/28/CE. *Jornal Oficial Da União Europeia*, *2008*(2), 16–62. https://doi.org/10.3000/17252555.L_2009.140.eng

European Parliament. (2018). DIRECTIVE (EU) 2018/2001 OF THE EUROPEAN PARLIAMENT AND OF THE COUNCIL of 11 December 2018 on the promotion of the use of energy from renewable sources (recast). *Official Journal of the European Union*, *2018*(December). Retrieved from https://eur-lex.europa.eu/legal-content/EN/TXT/PDF/?uri=CELEX:32018L2001&from=EN

finanzen.nl. (2019). Ethanolprijs in Euro. Retrieved November 5, 2019, from https://www.finanzen.nl/grondstoffen/ethanolprijs/euro

Fritsche, U. R., & Iriarte, L. (2014). Sustainability criteria and indicators for the bio-based economy in Europe: State of discussion and way forward. *Energies*, *7*(11), 6825–6836. https://doi.org/10.3390/en7116825

Geraedts, S. (2018). Goodfuels: Potential for Pyrolysis in the Marine market.

Giuntoli, J., Agostini, A., Edwards, R., & Marelli, L. (2017). Solid and gaseous bioenergy pathways: input values and GHG emissions. https://doi.org/10.2790/27486

Goedkope energie en Gas.nl. (2019). kWh-Prijs in 2019 - Hoe hoog ligt de prijs per kWh? Retrieved November 5, 2019, from https://goedkopeenergieengas.nl/energie/prijs-per-kwh/

Hannula, I., & Kurkela, E. (2013). *Liquid transportation fuels bed gasification of lignocellulosic biomass*. *VTT Technology* (Vol. 91). Retrieved from http://www.vtt.fi/publications/index.jsp

Hoefnagels, R., Smeets, E., & Faaij, A. (2010). Greenhouse gas footprints of different biofuel

production systems. *Renewable and Sustainable Energy Reviews*, *14*(7), 1661–1694. https://doi.org/10.1016/j.rser.2010.02.014

Hofbauer, H., Rauch, R., & Ripfel-Nitsche, K. (2007). *Report on Gas Cleaning for Synthesis Applications Work Package 2E: Gas treatment Deliverable: 2E-3 prepared by*. Retrieved from www.thermalnet.co.uk.

Iglesias Gonzalez, M., Kraushaar-Czarnetzki, B., & Schaub, G. (2011). Process comparison of biomass-to-liquid (BtL) routes Fischer-Tropsch synthesis and methanol to gasoline. *Biomass Conversion and Biorefinery*, *1*(4), 229–243. https://doi.org/10.1007/s13399-011-0022-2

IMO. (2015). *Third IMO GHG Study 2014: Executive Summary and Final Report*. Retrieved from www.imo.org

International Panel Climate Change. (2016). Global Warming Potential Values. *Greenhouse Gas Protocol*, *2014*(1995), 2–5. Retrieved from www.ipcc.ch

IPCC. (2006). IPCC Guidelines for National Greenhouse Gas Inventories. Chapter 11: N2O emissions from managed soils, and CO2 emissions from lime and urea application, *4*, 11.1-11.54. Retrieved from https://www.ipcc-nggip.iges.or.jp/public/2006gl/pdf/4_Volume4/V4_11_Ch11_N2O&CO2.pdf

IRENA. (2016). *INNOVATION OUTLOOK ADVANCED LIQUID BIOFUELS Copyrightt©©IRENAAAAAA*. Retrieved from https://www.irena.org/-/media/Files/IRENA/Agency/Publication/2016/IRENA_Innovation_Outlook_Advanced_Liquid_Biofuels_2016.pdf

ISO. (2006). *ISO 14040:2006(en), Environmental management — Life cycle assessment — Principles and framework*. Retrieved from https://www.iso.org/obp/ui/#iso:std:iso:14040:ed-2:v1:en

Jonker, J. G. G., van der Hilst, F., Junginger, H. M., Cavalett, O., Chagas, M. F., & Faaij, A. P. C. (2015). Outlook for ethanol production costs in Brazil up to 2030, for different biomass crops and industrial technologies. *Applied Energy*, *147*, 593–610. https://doi.org/10.1016/j.apenergy.2015.01.090

JRC, & Hoefnagels, R. (2011). Excel calculation model: Supply costs and GHG emissions of various supply chains.

Junginger, M. (2018). Forest carbon accounting Basic principle of GHG emission reductions through bioenergy.

Kampman, B., Delft, C. E., Verbeek, R., Van Grinsven, A., Pim Van Mensch,), Croezen, H., & Patuleia, A. (2013). *Bringing biofuels on the market Options to increase EU biofuels volumes beyond the current blending limits Author(s): 4.567.1-Bringing biofuels on the market Publication Data*. Retrieved from www.cedelft.eu

Kan, T., Strezov, V., & Evans, T. J. (2016). Lignocellulosic biomass pyrolysis : A review of product properties and effects of pyrolysis parameters. *Renewable and Sustainable Energy Reviews*, *57*, 1126–1140. https://doi.org/10.1016/j.rser.2015.12.185

Karatzos, S., Mcmillan, J. D., & Saddler, J. N. (2014). *The Potential and Challenges of Drop-in Biofuels A Report by IEA Bioenergy Task 39 AUTHORS*. Retrieved from http://task39.sites.olt.ubc.ca/files/2014/01/Task-39-Drop-in-Biofuels-Report-FINAL-2-Oct-2014-ecopy.pdf

Khanna, M., & Zilberman, D. (2017). *Handbook of bioenergy economics and policy: Volume II modeling land use and greenhouse gas implications conclusion*. *Handbook of Bioenergy*

Economics and Policy, Vol Ii: Modeling Land Use and Greenhouse Gas Implications (Vol. 40). Retrieved from http://www.springer.com/series/6360

Kumar, D., & Murthy, G. S. (2012). Life cycle assessment of energy and GHG emissions during ethanol production from grass straws using various pretreatment processes. *The International Journal of Life Cycle Assessment*, *17*(4), 388–401. https://doi.org/10.1007/s11367-011-0376-5

Lücking, L. . (2017). Methanol Production from Syngas. *At the Delft University of Technology,* 113.

Mehmeti, A., Angelis-Dimakis, A., Arampatzis, G., McPhail, S., & Ulgiati, S. (2018). Life Cycle Assessment and Water Footprint of Hydrogen Production Methods: From Conventional to Emerging Technologies. *Environments*, *5*(2), 24. https://doi.org/10.3390/environments5020024

Mu, D., Seager, T., Rao, P. S., & Zhao, F. (2010). Comparative Life Cycle Assessment of Lignocellulosic Ethanol Production: Biochemical Versus Thermochemical Conversion. *Environmental Management*, *46*(4), 565–578. https://doi.org/10.1007/s00267-010-9494-2

Mundi Index. (2015). Cotton - Daily Price - Commodity Prices - Price Charts, Data, and News. Retrieved November 5, 2019, from https://www.indexmundi.com/commodities/?commodity=jet-fuel

Nanda, S., A. Kozinski, J., & K. Dalai, A. (2015). Lignocellulosic Biomass: A Review of Conversion Technologies and Fuel Products. *Current Biochemical Engineering*, *3*(1), 24–36. https://doi.org/10.2174/2213385203666150219232000

Nanda, S., Mohammad, J., & Reddy, S. N. (2014). Pathways of lignocellulosic biomass conversion to renewable fuels, 157–191. https://doi.org/10.1007/s13399-013-0097-z

National Energy technology Laboratory. (2019). 10.4. Conversion of Methanol to Gasoline | netl.doe.gov. Retrieved May 14, 2019, from https://www.netl.doe.gov/research/coal/energy-systems/gasification/gasifipedia/methanol-to-gasoline

Nieuwlaar, E. (2017). Energy conversion technologies.

Olofsson, J., Barta, Z., Börjesson, P., & Wallberg, O. (2017). Integrating enzyme fermentation in lignocellulosic ethanol production: life-cycle assessment and techno-economic analysis. *Biotechnology for Biofuels*, *10*(1), 51. https://doi.org/10.1186/s13068-017-0733-0

Papadokonstantakis, S. (2018). *Advancefuel Project: D3.2 Definition of biomass ref-erence technologies with re-spect to TRL and performance indicators*. Retrieved from www.ADVANCEFUEL.eu

Papadokonstantakis, S., & Johnsson, F. (2018). *Advancefuel Project: Biomass conversion technol-ogies-Definitions D3.1 Report on definition of parameters for defining biomass conversion tech-nologies*. Retrieved from www.ADVANCEFUEL.eu

Pierobon, F., Eastin, I. L., & Ganguly, I. (2018). Life cycle assessment of residual lignocellulosic biomass-based jet fuel with activated carbon and lignosulfonate as co-products. *Biotechnology for Biofuels*, *11*, 139. https://doi.org/10.1186/s13068-018-1141-9

Plevin, R. J., Delucchi, M. A., & Creutzig, F. (2014). Using Attributional Life Cycle Assessment to Estimate Climate-Change Mitigation Benefits Misleads Policy Makers. *Journal of Industrial Ecology*, *18*(1), 73–83. https://doi.org/10.1111/jiec.12074

PricewaterhouseCoopers et al. (2017). Sustainable and optimal use of biomass for energy in the EU beyond 2020, (May 2017), 198. Retrieved from https://ec.europa.eu/energy/sites/ener/files/documents/biosustain_report_final.pdf

Rehl, T., Lansche, J., & Müller, J. (2012). Life cycle assessment of energy generation from biogas—Attributional vs. consequential approach. *Renewable and Sustainable Energy Reviews*, *16*(6), 3766–3775. https://doi.org/10.1016/J.RSER.2012.02.072

Scarlat, N., & Dallemand, J.-F. (2011). Recent developments of biofuels/bioenergy sustainability certification: A global overview. *Energy Policy*, *39*(3), 1630–1646. https://doi.org/10.1016/J.ENPOL.2010.12.039

Searchinger, T., Heimlich, R., Houghton, R. A., Dong, F., Elobeid, A., Fabiosa, J., … Yu, T.-H. (1989). Supporting Online Material Use of U.S. Croplands for Biofuels Increases Greenhouse Gases Through Emissions from Land-Use Change. *24. R. Hammerschlag, Environ. Sci. Technol*, *24*(23), 30. https://doi.org/10.1126/science.1152747

Ship and Bunker. (2018). World Bunker Prices. Retrieved November 5, 2019, from https://shipandbunker.com/prices

Skowroñska, M., & Filipek, T. (2014). Life cycle assessment of fertilizers: A review. *International Agrophysics*, *28*(1), 101–110. https://doi.org/10.2478/intag-2013-0032

SkyNRG. (2019). SkyNRG | the market leader for Sustainable Aviation Fuel. Retrieved July 5, 2019, from https://skynrg.com/

Stehfest, E., & Bouwman, L. (2006). N2O and NO emission from agricultural fields and soils under natural vegetation: summarizing available measurement data and modeling of global annual emissions. *Nutrient Cycling in Agroecosystems* , *74*, 207–228. Retrieved from https://link.springer.com/content/pdf/10.1007%2Fs10705-006-9000-7.pdf

Swanson, R. M., Satrio, A. J., Brown, C. R., Planton, A., & David, D. H. (2010). Techno-Economic Analysis of Biofuels Production Based on Gasification. *National Renewable Energy Laboratory*. Retrieved from https://www.nrel.gov/docs/fy11osti/46587.pdf

Tews, I. J., Zhu, Y., Drennan, C., Elliott, D. C., Snowden-Swan, L. J., Onarheim, K., … Beckman, D. (2014). *Biomass Direct Liquefaction Options. TechnoEconomic and Life Cycle Assessment*. https://doi.org/10.2172/1184983

Tijmensen, M. J. A., Faaij, A. P. C., Hamelinck, C. N., & van Hardeveld, M. R. M. (2002). Exploration of the possibilities for production of Fischer Tropsch liquids and power via biomass gasification. *Biomass and Bioenergy*, *23*(2), 129–152. https://doi.org/10.1016/S0961-9534(02)00037-5

United Nations Climate Change. (2015). What is the Paris agreement? *The Paris Agreement*. Retrieved from https://unfccc.int/process-and-meetings/the-paris-agreement/what-is-the-paris-agreement

Uslu, A., Detz, R. J., & Mozaffarian, H. (2018). *Advancefuel Project: Barriers to advanced liquid biofuels & renewable liquid fuels of non-biological origin D1.1 Key barriers to advanced fuels-Results of the stakeholder consultation*. Retrieved from www.ADVANCEFUEL.eu

van der Hilst, F., Hoefnagels, R., Junginger, M., Londo, M., Shen, L., & Wicke, B. (2018). Biomass Provision and Use: Sustainability Aspects. *Energy from Organic Materials (Biomass)*, 1353–1381. https://doi.org/10.1007/978-1-4939-7813-7_1048

van Dijck. (2019). van Dijck MC products. Retrieved November 5, 2019, from https://www.vandijckmx.nl/racing-fuels-race-benzine-racebenzine-van-dijck-racing-fuels/methanol-drum-200ltr/

van Vliet, O. P. R., Faaij, A. P. C., & Turkenburg, W. C. (2009). Fischer-Tropsch diesel production in a well-to-wheel perspective: A carbon, energy flow and cost analysis. *Energy Conversion and*

Management, *50*(4), 855–876. https://doi.org/10.1016/j.enconman.2009.01.008

Walther, G.-R., Post, E., Convey, P., Menzel, A., Parmesan, C., Beebee, T. J. C., … Bairlein, F. (2002). Ecological responses to recent climate change. *Nature*, *416*(6879), 389–395. https://doi.org/10.1038/416389a

Wang, L., Littlewood, J., & Murphy, R. J. (2013). Environmental sustainability of bioethanol production from wheat straw in the UK. *Renewable and Sustainable Energy Reviews*, *28*, 715–725. https://doi.org/10.1016/J.RSER.2013.08.031

Wang, M. Q., Han, J., Haq, Z., Tyner, W. E., Wu, M., & Elgowainy, A. (2011). Energy and greenhouse gas emission effects of corn and cellulosic ethanol with technology improvements and land use changes. *Biomass and Bioenergy*, *35*(5), 1885–1896. https://doi.org/10.1016/J.BIOMBIOE.2011.01.028

Wicke, B. (2017). Sustainability of the biobased economy : Who am I ?, 1–66.

Wiloso, E. I., Heijungs, R., & de Snoo, G. R. (2012). LCA of second generation bioethanol: A review and some issues to be resolved for good LCA practice. *Renewable and Sustainable Energy Reviews*, *16*(7), 5295–5308. https://doi.org/10.1016/J.RSER.2012.04.035

Wu, M., Wang, M., & Huo, H. (2006). Fuel-Cycle Assessment of Selected Bioethanol Production Pathways in the United States. *Anl/Esd/06-7*, 65.

Zabed, H., Sahu, J. N., Boyce, A. N., & Faruq, G. (2016). Fuel ethanol production from lignocellulosic biomass : An overview on feedstocks and technological approaches. *Renewable and Sustainable Energy Reviews*, *66*, 751–774. https://doi.org/10.1016/j.rser.2016.08.038

Zactruba, J. (2010). The Efficiency of Power Plants of Different Types. Retrieved October 9, 2019, from https://www.brighthubengineering.com/power-plants/72369-compare-the-efficiency-of-different-power-plants/

Appendix

A. Formulas N_2O field emissions

The following formulas can be used to calculate the N_2O field emissions of a specific piece of land using specific amounts of fertilizers. The formulas cohere the RED-II methodology (Edwards et al., 2019; IPCC, 2006).

$$N_2O_{Total} = N_2O_{Direct\ for\ mineral\ soils} + N_2O_{Direct\ for\ organic\ soils} + N_2O_{Indirect\ for\ mineral\ \&\ organic\ soils}$$

Where,

$$N_2O_{Direct\ for\ mineral\ soils} = (F_{SN} + F_{ON}) * EF_{ij} + F_{CR} * EF_1$$

$$N_2O_{Direct\ for\ organic\ soils} = (F_{SN} + F_{ON}) * EF_1 + F_{CR} * EF_1 + F_{OS,CG,TEMP} * EF_{2CG,TEMP} + F_{OS,CR,TROP} * EF_{2CG,TROP}$$

$$N_2O_{Indirect\ for\ mineral\ \&\ organic\ soils} = (F_{SN} * Frac_{GASF} + F_{ON} * Frac_{GASM}) * EF_4 + (F_{SN} + F_{ON} + F_{CR}) * Frac_{Leach} * EF_5$$

With,

N_2O_{Total} = Total direct & indirect annual N_2O emission produced from organic and mineral soils (kg N/ha/y)

$N_2O_{Direct\ for\ mineral\ soils}$ = Total direct annual N_2O emissions produced from mineral soils (kg N/ha/y)

$N_2O_{Direct\ for\ organic\ soils}$ = Total direct annual N_2O emissions produced from organic soils (kg N/ha/y)

$N_2O_{Indirect\ for\ mineral\ \&\ organic\ soils}$ = Total indirect annual N_2O emissions produced from mineral & organic soil (kg N/ha/y)

F_{SN} = annual synthetic N fertilizers input (kg N/ha/y)

F_{ON} = annual animal manure N applied as fertilizer (kg N/ha/y)

F_{CR} = annual amount of N in crop residues (kg N/ha/y)

$F_{OS,CG,TEMP}$ = annual area of managed/drained organic soils under cropland in temperate climate (ha/y)

$F_{OS,CR,TROP}$ = annual area of managed/drained organic soils under cropland in tropical climate (ha/y)

$Frac_{GASF}$ = 0.10 ((kg N NH_3 + NO_x)/kg N applied)

$Frac_{GASM}$ = 0.20 ((kg N NH_3 + NO_x)/kg N applied)

$Frac_{Leach}$ = 0.30 (kg N/ kg N additions)

EF_1 = 0.01 (kg N/ Kg N input)

EF_{ij} = Crop and site-specific emission factors (Stehfest & Bouwman, 2006)

$EF_{2CG,TEMP}$ = 8 (kg N/ha/y)

$EF_{2CG,TROP}$ = 16 (kg N/ha/y)

EF_4 = 0.01 ((kg N/ (kg N NH_3 + NO_x))

EF_5 = 0.0075 (kg N/ kg N leaching)

B. Cultivation input values

Table 12 - Cultivation input values of dedicated energy feedstocks

Category	Feedstock						Unit
	SRC Eucalyptus	SRC Poplar WF	SRC Poplar WOF	SRC Willow	Switchgrass	Miscanthus	
Yield	25800	28000	20000	26500	1090	1090	kg ha-1 year-1
Moisture content	0.5	0.5	0.5	0.5	0.3	0.3	
Energy consumption							
Diesel	1469	3352.8352	3352.8352	4240	97.68763774	96.74762174	MJ ha-1 year-1
Agro chemicals							
Synthetic N-fertiliser (kg N)	228.2	76.72	0	68.37	2.53734124	2.51292524	kg N ha-1 year-1
Manure	0	20000	20000	0	0	0	kg N ha-1 year-1
CaO-fertiliser (calculated as kg CaO)	266.3	60.48	0	0	25	25	kg CaO ha-1 year-1
K2O-fertiliser (kg K2O)	182.6	51.24	0	0	82.7	82.7	kg K2O ha-1 year-1
P2O5-fertiliser (kg P2O5)	87.5	25.48	0	0	10.2	10.2	kg P2O5 ha-1 year-1
Pesticides	1.6	3.92	4	7.95	0.012686706	0.012564626	kg ha-1 year-1
Field CO2 emissions (acidification)	74.2653			0			kg ha-1 year-1
Seeding material							
Seeds-eucalyptus cuttings	51.471	55.86	39.9	0	0	0	kg ha-1 year-1
Field N2O emissions	4.73	1.7822	0	1.7	0.062254696	0.06168092	kg ha-1 year-1
Source	(Edwards et al., 2019; Giuntoli et al., 2017)	(Edwards et al., 2019; Giuntoli et al., 2017)	(Edwards et al., 2019; Giuntoli et al., 2017)	(Edwards et al., 2019; Giuntoli et al., 2017)	(JRC & Hoefnagels, 2011)	(JRC & Hoefnagels, 2011)	

C. Formulas carbon stock

The calculation for the carbon stock of a piece of land can be done with the formulas below which are based upon European Commission (2010). The calculations are coherent with the RED-II calculations. For extra explanation see the report of (European Commission, 2010). To the total carbon stock of a piece of land i is expressed as CS_i where:

$$CS_i = (SOC + C_{VEG}) * A$$

$$SOC = SOC_{ST} * F_{LU} * F_{MG} * F_l$$

$$C_{VEG} = C_{BM} + C_{DOM}$$

$$C_{BM} = C_{AGB} + C_{BGB}$$

$$C_{AGB} = B_{AGB} * CF_B$$

$$C_{BGB} = B_{BGB} * CF_B$$

$$C_{DOM} = C_{DW} + C_{LI}$$

$$C_{DW} = DOM_{DW} * DF_{DW}$$

$$C_{LI} = DOM_{LI} * CF_{LI}$$

All formulas can be rewritten in 1 formula making:

$$CS_i = \Big(\big((DOM_{LI} * CF_{LI}) + (DOM_{DW} * CF_{DW})\big) + \big((B_{BGB} * CF_B) + (B_{AGB} * CF_B)\big)\Big) + (SOC_{ST} * F_{LU} * F_{MG} * F_l)\Big) * A$$

With,

DOM_{LI} = Weight of litter (measured as mass of dry matter per hectare).

CF_{LI} = 0.4 Carbon fraction of dry matter in litter (measured as mass of carbon per mass of dry matter).

DOM_{DW} = Weight of dead wood pool (measured as mass of dry matter per hectare).

CF_{DW} = 0.5 Carbon fraction of dry matter in dead wood pool (measured as mass of carbon per mass of dry matter).

B_{BGB} = Weight of below ground living biomass (measured as mass of dry matter per hectare).

CF_B = 0.47 Carbon fraction of dry matter in living biomass (measured as mass of carbon per mass of dry matter).

B_{AGB}= Weight of above ground living biomass (measured as mass of dry matter per hectare).

CF_B = 0.47 Carbon fraction of dry matter in living biomass (measured as mass of carbon per mass of dry matter).

SOC_{ST} = Standard soil organic carbon in the 0-30 centimetre topsoil layer (measured as mass of carbon per hectare), value can be found in point 6 of the report of European Commission (2010).

F_{LU} = Land use factor reflecting the difference in soil organic carbon associated with the type of land use compared to the standard soil organic carbon, value can be found in point 7 of the report of European Commission (2010).

F_{MG} = Management factor reflecting the difference in soil organic carbon associated with the principle management practice compared to the standard soil organic carbon, value can be found in point 7 of the report of European Commission (2010).

F_l = Input factor reflecting the difference in soil organic carbon associated with different levels of carbon input to soil compared to the standard soil organic carbon, value can be found in point 7 of the report of European Commission (2010).

A = Factor scaling to the area concerned (measured as hectares per unit area).

D. Emission factors and economic value of fuels & electricity

Table 13 -GHG emission factors of fuels and average electricity mix Europe

Fuel characteristics (1)	gCO_2/ MJ	gCH_4/ MJ	gN_2O/ MJ	Combustion gCO2-eq/MJ	TOT $gCO_{2\text{-}eq}$/MJ	Source
Diesel	95.1				95.1	(Edwards et al., 2019)
Gasoline	93.3				93.3	(Edwards et al., 2019)
Heavy Oil	94.2	0	0		94.2	(Edwards et al., 2019)
Ethanol					0	JEC E3-database (version 31-7-2008)
Methanol	28.2	0.0001	0	68.9	97.1025	(Edwards et al., 2019)
RJF						(Edwards et al., 2013)
DME					0	JRC scientific report EUR 27215 EN *
HFO for maritime use	94.2				94.2	(Edwards et al., 2019)
Natural gas (2500, EU Mix quality)	5.4	0.17	0.000167	56.2	65.899766	(Edwards et al., 2019)
Propane	60				60	(Engineering ToolBox, 2003)
Methane	5.4				65.899766	(Engineering ToolBox, 2003)
Electricity EU mix HV	126.8	0.3	0.006		136.088	(Edwards et al., 2019)
Electricity EU mix MV	131.6	0.31	0.006		141.138	(Edwards et al., 2019)
Electricity EU mix LV	139.9	0.33	0.01		151.13	(Edwards et al., 2019)

Table 14 – Energy density fuels

Fuel characteristics (2)	kg/m³ (at 0% water, unless otherwise stated)	LHVdry (at 0% water, unless otherwise stated)	Source
Diesel	832	43.1	(Edwards et al., 2019)
Gasoline	745	43.2	(Edwards et al., 2019)
Heavy Oil	970	40.5	(Edwards et al., 2019)
Ethanol	794	26.81	JEC E3-database (version 31-7-2008)
Methanol	793	19.9	(Edwards et al., 2019)
RJF	832	43.1	(Edwards et al., 2019)
DME	670	28.4	(Edwards et al., 2019)
HFO for maritime use	970	40.5	(Edwards et al., 2019)
Natural gas (2500, EU Mix quality)			(Edwards et al., 2019)
Propane		50.4	(Engineering ToolBox, 2003)
Methane		50	(Engineering ToolBox, 2003)
Hydrogen		120 LHV 141.7 HHV	(Engineering ToolBox, 2003)

Table 15 – Economic value fuels and electricity

Fuel characteristics (3)	Retail price (Euro/L)	Retail price (Euro/MJ)	Source
Diesel	1.4	0.027025522	(ANWB, 2019)
Gasoline	1.65	0.028454861	(ANWB, 2019)
HFO	0.46	0.011017284	(Ship and Bunker, 2018)
Ethanol	1	0.029615815	(finanzen.nl, 2019)
Methanol	2.115	0.084281156	(van Dijck, 2019)
RJF	0.65	0.012547564	(Mundi Index, 2015)
DME	2.115	0.049896127	(van Dijck, 2019)
HFO for maritime transport	0.46	0.011017284	(Ship and Bunker, 2018)
Electricity		0.063666667	(Goedkope energie en Gas.nl, 2019)

Table 16 – GHG emission factors of electricity mixes of specific countries used in case studies

	gCO_2/MJ	gCH_4/MJ	gN_2O/MJ	TOT $gCO_{2\text{-eq}}$/MJ	Source
The Netherlands	141	0.159	0.00575	141	(JRC & Hoefnagels, 2011)
Brazil	28.5	0.0579	0.00293	28.5	(JRC & Hoefnagels, 2011)
Canada	52.1	0.0779	0.00193	52.1	(JRC & Hoefnagels, 2011)
USA	170	0.341	0.00564	170	(JRC & Hoefnagels, 2011)
France	21.6	0.0334	0.000978	21.6	(JRC & Hoefnagels, 2011)

E. Conversion chemicals and inputs characteristics

Table 17 – GHG emission factors of agricultural inputs

Agricultural inputs	**gCO_2/kg**	**gCH_4/kg**	**gN_2O/kg**	**TOT $gCO_{2\text{-eq}}$/kg**	**Source**
Synthetic N-fertiliser (kg N)	3877	2.17	2.15	4571.95	(Edwards et al., 2019)
P2O5-fertiliser (kg P2O5)				541.7	(Edwards et al., 2019)
K2O-fertiliser (kg K2O)				416.7	(Edwards et al., 2019)
CaO-fertiliser (calculated as kg CaO)				69.7	(Edwards et al., 2019)
Pesticides	11209.6	11.98	1.68	12009.74	(Edwards et al., 2019)

Table 18 - GHG emission factors of conversion chemicals

Conversion chemicals inputs	**gCO2/kg**	**gCH4/kg**	**gN2O/kg**	**COM gCO2-eq/kg**	**TOT gCO2-eq/kg**	**Source**
Sodium hydroxide (NaOH)	485.5	1.445	0.027		529.671	(Edwards et al., 2019)
Corn steep liquor	810	1.93	2.78		1686.69	(Edwards et al., 2019)
DEPG	2140	4.3	0.15		2292.2	(Edwards et al., 2019)
Olivine	386.55	0.69	0.0059		405.5582	(Edwards et al., 2019)
Dolomite	16.3	0.02193	0.00016		16.89593	(Edwards et al., 2019)
Urea	1390				1390	(Edwards et al., 2019)
Tar catalyst	4160	10.99	1.86		4989.03	(Skowroñska & Filipek, 2014)
Synthesis catalyst	3520	12.5	1.3		4219.9	(Edwards et al., 2019)
Yeast	2149	6.57	0.0063		2315.1274	(Edwards et al., 2019)
Pure CaO for processes	1188.47	0.1	0.008		1193.354	(Argonne National Laboratory, 2018b)
Cellulase	1556	3.9	1.55		2115.4	(Edwards et al., 2019)
Sulphuric acid (H2SO4)	210.2	0.236	0.005		217.59	(Argonne National Laboratory, 2018b)
Ammonia (NH3)	2350.6	0.003	0.002		2351.271	(Edwards et al., 2019)
Alpha-amylase	1000	0	0		1000	(Edwards et al., 2019)
Gluco-amylase	7500	0	0		7500	(Edwards et al., 2019)
Diammonium phosphate (DAP)	653.2	0.808			673.4	(Edwards et al., 2019)

F. Feedstock characteristics

Table 19 – Feedstock energy content in LHV_{dry} and corrected LHV_{dry}

Type of feedstock	Moisture content	LHV_{dry} (MJ/Kg)	Corrected LHV_{dry} for MC (MJ/Kg)	Source
Woodchips forest residues 50%MC	50%	19	17.779	(Giuntoli et al., 2017)
Woodchips forest residues 30%MC	30%	19	18.2674	
Pellets forest residues 10%MC	10%	19	18.7558	
Woodchips eucalyptus (SRC) 50%MC	50%	19	17.779	
Woodchips eucalyptus (SRC) 30%MC	30%	19	18.2674	
Pellets eucalyptus (SRC) 10%MC	10%	19	18.7558	
Woodchips poplar with fertilizer 50%MC	50%	19	17.779	
Woodchips poplar with fertilizer 30%MC	30%	19	18.2674	
Pellets poplar with fertilizer 10%MC	10%	19	18.7558	
Woodchips poplar without fertilizer 50%MC	50%	19	17.779	
Woodchips poplar without fertilizer 30%MC	30%	19	18.2674	
Pellets poplar without fertilizer 10%MC	10%	19	18.7558	
Woodchips stemwood 50%MC	50%	19	17.779	
Woodchips stemwood 30%MC	30%	19	18.2674	
Pellets stemwood 10%MC	10%	19	18.7558	
Woodchips willow 50%MC	50%	19	17.779	
Woodchips willow 30%MC	30%	19	18.2674	
Pellets willow 10%MC	10%	19	18.7558	
Woodchips bagasse 50%MC	50%	17	15.779	
Pellets bagasse 10%MC	10%	17	16.7558	
Fresh switchgrass 30%MC	30%	17.36	16.6274	(JRC & Hoefnagels, 2011)
Bales switchgrass 13.5%MC	14%	17.36	17.03033	(JRC & Hoefnagels, 2011)
Pellets switchgrass 10%MC	10%	17.36	17.1158	(JRC & Hoefnagels, 2011)
Fresh miscanthus 30%MC	30%	17.2	16.4674	(JRC & Hoefnagels, 2011)
Bales miscanthus 13.5%MC	14%	17.2	16.87033	(JRC & Hoefnagels, 2011)
Pellets miscanthus 10%MC	10%	17.2	16.9558	(JRC & Hoefnagels, 2011)
Woodchips industry residues 30%MC	30%	19	16.4674	(Giuntoli et al., 2017)
Pellets industry residues 10%MC	10%	17.2	18.7558	
Fresh straw 30%MC	30%	17.2	16.4674	
Bales straw 13.5%MC	14%	17.2	16.87033	
Pellets straw 10%MC	10%	17.2	16.9558	
Pellets agricultural residues 10%MC	10%	17.2	16.9558	
Sawdust (wet and dry)	14%	17.2	16.87033	
Sawdust (wet)	30%	17.2	16.4674	
Sawdust (dry)	0.1	17.2	16.9558	

G. Transportation characteristics

Table 20 - Transportation characteristics

Type of transport and their characteristics	Fuel	CH4 emissions (g/t*km)	N02 emissions (g/t*km)	CO2 emissions (g/t*km)	Tot emissions (g/t*km)	Source
Truck (40 ton) for dry product (Diesel)	Diesel	0.003382	0.001501	77.42408	77.955928	(Edwards et al., 2019; Giuntoli et al., 2017)
Truck (40 ton) for chips (and similar size dry product) (Diesel)	Diesel	0.003512077	0.001558731	80.10083678	80.65314047	(Edwards et al., 2019; Giuntoli et al., 2017)
Truck (40 ton) for pellets (Diesel)	Diesel	0.00365256	0.00162108	83.30487025	83.87926609	(Edwards et al., 2019; Giuntoli et al., 2017)
Truck (40 ton) for liquids (Diesel)	Diesel	0.003642154	0.001616462	83.06753444	83.64029382	(Edwards et al., 2019; Giuntoli et al., 2017)
Truck (40 ton) for manure (Diesel)	Diesel	0.00365256	0.00162108	83.30487025	83.87926609	(Edwards et al., 2019; Giuntoli et al., 2017)
Truck (40 ton) for biowaste (Diesel)	Diesel	0.003512077	0.001558731	80.10083678	80.65314047	(Edwards et al., 2019; Giuntoli et al., 2017)
Truck (40 ton) for sugar cane transport	Diesel	0.000601879	0.003919554	130.6717557	131.8548297	E3-database (june 2014)
Truck (40 ton) for sugar cane transport (brazil)	Diesel	0.01529	0.00298	158.97	160.24029	(Jonker et al., 2015)
Truck (20 ton) for Jatropha seed transport (Diesel)	Diesel	0.0016	0.0012	171.18	171.5776	E3-database (June 2014)
Truck (12 ton) for FFB transport (Diesel)	Diesel	0.00199	0.0015	212.8162381	213.3129881	E3-database (June 2014)
Dumpster truck MB2213 for filter mud transport	Diesel	0	0	342.36	342.36	E3-database (June 2014)
Tanker truck MB2318 for vinasse transport	Diesel	0	0	205.416	205.416	E3-database (June 2014)
Tanker truck MB2318 for cane seed transport	Diesel	0	0	248.074056	248.074056	E3-database (June 2014)
Tanker truck with water cannons for vinasse transport	Diesel	0	0	89.0136	89.0136	E3-database (June 2014)
Ocean bulk carrier Panamax (Fuel oil)	HFO for maritime transport	0	0	9.5072292	9.5072292	E3-database (June 2014)
Inland bulk carrier 8.8 kt (diesel)	Diesel	0.093	0.0004	30.8124	33.2566	E3-database (June 2014)
Inland ship for oil transport, 1.2 kt (diesel)	HFO for maritime transport	0.03		47.4768	48.2268	E3-database (June 2014)
Chemical tanker for vegetable oil transport	HFO for maritime transport			8.99333523	8.99333523	E3-database (June 2014)
Product tanker 22.56 kt (Fuel oil)	HFO for maritime transport			8.99333523	8.99333523	E3-database (June 2014)
Product tanker 15 kt (Fuel oil)	HFO for maritime transport			16.12947978	16.12947978	E3-database (June 2014)
Product tanker 12.617 kt (Fuel oil)	HFO for maritime transport			10.84709232	10.84709232	E3-database (June 2014)
Bulk Carrier "Handysize" - wood chips (Fuel oil) with bulk density 220 kg/m3	HFO for maritime transport			22.68778736	22.68778736	E3-database (June 2014)
Bulk Carrier "Supramax" - wood chips (Fuel oil) with bulk density 220 kg/m3	HFO for maritime transport			14.347973	14.347973	E3-database (June 2014)
Bulk Carrier "Handysize" - pellets (Fuel oil) with bulk density 650 kg/m3	HFO for maritime transport			9.5530104	9.5530104	E3-database (June 2014)
Bulk Carrier "Supramax" - pellets (Fuel oil) with bulk density 650 kg/m3	HFO for maritime transport			6.178067643	6.178067643	E3-database (June 2014)

Bulk Carrier "Handysize" - agri-residues with low bulk density (125 kg/m3)	HFO for maritime transport			37.47732899	37.47732899	E3-database (June 2014)
Bulk Carrier "Supramax" - agri-residues with low bulk density (125 kg/m3)	HFO for maritime transport			23.42266352	23.42266352	E3-database (June 2014)
Bulk Carrier "Handysize" - agri-residues with high bulk density (300 kg/m3)	HFO for maritime transport			17.56514386	17.56514386	E3-database (June 2014)
Bulk Carrier "Supramax" - agri-residues with high bulk density (300 kg/m3)	HFO for maritime transport			11.18169519	11.18169519	E3-database (June 2014)
Bulk Carrier "Handysize" - PKM	HFO for maritime transport			11.82681	11.82681	E3-database (June 2014)
Bulk Carrier "Supramax" - PKM	HFO for maritime transport			6.7552704	6.7552704	E3-database (June 2014)
Freight train USA (diesel)	Diesel	0.005	0.001	23.775	24.198	E3-database (June 2014)
Rail (Electric, MV)	Electricity EU mix MV	0	0	29.63898	29.63898	E3-database (June 2014)

H. Auxiliary services characteristics

Table 21 - Hydrogen production technologies and their GHG emission values

Hydrogen production technology		gCO2/MJ H2	g CH4/ MJ H2	g N2O/MJ H2	gCO2eq/ MJ H2	Source
Steam methane reforming	Natural gas consumption	84.7	0.23375	0.000229 625	90.61217 825	(Mehmeti et al., 2018)
	Electricity consumption (MV)	4.38228	0.010323	0.000199 8	4.699895 4	(Mehmeti et al., 2018)
	Total	89.08228	0.244073	0.000429 425	95.31207 365	(Mehmeti et al., 2018)
Electrolysis E-PEM (proton exchange membrane) using EU average electricity mix	Natural gas consumption	0	0	0	0	(Mehmeti et al., 2018)
	Electricity consumption (MV)	215.5608	0.50778	0.009828	231.1840 44	(Mehmeti et al., 2018)
	Total	215.5608	0.50778	0.009828	231.1840 44	(Mehmeti et al., 2018)
Electrolysis SOEC (solid oxide electrolysis cells) using EU average electricity mix	Natural gas consumption (MV)	25.95413 333	0.071626 667	7.03627E -05	27.76576 807	(Mehmeti et al., 2018)
	Electricity consumption	142.6807 2	0.336102	0.006505 2	153.0218 196	(Mehmeti et al., 2018)
	Total	168.6348 533	0.407728 667	0.006575 563	180.7875 877	(Mehmeti et al., 2018)

Table 22 - Auxiliary boilers with corresponding efficiencies and emission values

Auxiliary boilers	Efficiency heat	Efficiency Electricity	gCO2/MJ Heat (fuel itself)	gCH_4/MJ Heat	gN_2O/MJ Heat	tot gCO2eq/m j	Source
Bagasse pellet boiler	0.85			0.0019471 67	0.0007788 61	0.2807797 78	E3-database (june 2014)
Bagasse pellet CHP	0.461	0.167		0.0053314 05	0.0026657 03	0.9276644 97	(Giuntoli et al., 2017)
Lignite CHP	0.71	0.16		0.0019998 83	0.0042496 09	1.3163804 77	E3-database (june 2014)
NG boiler	0.9		73.22196222	0.0027941 67	0.0011176 39	73.624872 78	(Giuntoli et al., 2017)
NG CHP	0.42	0.33		0.01	0.0023809 52	0.9595238 1	E3-database (june 2014)
Sawdust boiler	0.7501875 47			0.0065	0.0013	0.5499	(Giuntoli et al., 2017)
Wood chip boiler	0.8503401 36			0.0057462 06	0.0011483 96	0.4858772 83	(Giuntoli et al., 2017)
Wood chip CHP	0.47	0.17		0.0103962 34	0.0020777 18	0.8790658 61	(Giuntoli et al., 2017)
Wood pellet boiler	0.8896797 15			0.0033375 9	0.0006675 18	0.2823601 13	(Giuntoli et al., 2017)

Table 23 - Thermal power generation efficiency

		Efficiency (MJ steam/MJ electricity)	Efficiency (%)	Source
Thermal to electrical power generation	Gas/Steam turbine	2.5	40%	(Zactruba, 2010)

I. Feedstock processing steps and characteristics

Table 24 – Woody residues and dedicated energy crops processing steps and characteristics. The value presented are used as base values for the individual feedstock conversion processes, however they are changed within the model due to upstream and downstream efficiency changes in the supply chain.

Type of process			**Residues wood feedstocks**			**Dedicated wood energy feedstocks**		
Collection (50%MC)			Forest residues	Pulpgrade stemwood	Bagasse	Eucalyptus	Poplar WF	Poplar WOF
	I/O	Unit	amount	amount	amount	amount	amount	amount
Diesel	Input	MJ/MJ woodchips	0.012	0.0107	0	0	0	0
CH4	output	g/MJ woodchips	0.0000092	0.00000816	0			
N2O	output	g/MJ woodchips	0.0000385	0.0000341	0	0	0	0
Chipping (MC 30%)								
	I/O	Unit	amount	amount	amount	amount	amount	amount
Wood	Input	MJ/MJ woodchips	1.025	1	1	1	1	1
Diesel	Input	MJ/MJ woodchips	0.00336	0	0	0	0	0
Woodchips	Output	MJ	1	1	1	1	1	1
CH4	Output	g/MJ woodchips	0.00000257	0	0	0	0	0
N2O	Output	g/MJ woodchips	0.0000107	0	0	0	0	0
Pellet Mill (50>10%MC)								
	I/O	Unit	amount	amount	amount	amount	amount	amount
Electricity	Input	MJ/MJ pellets	0.05	0.05		0.05	0.05	0.05
Heat required	Input	MJ/MJ pellets	0.185263158	0.185263158	0.207058824	0.185263158	0.185263158	0.185263158
Diesel	Input	MJ/MJ pellets	1	0.002		0.002	0.002	0.002
Additional chips		MJ/MJ pellets	0.28134456	0.28134456	0.325269899	0.28134456	0.28134456	0.28134456
CH4	Output	g/MJ pellets	0.00000153	0.00000153	0.00000153	0.00000153	0.00000153	0.00000153
N2O	Output	g/MJ pellets	0.0000064	0.0000064	0.0000064	0.0000064	0.0000064	0.0000064
Source			(Giuntoli et al., 2017)					

Table 25 - Dedicated energy perennial grasses and residue perennial grasses processing steps and characteristics. The value presented are used as base values for the individual feedstock conversion processes, however they are changed within the model due to upstream and downstream efficiency changes in the supply chain.

			Dedicated energy grasses			**Residue grasses**		
Collection (50%MC)			Switchgrass	Miscanthus	Willow	Straw	Agricultural residues	Industry residues
	I/O	Unit	amount	amount	amount	Amount	amount	amount
Diesel	Input	MJ/MJ woodchips	0	0	0	0.01	0	0
CH4	output	g/MJ woodchips	0	0	0	0.0000123	0	0
N2O	output	g/MJ woodchips	0	0	0	0.0000303	0	0
Processing/baling (30%>13.5%MC)								
	I/O	Unit	Amount	Amount		Amount	Amount	Amount
Electricity	Input	MJ/MJ bale	0.0025	0.0025		0	0	0
Diesel	Input	MJ/MJ bale	0.0092	0.0092		0.01	0.01	0
CH4	Output	MJ/MJ bale	0	0		0.0000123	0.0000123	0
N2O	Output	MJ/MJ bale	0	0		0.0000303	0.0000303	0
Chipping (MC 30%)								
	I/O	Unit	amount	amount	amount	amount	amount	amount
Wood	Input	MJ/MJ woodchips	1	1	1	1	1.025	1
Diesel	Input	MJ/MJ woodchips	0	0	0	0	0.00336	0
Woodchips	Output	MJ/MJ woodchips	1	1	1	1	1	1
CH4	Output	g/MJ woodchips	0	0	0	0	0.00000257	0
N2O	Output	g/MJ woodchips	0	0	0	0	0.0000107	0
Pellet Mill (50>10%MC)								
	I/O	Unit	amount	amount	amount	amount	amount	amount
Electricity	Input	MJ/MJ pellets	0.028	0.028	0.05	0.02	0.02	0.028
Heat required	Input	MJ/MJ pellets	0	0	0.185263158	0	0.010350854	0.010350854
Diesel	Input	MJ/MJ pellets	0	0	0.002	0	0	0.0016
Additional chips	Input	MJ/MJ pellets	0	0	0.28134456	0	0.012445828	0.014130635
CH4	Output	g/MJ pellets						0.00000123
N2O	Output	g/MJ pellets						0.0000512
Source			(JRC & Hoefnagels, 2011)		(Antonissen, 2016; Argonne National Laboratory, 2018a)	(Giuntoli et al., 2017)		

J. All feedstock conversion reactor characteristics

J.1 Gasification pathways

Table 26 - FT reactors and their characteristics

Type of reactor	MC feedstock in	Co-products input	Efficiency main product based on LHV	Main product out	Co-products output	Source
FT-reactor Recycled design	30%		46%	FT-Diesel	Electricity	(Argonne National Laboratory, 2018b)
FT-reactor One-through design	30%		31%	FT-Diesel	Electricity	
PTL 80 SMDS	10%		42%	FT-Diesel	Electricity	(van Vliet et al., 2009)
PLT 400	10%		43%	FT-Diesel	Electricity	
PLT 2000	10%		43%	FT-Diesel	Electricity	
PTL 2000 CCS	10%		43%	FT-Diesel	Electricity	
TTL 2000 CCS	10%		42%	FT-Diesel	Electricity	
BTL 300 CGP	35%		44%	FT-Diesel	Electricity	
PTL 80 SMDS	10%		7%	FT-Gasoline	Electricity	
PLT 400	10%		8%	FT-Gasoline	Electricity	
PLT 2000	10%		8%	FT-Gasoline	Electricity	
PTL 2000 CCS	10%		8%	FT-Gasoline	Electricity	
TTL 2000 CCS	10%		8%	FT-Gasoline	Electricity	
BTL 300 CGP	35%		8%	FT-Gasoline	Electricity	
FT-reactor One-through design	30%		8%	FT-RJF	Electricity, Diesel, Gasoline, Propane, Methane	(De Jong et al., 2017; Swanson, Satrio, Brown, Planton, & David, 2010)

Table 27 - Methanol and DME reactors and their characteristics

Type of reactor	MC feedstock in	Co-products input	Efficiency main product based on LHV	Main product out	Co-products output	Source
Methanol reactor	30%		43%	Methanol	Electricity	(Argonne National Laboratory, 2018b)
Methanol reactor	50% & 30%		61%	Methanol	Electricity	(Hannula & Kurkela, 2013)
Methanol reactor	50% & 30%		58%	Methanol		(Argonne National Laboratory, 2018b)
DME reactor	30%		25%	DME	Electricity	(Argonne National Laboratory, 2018b)
DME reactor	50% & 30%		60%	DME	Electricity	(Hannula & Kurkela, 2013)
DME reactor	50% & 30%		55%	DME		(Argonne National Laboratory, 2018b)g

Table 28 - Syngas fermentation into ethanol reactors and their characteristics

Type of reactor	MC feedstock in	Co-products input	Efficiency main product based on LHV	Main product out	Co-products output	Source
Gasification & Fermentation	30%	Diesel	35%	Ethanol		(Argonne National Laboratory, 2018b)
Gasification & Fermentation	14%	Diesel	43%	Ethanol	Electricity	
Gasification & Fermentation	10%	Diesel	39%	Ethanol		

Table 29 - Conversion chemicals and other inputs of syngas fermentation into ethanol reactor

Conversion input	Woodchips willow 30%MC	Woodchips poplar 30%MC	Bales switchgrass 13.5%MC	Bales miscanthus 13.5%MC	Pellets 10%MC	Unit	Source
Diesel	0.005591987	0.005591987	0.003175261	0.003175261	0.003175261	MJ/MJ ethanol	(Argonne National Laboratory, 2018a)
Natural gas						MJ/MJ ethanol	
Biomass	2.844255619	2.844255619	2.354497215	2.33279678	2.237857376	MJ/MJ ethanol	
Electricity EU mix MV	0	0	-0.01140553	-0.011511628	0	MJ/MJ ethanol	
Sodium hydroxide (NaOH)	0.000260609	0.000260609	0.000238114	0.000235919	0.000226318	Kg/MJ ethanol	
Pure CaO for processes	0	0	0	0	0	Kg/MJ ethanol	
Urea	0	0	0	0	0	Kg/MJ ethanol	
Synthesis catalyst	1.24099E-05	1.24099E-05	1.13388E-05	1.12343E-05	1.0777E-05	Kg/MJ ethanol	
DEPG	1.11689E-06	1.11689E-06	1.02049E-06	1.01108E-06	9.69934E-07	Kg/MJ ethanol	
Olivine	0.000347975	0.000347975	0.000317939	0.000315009	0.000302188	Kg/MJ ethanol	
Tar catalyst	1.19135E-05	1.19135E-05	1.08852E-05	1.07849E-05	1.0346E-05	Kg/MJ ethanol	

J.2 Biochemical pathways

Table 30 - Dilute acid pre-treatment and fermentation reactors and their characteristics

Type of reactor	MC feedstock in	Co-products input	Efficiency main product based on LHV	Main product out	Co-products output	Source
Simultaneous saccharification and fermentation (1)	50%	Diesel	38%	Ethanol	Electricity	(Mu et al., 2010)
Simultaneous saccharification and fermentation (2)	30%	Diesel	36%	Ethanol	Electricity	(Argonne National Laboratory, 2018b)

Table 31 - Conversion chemicals and other inputs of dilute acid pre-treatment and fermentation reactor 1

	Forest residues 50%MC	Unit	Source
Biomass	2.603265613	MJ/MJ ethanol	(Mu et al., 2010)
Electricity EU mix MV	-0.115674862	MJ/MJ ethanol	
Dolomite		Kg/MJ ethanol	
Alpha-amylase		Kg/MJ ethanol	
Gluco-amylase		Kg/MJ ethanol	
Cellulase	0.000999652	Kg/MJ ethanol	
Yeast		Kg/MJ ethanol	
Sulphuric acid (H2SO4)	0.005406013	Kg/MJ ethanol	
Ammonia (NH3)		Kg/MJ ethanol	
Corn steep liquor	0.002117684	Kg/MJ ethanol	
Diammonium phosphate (DAP)	0.000249913	Kg/MJ ethanol	
Sodium hydroxide (NaOH)	7.99064E-05	Kg/MJ ethanol	
Pure CaO for processes	0.003937774	Kg/MJ ethanol	
Urea	8.87849E-06	Kg/MJ ethanol	

Table 32 - Conversion chemicals and other inputs of dilute acid pre-treatment and fermentation reactor 2

Conversion input	Woodchips willow 30%MC	Woodchips poplar 30%MC	Bales switchgrass 13.5%MC	Bales miscanthus 13.5%MC	Unit	Source
Diesel	0.005591987	0.005591987	0.003175261	0.003175261	MJ/MJ ethanol	(Argonne National Laboratory, 2018a)
Natural gas					MJ/MJ ethanol	
Biomass	2.773985774	2.773985774	2.534547002	2.511187122	MJ/MJ ethanol	
Electricity EU mix MV	-0.107747447	-0.107747447	-0.107747447	-0.107747447	MJ/MJ ethanol	
Dolomite					Kg/MJ ethanol	
Alpha-amylase	0	0	0	0	Kg/MJ ethanol	
Gluco-amylase	0	0	0	0	Kg/MJ ethanol	
Cellulase	0	0	1.33397E-06	1.32168E-06	Kg/MJ ethanol	
Yeast	0	0	3.32159E-07	3.29098E-07	Kg/MJ ethanol	
Sulphuric acid (H2SO4)	0.004296656	0.004296656	0.003925786	0.003889604	Kg/MJ ethanol	
Ammonia (NH3)	0.000515599	0.000515599	0.000471094	0.000466752	Kg/MJ ethanol	
Corn steep liquor	0.001632729	0.001632729	0.001491799	0.00147805	Kg/MJ ethanol	
Diammonium phosphate (DAP)	0.000171866	0.000171866	0.000157031	0.000155584	Kg/MJ ethanol	
Sodium hydroxide (NaOH)	0.001460863	0.001460863	0.001334767	0.001322465	Kg/MJ ethanol	
Pure CaO for processes	0.000945264	0.000945264	0.000863673	0.000855713	Kg/MJ ethanol	
Urea	0.000257799	0.000257799	0.000235547	0.000233376	Kg/MJ ethanol	

Table 33 - Steam explosion pre-treatment and fermentation reactor and their characteristics

Type of reactor	MC feedstock in	Co-products input	Efficiency main product based on LHV	Main product out	Co-products output	Source
Separate hydrolysis and fermentation	30%		34%	Ethanol	Electricity	(L. Wang et al., 2013)

Table 34 - Conversion chemicals of steam explosion pre-treatment and fermentation reactor

	Straw 13.5%MC	Unit	Source
Diesel	0	MJ/MJ ethanol	(L. Wang et al., 2013)¦
Natural gas	0	MJ/MJ ethanol	
Biomass	2.91062851	MJ/MJ ethanol	
Electricity EU mix MV	-0.188609482	MJ/MJ ethanol	
Dolomite	0	Kg/MJ ethanol	
Alpha-amylase	0.005369116	Kg/MJ ethanol	
Gluco-amylase		Kg/MJ ethanol	
Cellulase		Kg/MJ ethanol	
Yeast	0	Kg/MJ ethanol	
Sulphuric acid (H2SO4)	0	Kg/MJ ethanol	
Ammonia (NH3)	0	Kg/MJ ethanol	
Corn steep liquor	0.002398232	Kg/MJ ethanol	
Diammonium phosphate (DAP)	0.000316786	Kg/MJ ethanol	

Table 35 - Ethanol upgrading into RJF reactor and their characteristics

Type of reactor	Feedstock	Co-products input	Efficiency main product based on LHV	Main product out	Co-products output	Source
Ethanol upgrading reactor	Ethanol	Hydrogen, electricity	67%	RJF	Gasoline, Diesel	(De Jong et al., 2017)

J.3 Thermochemical pathways

Table 36 - Pyrolysis reactors and their characteristics

Type of reactor	MC feedstock in	Co-products input	Efficiency main product based on LHV	Main product out	Co-products output	Source
Pyr in H2 with drying	50% & 30%	Electricity	15%	Diesel	Gasoline, Heavy hydrocarbons	(Tews et al., 2014)
Pyr in H2 without drying	10%		15%	Diesel	Electricity, Gasoline, Heavy hydrocarbons	
Pyr ex H2 with drying	50% & 30%	Hydrogen	15%	Diesel	Electricity, Gasoline, Heavy hydrocarbons	
Pyr ex H2 without drying	10%	Hydrogen	15%	Diesel	Electricity, Gasoline, Heavy hydrocarbons	
Pyr in H2 with drying	50% & 30%	Electricity	36%	Gasoline	Diesel, heavy hydrocarbons	
Pyr in H2 without drying	10%		36%	Gasoline	Electricity, Diesel, Heavy hydrocarbons	
Pyr ex H2 with drying	50% & 30%	Hydrogen	36%	Gasoline	Electricity, Diesel, Heavy hydrocarbons	
Pyr ex H2 without drying	10%	Hydrogen	36%	Gasoline	Electricity, Diesel, Heavy hydrocarbons	
Pyr ex H2 with drying	50% & 30%	Hydrogen	4%	RJF	Electricity, Diesel, Gasoline, Heavy hydrocarbons	(De Jong et al., 2017; Tews et al., 2014)
Pyr in H2 with drying	50% & 30%	Electricity	4%	RJF	Electricity, Diesel, Gasoline, Heavy hydrocarbons	

Table 37 - HTL reactors and their characteristics

Type of reactor	MC feedstock in	Co-products input	Efficiency main product based on LHV	Main product out	Co-products output	Source
HLT in H2	50% & 30%	Electricity	25%	Diesel	Gasoline, Heavy hydrocarbons	(Tews et al., 2014)
HTL ex H2	50% & 30%	Hydrogen	25%	Diesel	Electricity, Gasoline, Heavy hydrocarbons	
HLT in H2	50% & 30%	Electricity	31%	Gasoline	Diesel, Heavy hydrocarbons	
HTL ex H2	50% & 30%	Hydrogen	31%	Gasoline	Electricity, Diesel, Heavy hydrocarbons	
HLT ex H2	50% & 30%	Hydrogen, electricity	6%	RJF	Diesel, Gasoline, Heavy hydrocarbons	(De Jong et al., 2017; Tews et al., 2014)
HTL in H2	50% & 30%	Electricity	6%	RJF	Diesel, Gasoline, Heavy hydrocarbons	

K. Choices of supply chains and possible options

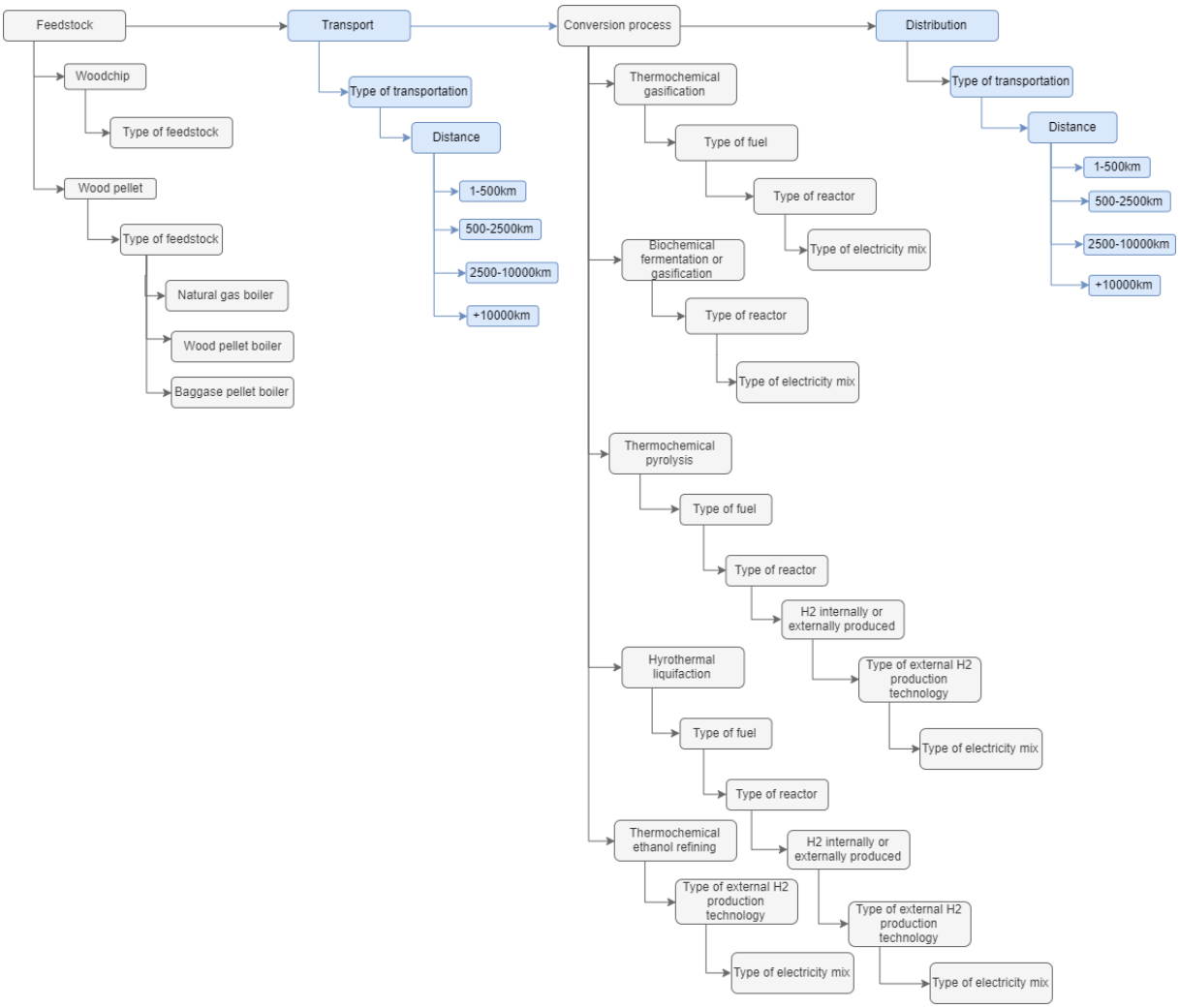

Figure 24 - Schematic representation of possible choices for advanced biofuel production systems

L. Total GHG emissions of feedstocks production over included distances.

Figure 25- GHG emission values of feedstock production with varying distances and appearances